Fourier Methods for Pricing Early-Exercise Options Under Lévy Dynamics

by

Tolulope Rhoda Fadina

Thesis presented in partial fulfilment of the requirements for the degree of Master of Science in Mathematics at Stellenbosch University

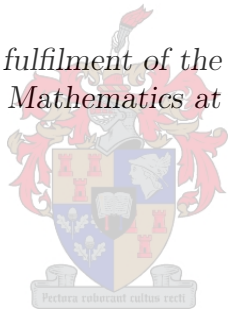

Department of Mathematics,
University of Stellenbosch,
Private Bag X1, Matieland 7602, South Africa.

Supervisor: Dr. P.W Ouwehand

January 2012

Declaration

By submitting this thesis electronically, I declare that the entirety of the work contained therein is my own, original work, that I am the owner of the copyright thereof (unless to the extent explicitly otherwise stated) and that I have not previously in its entirety or in part submitted it for obtaining any qualification.

Signature: .....
T.R Fadina

Date: 2012/01/08 .....

Abstract

The pricing of plain vanilla options, including early exercise options, such as Bermudan and American options, forms the basis for the calibration of financial models. As such, it is important to be able to price these options quickly and accurately. Empirical studies suggest that asset dynamics have jump components which can be modelled by exponential Lévy processes. As such models often have characteristic functions available in closed form, it is possible to use Fourier transform methods, and particularly, the Fast Fourier Transform, to price such options efficiently. In this dissertation we investigate and implement four such methods, dubbed the Carr-Madan method, the convolution method, the COS method and the Fourier space-time stepping method. We begin by pricing European options using these Fourier methods in the Black-Scholes, Variance Gamma and Normal Inverse Gaussian models. Thereafter, we investigate the pricing of Bermudan and American options in the Black-Scholes and Variance Gamma models. Throughout, we compare the four Fourier pricing methods for accuracy and computational efficiency.

Opsomming

Die prysbepaling van gewone vanilla opsies, insluitende opsies wat vroeg uitgeoefen kan word, soos Bermuda-en Amerikaanse opsies, is grondliggend vir die kalibrering van finansiële modelle. Dit is daarom belangrik dat die pryse van sulke opsies vinnig en akkuraat bepaal kan word. Empiriese studies toon aan dat batebewegings sprongkomponente besit, wat gemodelleer kan word met behulp van exponensiële Lévyprosesse. Aangesien hierdie modelle dikwels karakteristieke funksies het wat beskikbaar is in geslote vorm, is dit moontlik om Fourier-transform metodes, en in besonders die vinnige Fourier-transform, te gebruik om opsiepryse doeltreffend te bepaal. In hierdie proefskrif ondersoek en implementeer ons vier sulke metodes, genaamd die Carr-Madan metode, die konvolusiemetode, die COS-metode en die Fourier ruimte-tydstap metode. Ons begin deur die pryse van Europese opsies in die Black-Scholes, Gammavariansie (Engels: *Variance gamma*) en Normaal Invers Gauss (Engels: *Normal Inverse Gaussian*)-modelle te bepaal met behulp van die vier Fourier-metodes. Daarna ondersoek ons die prysbepaling van Bermuda-en Amerikaanse opsies in die Black-Scholes en Gammavariansiemodelle. Deurlopend vergelyk ons die vier Fourier-metodes vir akkuraatheid en berekeningsdoeltreffendheid.

Acknowledgements

To God be the glory great things he has done. I thank God for the gift of life and for his wisdom throughout this research. It has been God all the way.
My profound gratitude goes to my supervisor, Dr Peter Ouwehand. Thank you for the foundation you gave me and for your advice and support. I sincerely appreciate your efforts.
I sincerely appreciate the African Institute for Mathematical Sciences. And to the entire staff of Department of Mathematics, Stellenbosch University, I say THANK YOU.
To my parents, Prince and Mrs Michael Fadina , I say a very big thank you for the best legacy you set for me. To my siblings and in-laws, thanks for always been there. I love you all. To the entire RCCG family in Cape-town, thanks for your prayers and spiritual supports, God bless you all.

This research work was jointly funded by the African Institute for Mathematical Sciences (AIMS) and the Department of Mathematical Sciences at the University of Stellenbosch.

Dedications

To my loving parents
Prince and Mrs Michael Fadina

Contents

List of Figures

List of Tables

Chapter 1

Introduction

In financial markets, the act of determining fast and accurate prices and sensitivities of options is an active research field. An option contract is an agreement between two parties - the holder of the option and the writer of the option. The holder of the option is given the right to make certain decisions in order to receive a certain payoff or she/he loses the premium paid for the option. The payoff is the difference between the underlying asset price S_t at a prescribed date t in the future, and the predetermined strike price K. The two basic types of options are *call* options and *put* options. A call option gives the holder the right, not obligation, to buy S_t in the future t, for K, while a put option gives the holder the right, not obligation, to sell S_t in the future t, for K. A call option has a positive value when $S_t > K$, and a put option has a positive value when $K > S_t$. The payoff function of a call option is given by

$$(S_t - K)^+ = \begin{cases} S_t - K & \text{if } S_t \geq K, \\ 0 & \text{otherwise .} \end{cases}$$

And the payoff function of a put option is given by

$$(K - S_t)^+ = \begin{cases} K - S_t & \text{if } S_t \leq K, \\ 0 & \text{otherwise .} \end{cases}$$

Put-call parity establishes the relationship between the value of a call and a put option with similar strike price and maturity time T. The two commonly traded forms of vanilla options are European and early-exercise options.

A European option is a standard type of option contract with no special features except the simple maturity date T and the strike price K. This option can only be exercised at the maturity date, that is, the holder of this option can only make a decision at time T. The Bermudan option can be exercised at predetermined dates prior to, or on the maturity date while an American option can be exercised at any time before, or on the maturity date. In financial markets, practitioners prefer to know the worth of their options at all times in order to manage the risk associated with uncertainty, since the parameters of financial products constantly change over time. The Bermudan and American options are termed early-exercise options.

Starting from the work of Black and Scholes (1973), and Merton (1973), the dynamics of the underlying asset price is based on the assumption that underlying asset returns are normally distributed with Brownian motion noise but fixed volatility [1]. The pricing function for the European option in the form of a partial differential equation can be derived by hedging the option payoff function by the risk-neutral delta-hedging strategy. Observed option prices from financial markets show that different volatilities should be used for different strikes and maturities. The behaviour of observed prices distinguishes between maturities which contradict option prices from the model driven by Brownian motion with constant volatility, for observed prices move by jumps especially in short-dated options (options traded on in days and months). This reveals that the normality assumption in the Black-Scholes (BS) theory cannot capture heavy tails and discontinuities present in short-term trading in the practical log-returns. The real densities are usually too peaked in short-term trading compared to the normal density Cont and Tankov (2004); interpreting the BS model as unpredictable.

Diverse models have been established in literature to improve the fit of the option prices in the BS model. Hull *et al.* (1987), Stein *et al.* (1991) and Heston (1993) assume that the stochastic volatility of the underlying asset is a mean-reverting diffusion process, typically correlated with the underlying process itself. Dupire (1994) and Derman *et al.* (1994) pioneered a model that describes volatility as the deterministic function of the asset price, known as the local volatility model. The local volatility model retains the pure one-factor diffusion approach of the BS model, but with an extension, as it defines the underlying volatility function as a function of asset price and time. Other models that replace the source of continuity in the behaviour of the underlying asset with some discontinuity, are the Lévy models, the Variance Gamma model (VG) by Madan and Seneta (1990), the Normal Inverse Gaussian model (NIG) by Barndorff-Nielsen (1997), and the Carr-Geman-Madan-Yor model (CGMY) by Carr *et al.* (2002). All these models have their advantages and disadvantages. In this dissertation, the focus is on models of asset dynamics that do not suffer from the disadvantages of models driven by pure Brownian motion. Empirical studies reveal that underlying asset prices do jump and the phenomenon of implied volatility smile in financial markets shows that the risk-neutral returns are not normally distributed Barndorff-Nielsen (1997), Madan and Seneta (1990), Bates (1996), Cont and Tankov (2004), Tankov (2010). Thus, the focus here is on pricing options where the underlying assets are driven by the exponential Lévy model.

Exponential Lévy models can be divided into three; the continuous exponential Lévy models - processes with no jumps, the only example is the geometric Brownian motion, the BS model; the finite activity exponential Lévy model - a process with continuous sample paths and few jumps, examples are the Merton Jump Diffusion model Merton (1976) and the Kou model Kou (2002); and the infinite activity exponential Lévy model - a process with pure jumps, examples are the VG model, the NIG model and the CGMY model. Under these models, the characteristic functions

[1] The volatility measures the uncertainty associated with underlying asset pricing which is the same as annualized standard deviation of returns.

(CFs) of their distributions are available in closed-form. The Lévy-Khinchine representation is frequently used to obtain the CF's of Lévy processes, Schoutens (2003), **?**, Cont and Tankov (2004).

In the option pricing theory under the BS model, the risk-neutral valuation formula (see Equation 2.38) presents the pricing formula of options as an expectation of the product of the discounted payoff and the probability density function of the underlying process except for options with early exercise features. But in the case of Lévy processes, the risk-neutral densities often comprise special functions and infinite summations. Thus, it is difficult to find their integrals directly. The Feynman-Kač theorem relates the risk-neutral valuation formula to the solution of partial differential equations (PDEs) under the BS model, and partial integro-differential equation (PIDE) under the Lévy model. The PDE equation can be solved based on the terminal conditions. The PDE can be used to price several types of options once the payoff function is known. The PIDE comprises a diffusion term and an integral term. These terms are often treated separately.

Based on the risk-neutral valuation formula, many numerical methods have been employed to value options and to determine their sensitivities e.g. PIDE-based methods, Monte Carlo methods Boyle (1977), lattice methods Kéllezi and Webber (2004) and many more. Option pricing in Lévy models takes into account empirical facts which often result in a more complicated computation of option prices. In view of this, a more efficient method and fast algorithm have to be developed to cope with these models. For early-exercise options, the solution to the PIDE is not trivial. Diverse finite difference schemes have been proposed in literature Cont and Tankov (2004), Hirsa and Madan (2004), Andersen and Andreasen (2000), Forsyth and Vetzal (2002), but these methods are vulnerable to errors in convergence due to some factors that will be stated in Chapter 3 below, Lord *et al.* (2008), Jackson. *et al.* (2008), Surkov (2009). Thus, their results are not satisfactory.

Instead of applying the direct discounted expectation approach to evaluate the integral of the discounted payoff and risk neutral density function of the underlying process, it is easy to compute the integral of their Fourier transform once the CF of the distribution of the underlying asset is known. CF is the Fourier transform of the probability density function. In mathematical finance, diverse numerical integration methods based on Fourier methods have been established in literature. Some of these methods are the *transform-based methods*; the Carr Madan method Carr and Madan (1999), the Raible method Raible (2000), the convolution method (CONV method) Lord *et al.* (2008), the Lewis method Lewis (2001) and the Fourier space time-stepping method (FST method) Jackson. *et al.* (2008), Surkov (2009), and the Fourier-cosine series expansion (COS method) Fang and Oosterlee (2008), Fang (2010). The idea behind using the transform methods is to take an integral of the discounted payoff over the probability distribution obtained by inverting the corresponding Fourier transform; this originates in the convolution theorem (see Theorem 2.5.2) Carr and Madan (1999), Raible (2000), Lee (2004), Lord *et al.* (2008). The COS method substitutes the probability density function in the risk-

neutral valuation formula with the Fourier-cosine series expansion. In Lévy processes, the CF is often easier to handle than the density function itself Carr and Madan (1999), Lord *et al.* (2008), Cherubini *et al.* (2010). Thus, the Fourier methods are said to be effective approaches for pricing options in Lévy models because the CFs are readily available or can be calculated Raible (2000), Lord *et al.* (2008), Fang and Oosterlee (2008) and Fang and Oosterlee (2009b).

Fourier methods are computationally very efficient due to the availability of the Fast Fourier Transform (FFT), that is implemented in most of these methods Carr and Madan (1999), Lord *et al.* (2008), Surkov (2009). These methods are unique in pricing option with series of strikes in a single computation Carr and Madan (1999), Raible (2000), Surkov (2009), Fang and Oosterlee (2008), Lord *et al.* (2008). They can also be used to determine the hedge parameters at almost no additional computational cost, but in this dissertation, we will only focus on pricing, and not hedging, even though we know that pricing is very closely related to the ability to hedge. The FFT is an efficient algorithm for computing the sum of a finite sequence of complex number. It approximates a continuous Fourier Transform (CFT) by its discrete counterpart, Discrete Fourier Transform (DFT), for a carefully chosen vector Walker (1996), Cherubini *et al.* (2010).
Carr and Madan (1999) initiated the idea of pricing options using the FFT algorithm. An alternative formulation of transform-based methods for pricing and hedging of options in exponential Lévy models with the risk-neutral valuation formula is the FST method. The FST method involves solving the diffusion and the integral terms of the PIDE separately but in a proportional manner. The Fourier transform of the PIDE featured out the logarithm of the CF. Thus, the Fourier transform of the PIDE results in a system of ordinary differential equations (ODEs) that can be easily solved by breaking the equations up into simpler portions, solving each portion independently, and adding up the solutions. To price exotic options [2], the FST method is shown to handle prices and sensitivities effectively, Jackson. *et al.* (2008), Surkov (2009).

Furthermore, in pricing early exercise options, the Carr-Madan method is extended into a method that employs one of the crucial properties of the Fourier methods, the convolution theorem (Theorem 2.5.2). As explained earlier, the main idea is to recognise the option prices as the convolution of the risk-neutral density and the discounted payoffs. The COS method is also extended to price the early exercise option Fang and Oosterlee (2009b). The FST method allows the prices from one exercise time to be projected back to a second exercise time in one step of the algorithm. Thus, the algorithm for pricing European options remains unchanged for pricing early-exercise options. The price of an American option can be approximated directly by that of a Bermudian option with a larger exercise dates. To price American options efficiently using the CONV and COS methods, the Richardson extrapolation method can be applied to the price of the Bermudan options of its counterpart. Lord *et al.*

[2]Exotic options are path dependent options whose payoffs at maturity do not depend only on the price of the underlying asset at maturity but at several times before maturity, e.g. barrier, Bermudan and American options.

(2008) state that the pricing of American options using the PIDE approach is more favourable than the CONV method and the finite difference methods.

1.1 Motivation for research

Financial models always depend on unknown parameters. In order to provide parameters matching the real market price of liquid instruments (calibration), the pricing of series of a options is required. In financial markets, early-exercise options are often used as building blocks for more complicated products and for effective calibration. This is quite time-consuming. Thus, we aim to compute the values of these options as fast as possible. As stated earlier, diverse numerical methods have been implemented in literature to adequately price these options and derive their hedge. The efficiency of a numerical method for pricing options depends on the following:

- Accuracy - Precise calculation of option prices and their sensitivities are the bedrock for using numerical methods, although numerical methods give approximated results. In a financial market where huge number of assets change hands, a difference of 0.01 in the computed price can lead to a substantial loss or gain in a portfolio. Thus, the importance of good approximation cannot be overestimated.

- Speed - Practitioners operate in a highly competitive market. The ability to respond quickly to change in market conditions can give the practitioner an edge over competitors, especially in electronic financial markets where algorithm-trading is used in decision making on when and how options should be exercised.

- Convergence - The performance of numerical methods wholly depends on the rate at which the numerical solution converges to the exact solution as the number of points (N) involved in the computation increases. The difference between the approximated value and the exact value is the error. Higher-order convergence is preferred in most numerical methods, for the error decreases faster as N increases. In the case of exponential convergence, the error decreases exponentially as N increases. The computational speed is related to linear computational complexity, meaning the computational time (CPU-time) grows linearly only with respect to an increase in N. The convergence of the majority of numerical methods for solving financial problems are of first and second orders, Lord *et al.* (2008), Surkov (2009).

In this dissertation, Fourier's methods for pricing plain-vanilla and early-exercise options that give exponential convergence and second-order convergence under exponential Lévy models will be presented. The computer used for all programs is TOSHIBA with Pentium (R) Dual-core CPU, RAM 2.00GB (1.87 usable) and the system type is a 64 bits operating system. All programs are written in Python 2.6 on Linux 10.10.

1.2 Organisation of thesis

The general framework of our research, the exponential Lévy model, is explained in detail in Chapter 2 with applications to the option-pricing theory. Then, the risk-neutral valuation formula is presented. Chapter 3 introduces and explains the Fourier methods for approximating the risk neutral valuation integral. We conclude this chapter by presenting the numerical results obtained by pricing European style options in the BS, NIG and VG models using the Fourier methods. In Chapter 4, we extend the Fourier methods discussed in Chapter 3 to price Bermudan and American-style options. Lastly, we will summarize our findings and give concluding remarks.

Chapter 2

2. Models of asset prices

2.1 Introduction

In an arbitrage-free market the price of a contingent claim is given by the risk-neutral valuation formula. This formula has three main components: the risk free rate, the future payoff function and the risk-neutral distribution of the underlying asset returns. In this chapter, we discuss the risk-neutral distribution of the underlying asset.

The history of stochastic processes in finance can be traced back to Bachelier (1900), when Brownian motion was originally introduced as a stock-price model. One of the drawbacks of this model was that it accommodated negative stock prices which is not feasible in a real world market. After Bachelier's work, Samuelson (1965), corrected this flaw by modelling the dynamics of stock prices using geometric Brownian motion instead of arithmetic Brownian motion. This, Samuelson (1965) carried out prior to the derivation of the popularly used BS formula.

Brownian motion is a popularly used Lévy process and is often used to derive analytical formulae for solving option-pricing problems. The independent and stationary increments of Lévy processes motivate their applications to solving these problems. As stated earlier, financial models completely driven by geometric Brownian motion make up the BS model. Empirical studies show that an underlying asset driven by geometric Brownian motion does not work well in practice due to path-continuity and other factors Cont and Tankov (2004); many practitioners maintain that one need not to give up the continuity path if one accepts that a underlying asset is driven by stochastic volatility. Thus, it is important to work in a model where discontinuities cannot be ignored.

In financial modelling, the stationary increments, independent increments, stochastic continuity and the infinite divisible properties of asset returns motivate the use of *Lévy processes* to model asset prices. Lévy processes were founded and pioneered by Paul Lévy in 1930*s*. The class of infinitely divisible distribution is a crucial class of statistical distribution of Lévy processes. This is as a result of some properties: An infinitely divisible random variable can be expressed as a sum of large number of

independent and identically distributed (i.i.d) random variables. For every infinitely divisible distribution, there is an associated Lévy process Cont and Tankov (2004). These properties provide a means of representing changes in asset price as a result of a high rate of randomness in the financial market . The price changes in Lévy processes are consistent with the no-arbitrage assumption, and Lévy processes provide a good fit with observed prices from financial markets, Barndorff-Nielsen (1997), Carr *et al.* (2002), Cont and Tankov (2004). The availability of the CF of the Lévy processes is of great importance in option pricing.

There are two major types of Lévy processes: The jump-diffusion processes and infinite-activity processes. Jump-diffusion processes exhibit much small-scale finite variate of jumps due to diffusion, with a few larger jumps. Infinite-activity processes also exhibit small-scale variation due to jumps with infinitely many small jumps in any non-zero time interval. Nevertheless, in any bounded time interval, there are only a finite number of jumps of larger magnitude than a given $\varepsilon > 0$. A good example of a process with finite variation and infinite activity is the variance-gamma process.

Intuitively, we can say in jump-diffusion models, jumps arrive at distinct times and the interval between the jump times can be modelled as diffusion terms. Carr *et al.* (2002), speculate in their investigation that the presence of diffusion terms in the dynamics of the stock price is not necessary. In practice, jump-diffusion processes are rarely used because of their weak response to the addition of extra parameters to the activities of the diffusion processes. That is, they still, almost surely generate sample paths which are continuous with respect to time. In view of this, we focus on models driven by infinite activity processes, that is, NIG and VG models. Their empirical performance in fitting equity and asset prices have been remarkably proven in literature.

The majority of theorems and definitions given in this dissertation are fairly general. Only examples and proofs for theorems which are of interest to us are given, whereas references to proofs of more general results will be given and some proofs will be provided in the appendix. For detailed study, books in the literature of Lévy processes in finance are Schoutens (2003), Cont and Tankov (2004) and Kypriano (2010), and, some general books on Lévy processes are Sato (1999) and Applebaum (2004).

Section 2.2 presents the definition and properties of Lévy processes. We also present Lévy-Itô Decomposition that provides basic information on simulation of a Lévy sample path, and the Lévy-Khintchin formula that links Lévy processes to distributions. In section 2.3 , we shall discuss financial models driven by exponential Lévy models, and how to deal with complex discontinuities in the numerical computation of the CFs of their distributions. Section 2.4 explains the risk-neutral valuation formula. Lastly, we introduce the fundamental theory of Fourier methods.

2.2 Definitions and properties of Lévy processes

For a better understanding of the formal definition of Lévy processes, we need to know what càdlàg functions are. These kinds of functions appear throughout in financial mathematics and they play a vital roles in the theory of Lévy processes. Càdlàg functions are natural models for paths of processes with jumps.

Definition 2.2.1 (Càdlàg Function (continue á droite avec des limites á gauche)). *A stochastic process $(X_t)_{t\geq 0}$ is said to be càdlàg if, for every $t \in [0,T]$, the paths $t \to X_t$ are continuous from the right and limited from the left at every point. That is,*

$$\text{Left limit } X_{t-} = \lim_{s\to t, s<t} X_t$$
$$\text{Right limit } X_{t+} = \lim_{s\to t, s>t} X_t$$

exist and $X_t = X_{t+}$ Sato (1999). *Also the jump at time t is written as*

$$\Delta X_t = X_{t+} - X_{t-}.$$

It is important to note that all continuous functions are càdlàg functions but not all càdlàg functions are continuous.

Definition 2.2.2 (Lévy process). *A Lévy process is a càdlàg stochastic process $(X_t)_{t\geq 0}$ with $X_0 = 0$ defined on a filtered probability space $(\Omega, \mathbf{F}, \mathbb{F}, \mathbb{P})$ taking values in $\mathbb{R}$, where $\mathbf{F} = (\mathbb{F}_t)_{t\geq 0}$, and satisfies the following conditions* Sato (1999)*:*

1. *Independent increments: For every increasing sequence of times $t_0, \ldots, t_n$, given $j = 1, \ldots, n$, the random variables $X_{t_j} - X_{t_{j-1}}$ are independent.*
2. *Stationary Increments: $X_{t+u} - X_t$ does not depend on t but $X_{t+u} - X_t \sim X_u$. So that, the distribution of $X_{t+u} - X_t$ depends only on u, $\forall u > 0$.*
3. *Stochastic Continuity: For all $\varepsilon > 0, \lim_{h\to 0} \mathbb{P}(|X_{t+h} - X_t| \geq \varepsilon) = 0$.*

Condition 1 implies for a given information at time t, a change in the stochastic process $X_{t+u} - X_t$ is independent of the past information. Processes with stationary increments imply the increments in $X_{t+u} - X_t$, $\forall\ t, u > 0$ have the same distribution for every time t. i.e, a change in the distribution is independent on time. Condition 3 means that for a given time t, the probability of seeing a jump at t is zero. In other words, a jump appears at random times.

It is important to recall that Brownian motion is an example of a Lévy process, for it satisfies the above conditions. Sato (1999) gives a detailed study on Brownian motion as an example of Lévy processes. The class of Lévy processes include some other processes, for example; Poisson processes, Compound Poisson processes and many more, but the Poisson processes and the Brownian motion are the fundamental examples of Lévy processes. They can be thought of as the building blocks of Lévy processes because every Lévy process is a superposition of Brownian motion and, possibly an infinite number of independent Poisson processes, Cont and Tankov (2004). For more information on the examples of Lévy processes, see Appendix A.1.

2.2.1 Infinitely divisible distribution

Lévy processes are processes with some strong properties and one of the properties is *infinite divisibility.*

Definition 2.2.3 (Infinitely divisibility)**.** *A random variable Y (or distribution) is said to be infinitely divisible if it can be written as a sum of n independent and identically distributed random variables $\{Y_j\}$. That is*

$$Y \sim Y_1 + Y_2 + \cdots + Y_n, \qquad \text{for all } n \geq 2.$$

This implies the distribution of Y_j depends on n not on j. The distribution function $\mathbb{P}$ is infinitely divisible if and only if the CF $\Phi(\cdot)$ is, for every n, the n-th power of some CF $\Phi_n(\cdot)$.

Proposition 2.2.4. *Let X_t be a Lévy process that is sampled at a set of evenly spaced discrete time. For any $n \in \mathbb{N}$,*

$$Y_j = X_{\frac{t_j}{n}} - X_{\frac{t_{j-1}}{n}}$$

and

$$X_t = \sum_{j=1}^{n} Y_j. \tag{2.1}$$

Equation 2.1 implies Y_j is independently and identically distributed because X_t satisfies the independent stationary increments property, then, X_t has an infinitely divisible law. Conversely, given an infinitely divisible distribution $\mathbb{P}$, there exists a Lévy process X_t where the distribution of increments is governed by $\mathbb{P}$ Sato (1999). The normal, gamma, Poisson and α-stable distribution are examples of infinitely divisible distributions. This is known by studying their CFs, see Sato (1999) for details.

2.2.2 Characteristic function

One of the arguments that strengthens the use of CFs is that the CF of a random variable may be known in closed form, particularly for infinitely divisible random variables. As a result of the one-to-one relationship between the CF of a process and the probability density function, once the CF function is known, then the distribution function can be determined by the Fourier inversion (see Section 2.5 for detail). The COS method has shown to be a good method for obtaining densities from CF's.

Definition 2.2.5 (Characteristic function)**.** *Let X be a random variable, then its characteristic function $\Phi : \mathbb{R} \to \mathbb{C}$ is defined as*

$$\Phi_X(\omega) := \mathbb{E}[e^{i\omega \cdot X}], \quad \omega \in \mathbb{R}. \tag{2.2}$$

If the random variable has a probability density, $\mathbf{f}_X(x)$, then the CF is the Fourier transform of $\mathbf{f}_X(x)$. Thus, equation 2.2 becomes

$$\Phi_X(\omega) := \mathbb{E}[e^{i\omega \cdot X}] = \int_{\mathbb{R}} e^{i\omega \cdot X} \mathbf{f}_X(x) dx, \quad \omega \in \mathbb{R}. \tag{2.3}$$

Proposition 2.2.6 (Characteristic exponent)**.** *Let $(X_t)_{t\geq 0}$ be a Lévy process in $\mathbb{R}$ and $\mathbf{f}_X(x)$ be the probability density of X. Then, there exists a continuous function $\varrho : \mathbb{R} \to \mathbb{C}$ known as the characteristic exponent of X such that*

$$\mathbb{E}[e^{i\omega \cdot X_t}] := e^{t\varrho_X(\omega)}, \qquad \omega \in \mathbb{R} \tag{2.4}$$

and

$$\Phi_X(\omega) := \mathbb{E}[e^{i\omega \cdot X_t}] = \int_{\mathbb{R}} e^{i\omega \cdot X_t} \mathbf{f}_X(x) dx, \quad \omega \in \mathbb{R} \tag{2.5}$$

is the characteristic function of X_t. By virtue of equation 2.5,

$$\varrho_{X_t}(0) = 1.$$

The relationship between the moment-generating function $\mathcal{M}(\omega)$ and the CF $\Phi(\omega)$ is given by

$$\mathcal{M}(\omega) = \Phi(-i\omega). \tag{2.6}$$

Proposition 2.2.7 (Properties of Characteristic function)**.** *Let X be a Lévy process in $\mathbb{R}$ and $\Phi_X(\omega)$ denote the CF. The following are properties of CF* Sato (1999)*;*

- *Let X_1 and X_2 be two Lévy processes and $Y = X_1 + X_2$. The CF of $\Phi_Y(\omega)$ is the product of the CF of the two Lévy processes. i.e. $\Phi_Y(\omega) = \Phi_{X_1}(\omega) \cdot \Phi_{X_2}(\omega)$.*
- *Let X_1 and X_2 be two Lévy processes. For any linear function $X_1 = p + X_2 q$, $\Phi_{X_1}(\omega) = e^{ip\omega} \cdot \Phi_{X_2}(q\omega)$.*
- *$\mathbb{E}[e^{i\omega X}]$ always exists since $|e^{i\omega X}|$ is continuous and bounded by $1\ \forall\ \omega$.*
- *$\overline{\Phi_X(\omega)} = \Phi_X(-\omega)$.*
- *$\Phi_X(0) = 1$, for any distribution.*

Example 2.2.8 (Characteristic function of a normal distribution)**.** The probability density function of a normal distribution is given by

$$\mathbf{f}_X(x) = \frac{1}{\sqrt{2\pi\sigma^2}} e^{\frac{-(x-\mu)^2}{2\sigma^2}},$$

where X is a random variable. Using equation 2.5, the CF is given by

$$\Phi_X(\omega) = \int_{\mathbb{R}} e^{i\omega} \frac{1}{\sqrt{2\pi\sigma^2}} e^{\frac{-(x-\mu)^2}{2\sigma^2}} dx = e^{i\mu\omega - \frac{1}{2}\sigma^2\omega^2}. \tag{2.7}$$

And the characteristic exponent of a normal distribution is given as

$$\varrho(\omega) = \log(e^{i\mu\omega - \frac{\sigma^2\omega^2}{2}}) = i\mu\omega - \frac{\sigma^2\omega^2}{2}.$$

The moments

The derivation of the moments of a distribution from the CF is another crucial tool. The mean, variance, skewness and the kurtosis are the moments we care about in many risk-management applications. Let X be a real-valued random variable with probability distribution $\mathbb{P}$.

- The n-th moment $\mathcal{M}(X^n)$ of the distribution $\mathbb{P}$ is Sato (1999)

$$\mathcal{M} = (i^{-n})\frac{d^n\Phi_X(\omega)}{d\omega^n}\mid_{\omega=0} . \tag{2.8}$$

  Recall the characteristic exponent of X is the logarithm of the CF Φ_X.

- The n-th cumulant, c_n is defined as

$$c_n = (i^{-n})\frac{d^n \ln \Phi_X(\omega)}{d\omega^n}|_{\omega=0}. \tag{2.9}$$

- Mean of X: This can be calculated by setting $n = 1$ in equation (2.9), that is the first cumulant. It is also the expectation of the possible values of X in the distribution Cont and Tankov (2004).

$$\text{Mean} = c_1 = (i^{-1})\frac{d \ln \Phi_X(\omega)}{d\omega}\mid_{\omega=0}= \mathbb{E}[X]. \tag{2.10}$$

- Variance of X: Is the second cumulant, that is, $n = 2$ in equation (2.9). The expectation of the square of the difference between the random variable X and the expectation of X, is also known as the variance of X Cont and Tankov (2004). That is,

$$\text{Var} = c_2 = (i^{-2})\frac{d^2 \ln \Phi_X(\omega)}{d\omega^2}\mid_{\omega=0}= \mathbb{E}[(X - \mathbb{E}(X))^2]. \tag{2.11}$$

- Skewness of X : This measures the level of asymmetry of probability distribution $\mathbb{P}$ of a real-valued random variable X. If the tail on the left side of the probability density function is larger than the tail on the right side and more values lie to the right of the average, this is called negative skewness. If the tail on the right side of the probability density function is larger than the tail on the left side and more values lie to the left of the average, this is called positive skewness. If the size of the right tail is the same as with the left tail, that is, the values are evenly distributed on both sides of the average, this is called undefined skewness, Cont and Tankov (2004). Let $n = 3$ in equation (2.9),

$$c_3 = (i^{-3})\frac{d^3 \ln \Phi_X(\omega)}{d\omega^3}\mid_{\omega=0} . \tag{2.12}$$

  The skewness can be represented as:

$$\text{Skew} = \frac{c_3}{(\sqrt{c_2})^3} = \frac{\mathbb{E}[(X - \mathbb{E}(X))^3]}{(\sqrt{\mathbb{E}[(X - \mathbb{E}(X))^2]})^3} \tag{2.13}$$

- Kurtosis of X : This measures the peakedness of X in $\mathbb{P}$. The fourth cumulant that is, when $n = 4$ in equation (2.9) divided by the square of the second cumulant (variance) in equation (2.11) minus 3 is known as Kurtosis, Cont and Tankov (2004). Let

$$c_4 = (i^{-4})\frac{d^4 \ln \Phi_X(\omega)}{d\omega^4} \mid_{\omega=0}, \tag{2.14}$$

the kurtosis is given by

$$\text{Kurt} = \frac{c_4}{(c_2)^2} - 3 = \frac{\mathbb{E}[(X - \mathbb{E}(X))^4]}{(\mathbb{E}[(X - \mathbb{E}(X))^2])^2} - 3. \tag{2.15}$$

2.2.3 Lévy-Itô Decomposition

As the name implies, Lévy-Itô Decomposition decomposes a Lévy process X as the sum of continuous terms and discontinuous terms. The decomposition is useful since it allows one to compute the CF of any Lévy process with ease. Every Lévy process can be approximated by arbitrary precision of a jump-diffusion process that is, a sum of a compound Poisson process and Brownian motion with drift, possibly more than one, Cont and Tankov (2004). Note that the distribution of every Lévy process is uniquely determined by its characteristic triplet (γ, σ, ν) called Lévy triplet of the process. $\gamma \in \mathbb{R}$ is the drift parameter, $\sigma^2 \geq 0$ is the diffusion parameter and ν is the Lévy measure. The Lévy measure is the expected number of jumps in a given interval per unit time. The pure jump component is characterized by the jumps density, which is called the Lévy density Sato (1999).

Theorem 2.2.9. *Every Lévy process $(X_t)_{t\geq 0}$ on $\mathbb{R}$ can be written as*

$$X_t = \gamma t + \sigma B_t + X_t^l + \lim_{\varepsilon \downarrow 0} \hat{X}_t^{\varepsilon} \tag{2.16}$$

where

- *$(B_t)_{t\geq 0}$ is a Brownian motion.*
- *σ is the diffusion parameter.*
- *γ is the deterministic drift parameter.*
- *ν is a positive measure (Lévy measure) on $\mathbb{R}$ that satisfies:*

$$\int_{\mathbb{R}-\{0\}} (1 \wedge |x|^2)\nu(dx) < \infty. \tag{2.17}$$

  Equation 2.17 implies this measure has no mass at the origin, but infinitely many jumps can occur around the origin. Thus, the measure must be a squared integrable around the origin.

- *From equation (2.16), $\gamma t + \sigma B_t$ is a continuous Gaussian function and every Gaussian Lévy process is continuous. Thus, these are the continuous terms.*

- $X_t^l + \lim_{\varepsilon \downarrow 0} \hat{X}_t^\varepsilon$ *is the discontinuous part of equation* (2.16).
- $$\Delta X^l = |\Delta X| \geq 1 \quad \textit{and} \quad X_t^l = \sum_{0 \leq s \leq t} \Delta X_s^l,$$

  where ΔX *is the jump size,* ΔX^l *describes large jumps with an absolute size greater than* 1*, and* X_t^l *is the sum of a finite number of jumps in the time interval of* $0 \leq s \leq t$.
- $$\Delta X^\varepsilon = \varepsilon \leq |\Delta X| < 1 \quad \textit{and} \quad \hat{X}_t^\varepsilon = \sum_{0 \leq s \leq t} \Delta X_s^\varepsilon. \tag{2.18}$$

  $\hat{X}_t^\varepsilon$ *is the sum of a possibly infinite number of small jumps in the limit* $\varepsilon \downarrow 0$ *in the time interval of* $0 \leq s \leq t$*. In a situation where* $\varepsilon \downarrow 0$*, the process can have infinitely many small jumps, therefore* X_t^ε *may not converge. Thus, the infinite arrival rate of small jumps at zero exists.*

The case where the Lévy process X_t is of finite variation is a crucial condition for simplifying a Lévy-Itô Decomposition. For the proof of Theorem 2.2.9, see Sato (1999) and Cont and Tankov (2004).

2.2.4 Lévy-Khinchine Representation

The CF of a Lévy process is easily derived with the aid of the Lévy-Khinchine Representation, once the result of the Lévy-Itô Decomposition is available. This plays a crucial role in option pricing for it forms the basis for using Fourier methods. Recall the expression for Lévy-Khinchine representation:

$$\Phi_X(\omega) = \mathbb{E}[e^{i\omega \cdot X_t}] = e^{t\varrho_X(\omega)}, \quad \omega \in \mathbb{R} \tag{2.19}$$

with

$$\varrho_X(\omega) = -\frac{1}{2}\omega^2\sigma^2 + i\gamma\omega + \int_{\mathbb{R}} (e^{i\omega x} - 1 - i\omega \cdot x\mathbb{I}_{|x|\leq 1})\nu(dx), \tag{2.20}$$

where (γ, σ, ν) is the characteristic triplet of a Lévy process X_t with respect to the truncating function, $\varrho_X(\omega)$ is the characteristic or Lévy exponent, $\sigma^2 \geq 0$, $\gamma \in \mathbb{R}$ and ν is a positive measure on $\mathbb{R}$ such that $\int_{\mathbb{R}-\{0\}}(1 \wedge |x|^2)\nu(dx) < \infty$. For detail, see Theorem 8.1 in Sato (1999).

2.3 Models driven by exponential Lévy processes

In this section, we present some models driven by the exponential Lévy model. i.e, BS model, NIG model and VG model. These models are selected due to their empirical behaviour. We pay less attention to the density function and concentrate more on the CF of the distribution because the Fourier pricing formula mostly depend on the CF of the distribution and not the density function. We will compute the moments of the distribution, i.e, mean, variance, skewness and the kurtosis, and also discuss the

numerical behaviour of CF of the distribution of these exponential Lévy models. We continue by presenting the dynamics of the underlying stock price under exponential Lévy models.

Assume a market consisting of one risk-less asset (the bond) with a price process given by $\mathbf{B}_t = e^{rt}$, where r is the compound interest rate, and one risky asset (the stock), where the stock-price process $(S_t)_{t\in\mathbb{R}}$ is assumed to have the form:

$$S_t := S_0 e^{X_t} \tag{2.21}$$

and $(X_t)_{t\geq 0}$ is a stochastic process that satisfies some integrability condition (see Section 2.5).

2.3.1 Black-Scholes model as a continuous exponential Lévy model

The BS model is one of the most popular and famous pricing models in finance. This was pioneered by Black and Scholes (1973). The BS model is the only exponential Lévy model with a pure continuous sample path and the model is completely driven by Brownian motion that is normally distributed. Thus, the CF of the log-asset price is based on equation 2.7. This model is based on some assumptions: The interest rate and the volatility are functions of time which are fixed; no dividend is paid during the life of the option; trading can be done on any number of underlying assets; the transaction cost of hedging a portfolio is nothing; all risk-free portfolios must have the same return; the market is continuous which is not feasible in real-world markets because there are trading hours of stock exchanges. Let S be a function of t such that

$$\frac{\Delta S}{S} \tag{2.22}$$

is the relative change of the underlying asset price at small time-step Δt. Due to the instantaneous response of the market to new information about an underlying asset price, the change in the asset price from $t \to t + \Delta t$ is $S \to S + \Delta S$. Recall that a market is made up of risk-free and risky assets. Thus, the relative change in an underlying asset price, equation 2.22, is a combination of two different equations:

- The first part involves the underlying asset that would yield return with certainty (has no risk). For example, money kept in a bank account. The parameter μ (drift) is the average rate of growth of the underlying asset price. It is always fixed:
$$\mu\Delta t.$$
- The second part involves the random change in the price of the underlying asset by external factors. The parameter σ (volatility) often denotes the level of uncertainty in the model and ΔB is a sample from the normal distribution with the mean equals to zero and the variance equal to Δt:
$$\sigma\Delta B.$$

Thus, equation 2.22 can be written as

$$\frac{\Delta S}{S} = \mu \Delta t + \sigma \Delta B. \tag{2.23}$$

ΔB can be written as $B\sqrt{\Delta t}$ where B is a standard normal distribution with mean zero and variance 1. Thus, $\Delta B^2 \to \Delta t$ as $\Delta t \to 0$.

We can now use the Itô lemma on the asset's price (equation 2.23) and some assumptions based on the portfolio-hedging strategy to derive the Black-Scholes PDE equation:

$$\frac{\partial V(S_t,t)}{\partial t} + rS\frac{\partial V(S_t,t)}{\partial S} + \frac{1}{2}\sigma^2 S^2 \frac{\partial^2 V(S_t,t)}{\partial S^2} - rV(S_t,t) = 0. \tag{2.24}$$

For detail on the derivation of the Black-Scholes PDE, see Hull (2007). Equation 2.24 may have many solutions depending on the terminal condition. $V(S_t,t)$ can be a call or put option. For a European call and put option, the terminal conditions are given by the payoff function;

$$\Psi_c := (S_T - K)^+ \qquad \Psi_p := (K - S_T)^+.$$

The Black-Scholes partial differential equation for early exercise options (Bermudan and American options) does not satisfy the earlier proposed assumptions because there exists no arbitrage argument for Bermudan options unlike European options. Thus, arbitrage opportunities can occur. The equality condition in equation 2.24 is now inequality:

$$\frac{\partial V(S_t,t)}{\partial t} + rS\frac{\partial V(S_t,t)}{\partial S} + \frac{1}{2}\sigma^2 S^2 \frac{\partial^2 V(S_t,t)}{\partial S^2} - rV(S_t,t) \leq 0. \tag{2.25}$$

2.3.2 Normal inverse Gaussian as an infinite exponential Lévy model

The normal inverse Gaussian process was firstly introduced and proposed for modelling financial data by Barndorff-Nielsen (1997). Since then, this model has been widely studied in much literature for modelling the returns of asset prices and pricing of options under different frameworks, Rydberg (1997), Eberlein and Prause (2000), Webber and Ribeiro (2003), Kéllezi and Webber (2004), H.Albrecher and Predota (2004). The NIG is an infinitely divisible process with stationary independent increments, and an infinite variation process with stable-like small jumps. This model is a variance-mean mixture representation of the normal inverse Gaussian distribution with the inverse Gaussian as the mixing distribution. As a result of the mixture representation of the NIG distribution, we find that the NIG Lévy process X_t may be represented via a time change of Brownian motion as

$$X_t := X(t,\alpha,\beta,\delta) = \mu t + B_{L_t},$$

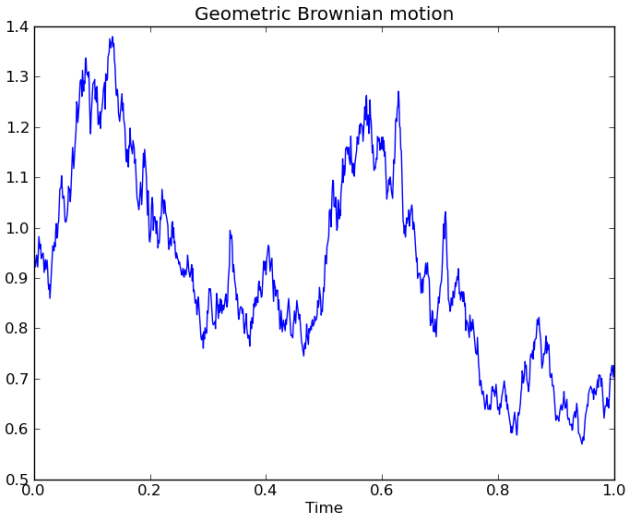

Figure 2.1: Sample path of a stock driven by geometric Brownian motion. Parameters used: $T = 1$, $r = 0.02$, and $\sigma = 0.7$.

where L_t is the inverse Gaussian Lévy process with a scaling parameter δ and $\sqrt{\alpha^2 - \beta^2}$, for α is the steepness parameter and β is the drift parameter, and B_t is the Brownian motion with the drift parameter and diffusion coefficient 1, and $\mu \in \mathbb{R}$ Barndorff-Nielsen (1997). This implies NIG is a time-changed Brownian motion and the time change t may be chosen as an inverse Gaussian process independent of the directing Brownian motion Geman (2002). The Lévy measure can be written as

$$\nu_{NIG} = \exp(\beta x)\frac{\delta\alpha}{\pi|x|}\mathcal{K}_1(\alpha|x|)dx \tag{2.26}$$

where $\alpha > 0$, $-\alpha < \beta < \alpha$, $\delta > 0$ and $\mathcal{K}_\rho(x)$ is the modified Bessel function of the third kind with index ρ Schoutens (2003). The NIG is described by the characteristic triplet $(\gamma, 0, \nu)$, where

$$\gamma = \frac{2\gamma\alpha}{\pi}\int_0^1 \sin h(\beta x)\mathcal{K}_1(\alpha x)dx,$$

$\sigma = 0$ and ν is given by equation 2.26. $\sigma = 0$ implies NIG has no Brownian component. Thus, the process is a pure jump process.

2.3.3 Variance-gamma model as an infinite exponential Lévy model

The variance-gamma process was introduced and firstly proposed to model the dynamics of an underlying asset price by Carr and Madan. (1998). In their paper, they describe the risk-neutral dynamics of asset prices driven by the VG process, and also derive a closed-form formula for the return density and for pricing European options. Afterwards, this model has been investigated and applied to price different types of

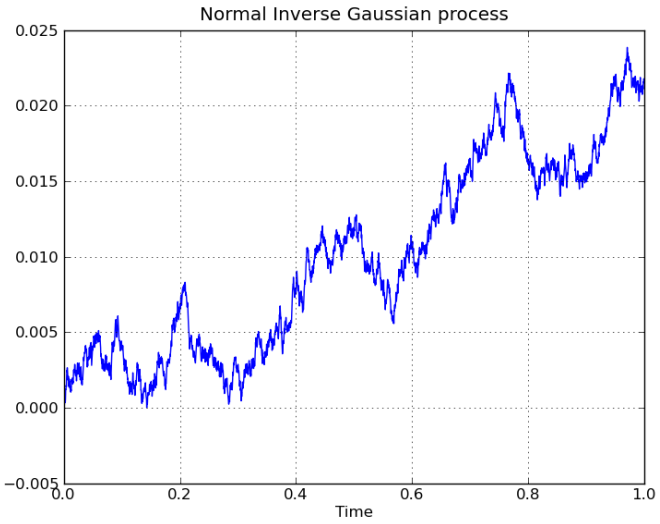

Figure 2.2: Sample path of Normal inverse Gaussian process: Parameters used: $T = 1$, $\sigma = 0$, $\theta = 4$ and $\alpha = 0.05$.

options by several authors: Madan and Seneta (1990), Carr *et al.* (2002), Hirsa and Madan (2004), F.Hubalek *et al.* (2006), Almendral and Oosterlee (2007).

The VG model is a three-parameter stochastic process that models the dynamics of the logarithm of an underlying asset price. θ is the drift term, σ is the volatility and κ is the variance rate. The VG process is obtained by evaluating Brownian motion with constant drift and volatility at a random time change given by the gamma process, that is, replacing the time in Brownian motion with gamma process Madan and Seneta (1990). Thus, the VG model is characterised with discontinuous sample path. Let

$$\beta(t; \theta, \sigma) = \theta t + \sigma B_t$$

be a Brownian motion with drift θ, volatility σ and a standard Brownian motion B_t. Also, there exists a process of independent gamma increments over non-overlapping intervals of time $(t, t + h)$, that is, a gamma process $\gamma(t; \mu, \kappa)$ with mean rate μ and variance rate κ, Carr and Madan. (1998). Besides the volatility and the drift of the time-changed Brownian motion, there exists an additional parameter in this model that controls kurtosis and skewness. The θ controls the skewness while the κ controls the kurtosis. This is the variance of the gamma-distributed time. Under the *VG* process, the unit period continuously-compound return is normally distributed, conditional on the realisation of a random time that has a gamma density. The VG process $X(t; \theta, \sigma, \kappa)$ in terms of the Brownian motion, with drift $\beta(t; \theta, \sigma)$ and gamma process with unit mean rate $\gamma(t; 1, \kappa,)$ can be written as Carr and Madan. (1998);

$$X(t; \theta, \sigma, \kappa) = \beta(\gamma(t, 1, \kappa), \theta, \sigma).$$

The VG process has no Brownian motion and it can be written as the difference of two independent gamma processes. With these properties, the Lévy density can be

expressed as

$$\nu_{VG}(dx) = \begin{cases} \frac{C\exp(G|x|)}{|x|}dx & \text{for } x < 0, \\ \frac{C\exp(-M|x|)}{|x|}dx & \text{for } x > 0 \end{cases}$$

where

$$C = \frac{1}{\kappa},$$
$$G = \left(\sqrt{\frac{\theta^2\kappa^2}{4} + \frac{\sigma^2\kappa}{2}} - \frac{\theta\kappa}{2}\right)^{-1},$$
$$M = \left(\sqrt{\frac{\theta^2\kappa^2}{4} + \frac{\sigma^2\kappa}{2}} + \frac{\theta\kappa}{2}\right)^{-1}.$$

The Lévy triplet of the VG model is given by $(\gamma, 0, \nu_{VG}(dx))$ where

$$\gamma = \frac{-C(G\exp(-M) - 1) - M(\exp(-G) - 1)}{MG}.$$

The drift parameter θ measures the directional premium since it affects the skewness of the process Carl *et al.* (2003). The parameter $C = \frac{1}{\kappa}$ controls the overall activity rate of the process while $\kappa = \frac{1}{C}$ controls the kurtosis of the model. The parameters G and M control the rate at which arrival rate reduces with the size of the move. The smaller the value of κ, the more the sample path of the VG model resemble the sample path of a typical stock-price. When $\theta > 0$, then $G > M$ and this results in a positive skewness in the distribution of the VG model. The reverse holds when $\theta < 0$. When $\theta = 0$, then $G = M$ and this makes the distribution of the VG process to be symmetric.

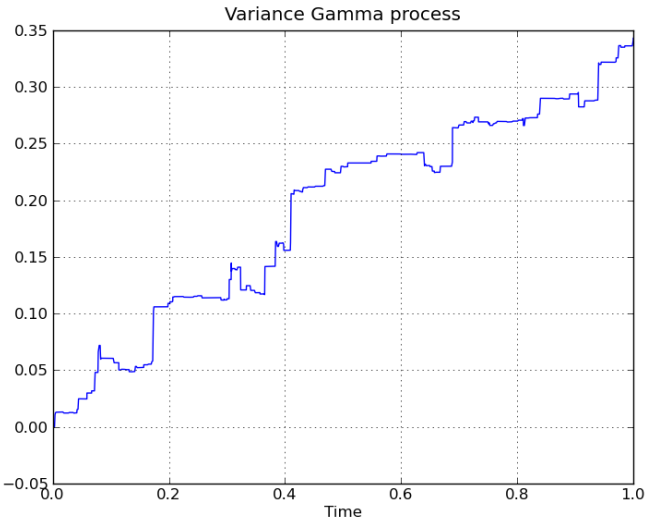

Figure 2.3: Sample path of a Variance Gamma process on a fixed grid. Parameters used: $T = 1$, $\sigma = 0.3$, $\theta = 4$ and $\kappa = 0.05$.

The direct computation of CF of the log-asset price of the NIG model and the VG model is not trivial. The use of a subordinator makes the computation of these CFs possible. This is as a result of the conditional Gaussian structure of the normal inverse process and the variance-gamma process which also simplifies computations and simulations significantly. A subordinator $(S_t)_{t\geq 0}$ is almost surely a non-decreasing Lévy process such as *time*, (a sequence with non-negative increments). Thus, a negative jump does not exist. The Lévy triplet can be expressed as $(\gamma_s, \sigma_s, \nu_s)$ where $\sigma_s = 0$. That is, S_t has no diffusion parameter. S_t has a positive drift and jump of finite variation. The increasing nature of a subordinator qualifies it to be represented as a time indicator. The transformation of an old Lévy process into a new Lévy process with the new characteristic triplet given in terms of the old Lévy process, is termed *Subordination*, Cont and Tankov (2004) and this is illustrated by Theorem 2.3.1.

Theorem 2.3.1 (Subordination of Lévy processes)**.** *Let $(X_t)_{t\geq 0}$ be a Lévy process on $\mathbb{R}$ with the Lévy triplet (γ, σ, ν) and its CF $\Phi_X(\omega)$ and characteristic exponent $\psi_X(\omega)$ as given in equations (2.19) and (2.20). Let $(S_t)_{t\geq 0}$ be a subordinator with triplet $(\gamma_s, 0, \nu_s)$ and Laplace exponent $\mathcal{L}_s(\omega)$. We assume $(X_t)_{t\geq 0}$ and $(S_t)_{t\geq 0}$ are independent. Let $(Y_t)_{t\geq 0}$ be a stochastic process by random time changing the old Lévy process $(X_t)_{t\geq 0}$ such that;*

$$Y_t = X_{S_t}$$

is a Lévy process and its CF $\Phi_Y(\omega)$ is given by;

$$\Phi_Y(\omega) = \mathbb{E}[e^{i\omega Y_t}] = e^{t\mathcal{L}_s(\psi_X(\omega))} \tag{2.27}$$

Thus, the CF of Y_t is derived by substituting the characteristic exponent $\psi_X(\omega)$ of the old Lévy process into the Laplace exponent of the subordinator $\mathcal{L}_s(\omega)$. The characteristic triplet of Y_t, $(\gamma_y, \sigma_y, \nu_y)$ is given by

$$\begin{aligned}\gamma_y &= \gamma_s\gamma + \int_0^\infty \nu_s(ds)\int 1_{|x|\leq 1} x\mathbb{P}_t^x(dx),\\ \sigma_y^2 &= {\gamma_s}^2\sigma^2,\\ \nu^y(dx) &= \gamma_s\nu(dx) + \int_0^\infty \mathbb{P}_t^x(dx)\nu_s(ds),\end{aligned}$$

where $\mathbb{P}_t^x$ is the probability distribution of X_t. $(Y_t)_{t\geq 0}$ is said to be subordinate to the process $(X_t)_{t\geq 0}$ Cont and Tankov (2004).

For more information on the types of subordination, see Appendix A.1.1. Sato (1999) give a detailed proof of Theorem 2.3.1 and Cont and Tankov (2004) give an outline of discussion of the theorem.

Below are the CF's of the BS, NIG and VG models[1] Barndorff-Nielsen (1997), Madan and Seneta (1990).

BS model	$\Phi(\omega,t) = \exp(i\omega\mu t - \frac{1}{2}\sigma^2\omega^2 t)$
NIG model	$\Phi(\omega,t) = \exp(i\omega\mu t - \frac{1}{2}\sigma^2\omega^2 t)\cdot \varrho_{NIG}(\omega;t;\alpha,\beta,\delta)$ $\varrho_{NIG}(\omega,t,\alpha,\beta,\delta) = \exp[\delta t(\sqrt{\alpha^2-\beta^2}) - (\sqrt{\alpha^2-(\beta+i\omega)^2})]$
VG model	$\Phi(\omega,t) = \exp(i\mu\omega t)\cdot \varrho_{VG}(\omega;t;\omega,\kappa,\theta)$ $\varrho_{VG}(\omega;t;\theta,\kappa) = (1 - i\omega\theta\kappa + \frac{1}{2}\sigma^2\kappa\omega^2)^{-\frac{t}{\kappa}}$

Table 2.1: The characteristic functions of the log-asset price of the BS, NIG and VG models, where ϱ_{NIG} and ϱ_{VG} are the characteristic exponents.

Knowing the CFs of the BS, NIG and VG models, we can easily compute their cumulants using equation 2.9. Table 2.2 presents the cumulants of these models.

BS model	NIG model	VG model
$c_1 = (r - \frac{1}{2}\sigma^2)t$	$c_1 = (r - \frac{1}{2}\sigma^2 + \mathbf{w})t + \delta t\beta(\alpha^2-\beta^2)^{-1/2}$	$c_1 = (\mu+\theta)t$
$c_2 = \sigma^2 t$	$c_2 = \delta t\alpha^2(\alpha^2-\beta^2)^{-3/2}$	$c_2 = (\sigma^2 + \kappa\theta^2)t$
$c_3 = 0$	$c_3 = 3\delta t\alpha^2\beta(\alpha^2-\beta^2)^{-5/2}$	$c_3 = 3(\sigma^2\theta\kappa + 2\theta^3\kappa^2)t$
$c_4 = 0$	$c_4 = 3\delta t\alpha^2(\alpha^2+4\beta^2)(\alpha^2-\beta^2)^{-7/2}$	$c_4 = 3(\sigma^4\kappa + 2\theta^4\kappa^3 + 4\sigma^2\theta^2\kappa^2)t$
	$\mathbf{w} = \delta(\sqrt{\alpha^2-\beta^2}) - (\sqrt{\alpha^2-(\beta+i\omega)^2})$	$\mathbf{w} = \frac{1}{\kappa}\ln(1-\theta\kappa-\frac{\sigma^2\kappa}{2})$

Table 2.2: The cumulants of the log-asset price of the BS, NIG and VG models, where $\mathbf{w}$ is the drift correlation term which satisfies $e^{-\mathbf{w}t} = \Phi(-i,t)$.

[1] μ is the drift in BS and NIG models, σ is the volatility, t is the time to maturity, $\alpha = \frac{\mu}{\sigma^2}$ and $\beta = \frac{\sqrt{\mu^2+2\frac{\sigma^2}{\mu}}}{\sigma^2}$, δ is the scaling factor in NIG , κ is the variance in VG and θ is the drift in the VG.

2.3.4 Complex discontinuities in characteristic functions

In financial modelling, CFs of the log-asset price of many option pricing distributions involve multivalued functions. These functions may introduce discontinuities into the CFs of the distributions of financial models, which leads to incorrect option prices, especially if the options are priced by Fourier inversion methods Lord (2008). An alternative to avoid discontinuity is to integrate the system of ODEs that evolves under the risk-neutral measure of the underlying asset of the model by numerical methods, as this will result in a continuous solution Lord and Kahl (2010).

From a computational perspective, Fourier methods are advantageous. Therefore, it is worthwhile to investigate how to do away with discontinuity in the solution. Recall the log of a complex variable $z = x+iy = re^{i(\arg(z)+2\pi n)}$ with $\arg(z) \in [-\pi, \pi)$, $n \in \mathbb{Z}$, and $r \in \mathbb{R}$ can be expressed as

$$\log z = \log r + i(\arg(z) + 2\pi n), \quad \text{where } r \text{ is the radius.} \tag{2.28}$$

If we restrict the $\log z$ to its principal branch, that is, setting $arg(z)$ to be the principal argument, $\arg(z) \in [-\pi, \pi)$, and $n = 0$, then the branch cut of the complex log is $(-\infty, 0]$ and the complex log is discontinuous along it, Kahl and Jäckel (2005). Thus restricting $\log z$ to its principal branch yield discontinuities in the CF. Hence, we have wrong option prices if we use the discontinuous CF. The restriction on $\arg(z) \in [0, \pi)$ implies we cut the complex plane along the negative real axis.

In a popular model of asset-price dynamics known as the Heston model, the log of complex arguments in the CF gives rise to numerical instability, and as a result of this, most implementations in the Heston model are not robust for long dated options, Kahl and Jäckel (2005). To show that exponential Lévy models may have complex discontinuities, we illustrate the effect of the principal branch on the NIG and VG models.

Example 2.3.2 (Variance-gamma model)**.** Let the expression for an underlying asset modelled by the VG process be given by

$$S_t = P_t \exp(\mathbf{w}t + \theta\mathcal{G}_t + \sigma B_{\mathcal{G}_t}) \tag{2.29}$$

where B_t is a standard Brownian motion, $\mathcal{G}_t$ is the gamma process with the variance rate $\nu > 0$, P_t is the forward price of S_t, $\sigma > 0$ and the parameter $\mathbf{w}$ (see Table 2.2) is chosen so that the expectation of the exponential part of equation 2.29 is a unit. For simplicity, let $p_t = \ln P_t$ and $\hat{p}_t = p_t + \mathbf{w}t$. Recall the conditional CF of the distribution of log-asset returns under the VG model

$$\Phi_{VG} = \frac{\exp(i\omega\hat{p}_t)}{(1 - i\omega\theta\kappa + \frac{1}{2}\sigma^2\kappa\omega^2)^{\frac{t}{\kappa}}}. \tag{2.30}$$

The ς^{th} moment of the underlying asset exists as long as the minimum ς_- and the maximum ς_+ is defined by

$$\varsigma_\pm = -\frac{\theta}{\sigma^2} \pm \sqrt{\frac{\theta^2}{\sigma^4} + \frac{2}{\nu\sigma^2}}$$

so that the extended CF in equation 2.30 is well-defined for $\omega \in \wedge_x$ which is defined by $\{\omega \in \mathbb{C}| - \mathcal{I}(\omega) \in (\varsigma_-, \varsigma_+)\}$. The bounded maximum and minimum moments does not depend on the maturity time T since the VG model is completely time-homogeneous. The multivalued function is present in

$$(1 - i\omega\theta\kappa + \frac{1}{2}\sigma^2\kappa\omega^2). \tag{2.31}$$

If we restrict the multivalued function to its principal branch, the CF of the distribution of the VG model will only be continuous if $(1 - i\omega\theta\kappa + \frac{1}{2}\sigma^2\kappa\omega^2)$ does not cross the negative real line. To satisfy this condition, the imaginary part of $(1 - i\omega\theta\kappa + \frac{1}{2}\sigma^2\kappa\omega^2)$ must be positive. This can only occur when $\omega = x + iy$, with $x = 0$ or $y = \frac{\theta}{\sigma^2}$. Then

$$1 - i\omega\theta\kappa + \frac{1}{2}\sigma^2\kappa\omega^2 = 1 - ix\theta\kappa + \theta\kappa y + \frac{1}{2}\sigma^2\kappa x^2 + \frac{1}{2}\sigma^2\kappa \cdot 2ixy - \frac{1}{2}\sigma^2\kappa y^2. \tag{2.32}$$

For $x = 0$, equation 2.32 becomes

$$1 - ix\theta\kappa + \theta\kappa y + \frac{1}{2}\sigma^2\kappa x^2 + \frac{1}{2}\sigma^2\kappa \cdot 2ixy - \frac{1}{2}\sigma^2\kappa y^2 = 1 + \theta\kappa y - \frac{1}{2}\sigma^2\kappa y^2, \quad \textit{for } \theta > 0. \tag{2.33}$$

For $y = \frac{\theta}{\sigma^2}$,

$$1 - ix\theta\kappa + \theta\kappa y + \frac{1}{2}\sigma^2\kappa x^2 + \frac{1}{2}\sigma^2\kappa \cdot 2ixy - \frac{1}{2}\sigma^2\kappa y^2 = 1 + \frac{\kappa\theta^2}{2\sigma} + \frac{1}{2}\sigma^2\kappa x^2 \geqslant 1, \quad \textit{for } \kappa, \theta > 0 \tag{2.34}$$

so that $(1 - i\omega\theta\kappa + \frac{1}{2}\sigma^2\kappa\omega^2)$ can never be negative. Now, we can say the principal branch of the complex power function is the right one, as this is the only one that gives real values for equation 2.31. Thus, the CF of the distribution of the VG model is continuous when the complex log is restricted to the principal branch despite the presence of the multi-valued function in the CF. Thus, the principal branch of a multivalued function works well for the VG model Lord and Kahl (2010).

2.4 Risk-neutral valuation formula

Pricing financial instruments is a subject which lies at the heart of Financial Mathematics. When valuing financial instruments, a risk-neutral framework must be used to avoid arbitrage opportunities. An arbitrage opportunity is a self-financing portfolio which admits a terminal gain, without any probability of intermediate or terminal loss. In order to price options in our models, the model must satisfy the fundamental theorems of asset pricing. *The First Fundamental Theorem of Asset Pricing* relates the notion of the existence of equivalent martingale measures (EMM) to an arbitrage-free opportunity, and *The Second Fundamental Theorem of Asset Pricing* relates the notion of uniqueness of the EMM to market completeness, Harrison and Pliska (1981).

The popularly known option pricing theory of the BS model depends on the fact that the payoff of every contingent claim can be replicated by a self-financing

portfolio. In other words, the risk of holding or selling an option can be completely replicated against it. Thus, the market is arbitrage-free. In such model, there exists a unique measure $\mathcal{Q}$ (risk neutral-measure) which is equivalent to the " real world measure " $\mathbf{P}$, and this makes the discounted price process a martingale:

$$S_s^* = \mathbb{E}^{\mathcal{Q}}[S_t^* | \mathbb{F}_s],$$

where

$$S_t^* = S_t e^{-rt}, \quad \text{for} \quad 0 \leq s < t \leq T.$$

Recall the expression for the underlying asset price from equation 2.21,

$$S_t = S_0 e^{X_t}$$

where X_t is a Lévy process under the real world measure $\mathbf{P}$.

A financial market is risk-neutral whenever the expected return of investment on the underlying asset is the same as the riskless rate of interest. Studying the Black-Scholes PDE, equation 2.24, the function depends on the underlying asset price S and time t, not on the investor's preferences. And the relevant parameters needed for the valuation of the options are the risk-free rate of interest r and the volatility σ, not the drift term μ. This leads to the work of Cox and Ross (1976) who developed a technique known as the *risk-neutral valuation technique* . This technique is based on the assumption that under option pricing, investors are indifferent to risk. i.e, the world is risk-neutral.
For a stock-price driven by the NIG model and the VIG model, there are many equivalent measures under which the discounted asset-price process is a martingale because the noise process has jumps of random sizes. A market built on a Lévy process cannot be replicated by a suitable portfolio. Instead, an additional condition must be used to select the appropriate martingale measure from the multiple equivalent martingale measure (EMM). Thus, financial markets driven by Lévy processes are incomplete, and the EMM is not unique. Only Lévy markets that are built on pure Brownian motion (BS model) or Poisson process are complete, Cont and Tankov (2004). To select the appropriate EMM under exponential Lévy models, six measures have been proposed in literature; the minimal martingale measure, Föllmer and Schweizer (1991), the Esscher martingale measure, Gerber and Shiu (1994), H.Bühlmann *et al.* (1996), the minimal entropy martingale measure, Miyahara (1999), the variance optimal martingale measure, Schweizer (1995), the mean correcting martingale measure and the utility martingale measure. Here, we discuss Boyarchenko and Levendorskii (2002) universal approach called the *EMM-condition* based on the Esscher martingale measure. Since X_t is a Lévy process, using the characteristic exponent of a Lévy process, $\varrho(\cdot)$,

$$S_0 = S_0 e^{-t(r+\varrho^{\mathcal{Q}}(-i))}$$

for

$$\varrho^{\mathcal{Q}}(0) = 0$$

and

$$r + \varrho^{\mathcal{Q}}(-i) = 0 \tag{2.35}$$

is called the EMM-condition. Using the Esscher transform, (see Miyahara (2002)) in terms of the characteristic exponent,

$$\varrho^{\mathcal{Q}}(\omega) = \varrho^{\mathbf{P}}(\omega - i\varsigma) - \varrho^{\mathbf{P}}(-i\varsigma) \tag{2.36}$$

where ς is real, $i = \sqrt{-1}$ and the EMM-condition becomes

$$r + \varrho^{\mathbf{P}}(\omega - i\varsigma) - \varrho^{\mathbf{P}}(-i\varsigma) = 0. \tag{2.37}$$

Thus,

$$S_t^* = S_0 e^{-t(r+\varrho^{\mathbf{P}}(\omega-i\varsigma)-\varrho^{\mathbf{P}}(-i\varsigma))}, \quad \text{and} \quad \mathcal{Q} \sim \mathbf{P}.$$

In Lévy models, we assume under the real-world measure $\mathbf{P}$, the existence of some equivalent martingale measure $\mathcal{Q}$ such that the discounted asset price process is a martingale. In the VG model, the three main parameters σ (volatility), ν (variance) and θ (drift), are also chosen to be risk-neutral. The unique pricing formula of a contingent claim is the expectation under the martingale measure of the discounted payoff at the maturity date.

Given the payoff function $\Psi(S_T)$ for a European option, the existence of an equivalent martingale measure $\mathcal{Q}$, not necessarily unique, in an arbitrage-free market, leads to the risk-neutral pricing formula $V(t_0, S_0)$ at time t_0 where $\Delta t = T - t_0$ such that

$$V(S_0, t_0) := e^{-r\Delta t}\mathbb{E}^{\mathcal{Q}}[\Psi(S_T)|\mathbb{F}_0] \tag{2.38}$$

where S_T is an adapted stochastic process, r is the risk-free rate of return and $\mathbb{F}_0(\mathbb{F}_0 = 0)$ is the filtration generated at time t by the risk-neutral distribution $\mathcal{Q}$. This expectation makes it possible to value the equation 2.38 by the means of the Monte Carlo methods. Since equation 2.38 is an expectation, we represent equation 2.38 as

$$V(x, t_0) := e^{-r\Delta t}\int_{-\infty}^{\infty} \Psi(y)\mathbf{f}(y|x; \Delta t)dy \tag{2.39}$$

and $\mathbf{f}(y|x; \Delta t)$ is the conditional probability density function representing the transition of x at time t_0 to y at time T where x and y are any monotonic functions of the underlying asset's price. For more information see Harrison and Pliska (1981).

By means of the risk-neutral pricing formula, the price of any option except for early exercise options can be written as an expectation of the product of the discounted payoff of the option price and the risk-neutral density function. Recall that the probability density function of most Lévy processes is not available in a closed form but can be calculated from the CF by the Fourier inversion method. This leads us to study some basic concepts of Fourier methods.

2.5 Some fundamentals of Fourier methods

Here, we present some mathematical properties of the Fourier methods that are useful to our discussion. For detailed study on Fourier methods in finance, see Cherubini *et al.* (2010), and for general books in literature on Fourier methods, see Brigham (1974), Boyd (2000), Press *et al.* (2007).

A function $\mathbf{f}(t)$ in the space domain can be transformed to a function $\hat{\mathbf{f}}(\omega)$ in the frequency domain,

$$\hat{\mathbf{f}}(\omega) := \mathcal{F}[\mathbf{f}(t)](\omega) = \int_{\mathbb{R}} e^{i\omega t}\mathbf{f}(t)dt. \tag{2.40}$$

The inverse Fourier transform which allows us to determine the function $\mathbf{f}(\mathbf{t})$ from its Fourier transform, is defined as

$$\mathbf{f}(t) := \mathcal{F}^{-1}[\hat{\mathbf{f}}(\omega)](t) = \frac{1}{2\pi}\int_{\mathbb{R}} e^{-i\omega t}\hat{\mathbf{f}}(\omega)d\omega, \quad \omega \in \mathbb{R}. \tag{2.41}$$

In general, the Fourier transform $\hat{\mathbf{f}}(\omega)$ is a complex quantity, $\hat{\mathbf{f}}(\omega) = \mathcal{R}(\omega) + i\mathcal{I}(\omega)$. As stated earlier, the characteristic function Φ_X is the Fourier transform of the density function. Thus:

$$\Phi_X(\omega) := \int_{\mathbb{R}} e^{i\omega t}\mathbf{f}_X(t)dt \quad \text{and} \quad \mathbf{f}_X(t) := \frac{1}{2\pi}\int_{\mathbb{R}} e^{-i\omega t}\Phi_X(\omega)d\omega. \tag{2.42}$$

To evaluate the risk-neutral integral in equation 2.38, we need the payoff function and the density function of the model. Since we know the CF of the distribution of our models, we can use the inverse integral in equation 2.42 to obtain the density function using numerical methods. This is made possible by the inversion method.

Remark 2.5.1. A sufficient condition for the existence of the Fourier transform of g and its inverse is that the function $g(x)$ is a piecewise continuous real function over $(-\infty, \infty)$ that is square integrable, i.e. satisfies

$$\int_{-\infty}^{\infty} |g(x)|^2 dx < \infty. \tag{2.43}$$

Theorem 2.5.2 (Convolution Theorem)**.** *Let* $\mathbf{f}$ *and* $\mathbf{g}$ *be two piecewise continuous functions, that is, square integrable such that* $\hat{\mathbf{f}}(\omega)$ *and* $\hat{\mathbf{g}}(\omega)$ *are the Fourier transform of* $\mathbf{f}$ *and* $\mathbf{g}$*. The convolution* $\mathbf{f} * \mathbf{g}$ *is given by*

$$[\mathbf{f} * \mathbf{g}] = \int_{-\infty}^{\infty} \mathbf{f}(t-y)\mathbf{g}(y)dy = \int_{-\infty}^{\infty} \mathbf{f}(y)\mathbf{g}(t-y)dy,$$

and

$$\mathcal{F}[\mathbf{f} * \mathbf{g}] = \hat{\mathbf{f}}(\omega)\hat{\mathbf{g}}(\omega). \tag{2.44}$$

The method we will discuss in Section 3.2 and 3.3 wholly depends on equation 2.44.

Theorem 2.5.3 (Parseval Identity)**.** *The product of two square integrable function* $\mathbf{f}$ *and* $\mathbf{g}$ *can be directly expressed as the product of their respective Fourier transforms such as*

$$\int_{-\infty}^{\infty} \mathbf{f}(t)\mathbf{g}(t)dt = \frac{1}{2\pi}\int_{-\infty}^{\infty} \hat{\mathbf{f}}(\omega)\hat{\mathbf{g}}(-\omega)d\omega. \tag{2.45}$$

The latter part of equation 2.44 and 2.45 can represent the risk-neutral valuation formula, where $\hat{\mathbf{f}}$ refers to the Fourier transform of the density function of the underlying process and $\hat{\mathbf{g}}$ the Fourier transform of the discounted payoff. Instead of integrating the product of the density function and the discounted payoff over an infinite interval, we can represent the transform integral of the option price as contour integral in the complex plane. This can be done by the help of the Parseval identity by shifting the contour and applying the Residual Calculus M.Schmelzle (2010). In equation 2.45, we set the imaginary part on the complex plane to zero because option prices are always real. It is important to note that the payoff of a call option is an unbounded function of the asset. Thus, the Fourier transform of the call payoff function is not square integrable and does not exist. But this can be circumvented numerically by introducing a dampened factor.

2.5.1 Discrete Fourier transform

To compute equation 2.40, we need to truncate the range of integration to a finite interval $[a, b]$ and then approximate the integral by a finite sum. The DFT needs a finite sequence of real or complex numbers, and for this reason it is ideal for processing information stored in computers. For efficient performance of the DFT, the FFT algorithm can be implemented. Since FFT algorithms are mostly employed to compute the DFT, the DFT and FFT are popularly used synonymously. DFT refers to a mathematical transformation, regardless of how it is computed, when FFT refers to any one of several efficient algorithms for the DFT.

Let N be the number of sample points of a smooth function on a space domain, and a frequency domain, such that Δt and $\Delta\omega$ are the sample interval on the space and frequency domain. Below are the basic steps to derive the discrete counterpart for integral of the form:

$$G := \int_a^b e^{i\omega t}\mathbf{g}(t)dt, \tag{2.46}$$

and we want to calculate equation 2.46 for different values of ω. Determining the sample interval on the domain: Divide the interval $[a, b]$ into N equal sub-intervals such that

$$\Delta t := \frac{b-a}{N}, \quad t_n := a + n\Delta t$$

and the sequence of the sampled values is $\{\mathbf{g}(t_n)\}$, for $n = 0, \ldots, N$, where $\mathbf{g}(a) = \mathbf{g}(t_0)$. In the entire space domain, there are $N + 1$ number of points. Then, we can approximate the integral in equation 2.46 by a sum

$$G \approx \Delta t \sum_{n=0}^{N-1} e^{i\omega t_n}\mathbf{g}(t_n) \tag{2.47}$$

which is approximately accurate to some extent, at least the error convergence at any rate is first-order, Press *et al.* (2007). Assuming $\omega_k = k\Delta\omega$ for k's sampling points on the frequency domain such that

$$k\Delta\omega := k\frac{2\pi}{N}, \tag{2.48}$$

then, the sequence of the sampled values is $\{\mathbf{g}(\omega_k)\}$, for $k = 0, \ldots, N$. Provided t_n and ω_k are equally spaced and have uniform grids, for some values of ω, the sum in equations 2.47 can be written as DFT and computed by the FFT algorithm. The FFT algorithm reduces the number of mathematical operations involved in the computation. It is important in the FFT algorithm for N to be a power of 2, that is, $N = 2^q$. Then, equation 2.47 can be written as

$$\hat{\mathbf{g}}(\omega_k) := \Delta t \sum_{n=0}^{N-1} e^{i\omega t_n} \mathbf{g}(t_n) = \Delta t e^{i2a\pi k/N} [DFT(\mathbf{g}(t_0), \ldots, \mathbf{g}(t_{N-1}))]_n. \tag{2.49}$$

Equation 2.49 maps N complex numbers $\mathbf{g}(t_n)$ into N complex numbers $\hat{\mathbf{g}}(\omega_k)$. The relation between the discrete Fourier transform, equation 2.49, and the integral in equation 2.46 when equation 2.49 is observed as the samples of a continuous function sampled on the interval Δ is,

$$G \approx \hat{\mathbf{g}}(\omega_k),$$

and the discrete form of the inverse Fourier transform, that recovers the sequence $\mathbf{g}(t_n)$ from $\hat{\mathbf{g}}(\omega_k)$, i.e. the inverse discrete Fourier transform, can be written as,

$$\mathbf{g}(t_n) := \frac{\Delta\omega}{b-a} \sum_{k=0}^{N-1} e^{-i\omega t_n} \hat{\mathbf{g}}(\omega_k) = \frac{e^{-i2a\pi k/N}}{N} [DFT^{-1}(\hat{\mathbf{g}}(\omega_0), \ldots, \hat{\mathbf{g}}(\omega_{N-1}))]_k. \tag{2.50}$$

Studying equation 2.46, where $\mathbf{g}(t)$ is a smooth function as in our case, the integral is oscillatory in nature. Thus, there are chances of errors in the expected result when equation 2.49 is used to approximate the integral. This arises when ω is large enough to cause many cycles in the interval $[a, b]$. Equation 2.48 shows that ω_k gives exactly k cycles, then we can be sure the value of $\hat{\mathbf{g}}(\omega_k)$ will be very small to the extent that it can be swallowed up by the truncation error. In the case where the integral in equation 2.46 is not oscillatory, the error would be $\Delta/(b-a)$ but never in the case when the integral is oscillatory in nature. Thus, as ω increases, equation 2.49 becomes inaccurate for approximating the integral in equation 2.46.

Assuming the N-dimensional vector of $\mathbf{g}(t_n)$ and $\hat{\mathbf{g}}(\omega_k)$ is

$$\mathcal{G} = (\mathbf{g}(t_0), \ldots, \mathbf{g}(t_{N-1}))^{\mathbf{T}} \quad and \quad \hat{\mathcal{G}} = (\hat{\mathbf{g}}(\omega_0), \ldots, \hat{\mathbf{g}}(\omega_{N-1}))^{\mathbf{T}}, \tag{2.51}$$

and we denote H^N as the $N \times N$ matrix with $(j,k)^{th}$ entry, such that

$$H^N_{j,k} = e^{2\pi i n k/N}, \quad \text{for } 1 \leq j \leq N, \quad j = k.$$

Let the discrete Fourier transform of $\mathcal{G}$ from equation 2.49 be written as

$$\hat{\mathcal{G}} = H^N \mathcal{G}. \tag{2.52}$$

Obviously, the computation of $\hat{\mathcal{G}}$ requires N^2 complex multiplications, with the addition of a very few numbers of operations. Thus, the discrete Fourier transform appears to be an $\mathcal{O}(N^2)$ process. Different methods have been independently developed in literature for computing DFT of a vector, Brigham (1974). But, if we

implement the FFT and we set $N = 2^q$, then we can be sure that the computation will only require $N/2 \log_2 N$ complex multiplications. This is possible because the DFT of length N can be re-expressed as the addition of two different DFT's, with one part consisting of the even-numbered points, and the other consisting of the odd-numbered points, each of length $N/2$, such that,

$$\mathcal{G}^e = (\mathbf{g}(t_0), \ldots, \mathbf{g}(t_{N-2}))^{\mathbf{T}} \quad and \quad \mathcal{G}^o = (\mathbf{g}(t_1), \ldots, \mathbf{g}(t_{N-1}))^{\mathbf{T}}.$$

Then, the M-dimensional vector is formed. i.e,

$$\hat{\mathcal{G}}^e = H^N \mathcal{G}^e \quad and \quad \hat{\mathcal{G}}^o = H^N \mathcal{G}^o.$$

The first N component of $\hat{\mathcal{G}}$ can now be written as

$$\hat{\mathbf{g}}(\omega_k) = \hat{\mathbf{g}}^e(\omega_k) + e^{2\pi ik/N} \hat{\mathbf{g}}^o(\omega_k)$$

and the last component,

$$\hat{\mathbf{g}}(\omega_{k+N}) = \hat{\mathbf{g}}^e(\omega_k) - e^{2\pi ik/N} \hat{\mathbf{g}}^o(\omega_k), \quad \text{for } k = 0, \cdots, N.$$

We observe that the operations on the matrix-vector complex multiplication have been reduced by two matrix-vector multiplications of the even and odd components. Using the FFT algorithm, the total number of multiplications is reduced from N^2 to $N^2/2$. Thus, FFT increases the computational efficiency by improving the computational speeds and saves time. For further information, see Brigham (1974), Press *et al.* (2007). In our numerical results, we use the in-built FFT algorithm.

2.5.2 Sampling Theorem and Nyquist rule

When implementing DFT, the following question about the frequency should be answered: What is the appropriate space-domain sampling interval (Δt)? The Sampling theorem places restrictions on the frequency content of the continuous time function $g(t)$. The sample rate ω_s gives information on how often samples are taken per unit time, that is,

$$\omega_s = \frac{1}{\Delta t} \tag{2.53}$$

and the highest frequency for any sampling interval *(Nyquist frequency)* is given by

$$\omega_c = \frac{\omega_s}{2}. \tag{2.54}$$

In order to recover $g(t)$ exactly on the frequency domain, it is necessary to sample $g(t)$ at a rate greater than twice the highest frequency. Mathematically,

$$\omega_s > 2\omega_c. \tag{2.55}$$

Thus, the minimal sample rate needed is just twice the highest frequency, irrespective of how many other frequency components are present. The consequences of sampling below ω_s results in aliasing. The concept of aliasing is when a frequency mistakenly takes on the identity of another different frequency when recovered.

Theorem 2.5.4 (Sampling theorem)**.** *Let $g(t)$ be a continuous time function and $\hat{g}(\omega)$ be the Fourier transform of $g(t)$. If $\hat{g}(\omega)$ is zero for all frequencies above $|\omega| \geq \omega_c$,*

$$\hat{g}(\omega) = 0 \ \forall \ |\omega| \geq \omega_c \tag{2.56}$$

then we can say that $g(t)$ is completely determined from its sampled values,

$$g_n = g(n\Delta t), \quad \text{for } n = \cdots, -1, 0, -1, \cdots. \tag{2.57}$$

To remove an aliased frequency from an already sampled function is far from trivial. Press *et al.* (2007) suggests a few ways to overcome aliasing before sampling: Knowing or enforcing a known bounded domain on the continuous function. Also, sampling at a rate that is sufficiently rapid to give a minimum of two points per cycle of the highest frequency in the domain. As an alternative, if the continuous function has already been sampled, then we can approximate the discrete samples of $\hat{g}(\omega)$ and assume $\hat{g}(\omega)$=0, for any frequency outside the range $-\omega_c < \omega < \omega_c$, Brigham (1974), Cherubini *et al.* (2010), Press *et al.* (2007). The below example give more insight on the application of Theorem 2.5.4.

Example 2.5.5. Recall from equation 2.42, the Fourier pair of the CF Φ_X and the probability density function $\mathbf{f}_X$:

$$\Phi_X(\omega) := \int_{-\infty}^{\infty} e^{i\omega x}\mathbf{f}_X(x)dx \quad \text{and} \quad \mathbf{f}_X(x) := \frac{1}{2\pi}\int_{-\infty}^{\infty} e^{-i\omega x}\Phi_X(\omega)d\omega \tag{2.58}$$

where ω is the Fourier argument and x is the log return of the process. In real-world modelling, it is important to restrict the support of the variable which is typically given to be unbounded to a bounded interval. Thus, we restrict the support of x to $[-X_c, X_c]$. As a result of this, we change the notation of the CF on the bounded interval to $\hat{\mathbf{f}}_X$. Now we want to use $\hat{\mathbf{f}}_X$ to approximate Φ_X so that outside the support of $\mathbf{f}_X(x)$, the value of the probability distribution function near zero is assumed to be zero in modelling. That is,

$$\mathbf{f}_X(x) < \epsilon, \quad |x| > X_c.$$

So, if the value of the asset is normalised with respect to today's price, even a small value of X_c, such as 5, means that we give a negligible probability to moves below 50% or beyond 150%, and this may be large enough especially in short-term trading. In view of this, we assume $\mathbf{f}_X(x) = 0$ for $|x| > X_c$. The CF is given by

$$\hat{\mathbf{f}}_X(\omega) = \int_{-X_c}^{X_c} e^{i\omega x}\mathbf{f}_X(x)dx, \tag{2.59}$$

and $\mathbf{f}_X(x) = 1$ for $|x| < X_c$, i.e

$$\hat{\mathbf{f}}_X(\omega) = \int_{-X_c}^{X_c} e^{i\omega x}dx, \quad |x| < X_c. \tag{2.60}$$

Evaluating the integral in equation 2.60

$$\hat{\mathbf{f}}_X(\omega) = \int_{-X_c}^{X_c} e^{i\omega x}dx = \frac{\sin(2\pi X_c\omega)}{\pi\omega}. \tag{2.61}$$

Recall from equation 2.53 and 2.54,

$$\Delta = \frac{1}{2X_c}$$

and

$$\hat{\mathbf{f}}_n = \hat{\mathbf{f}}(n\Delta),$$

then we compute equation 2.59 only at the sampling values $n\Delta$,

$$\hat{\mathbf{f}}_n = \int_{-X_c}^{X_c} \mathbf{f}_X(x) e^{i\omega x} dx. \tag{2.62}$$

Using the inverse Fourier transform formula

$$\mathbf{f}_X(x) = \frac{1}{2X_c} \sum_{n=-\infty}^{\infty} \hat{\mathbf{f}}_n e^{-i\omega x \Delta n}, \quad |x| < X_c. \tag{2.63}$$

To avoid the explicit constraint on $|x| < X_c$, we rewrite equation 2.64 in term of an indicator function such that

$$\mathbf{f}_X(x) = \frac{1}{2X_c} \mathbb{I}_{|x|<X_c} \sum_{n=-\infty}^{\infty} \hat{\mathbf{f}}_n e^{-i\omega x \Delta n}, \tag{2.64}$$

then we recover $\hat{\mathbf{f}}_X$ by applying the Fourier transform to $\mathbf{f}_X(x)$;

$$\hat{\mathbf{f}}_X(\omega) = \frac{1}{2X_c} \sum_{n=-\infty}^{\infty} \hat{\mathbf{f}}_n \int_{-\infty}^{\infty} e^{i\omega x(\omega - \Delta n)} \mathbb{I}_{|x|<X_c} dx. \tag{2.65}$$

and

$$\int_{-\infty}^{\infty} e^{i\omega x(\omega - \Delta n)} \mathbb{I}_{|x|<X_c} dx = \frac{\sin(2\pi X_c(\omega - n\Delta))}{\pi(\omega - \Delta n)}.$$

Thus, we conclude the Fourier space of the function $\mathbf{f}_X(x)$ with bounded interval is given by

$$\hat{\mathbf{f}}_X(\omega) = \frac{1}{2X_c} \sum_{n=-\infty}^{\infty} \hat{\mathbf{f}}_n \frac{\sin(2\pi X_c(\omega - n\Delta))}{\pi(\omega - \Delta n)}. \tag{2.66}$$

Equation 2.66 is the *Sampling theorem* and this shows the Fourier transform $\hat{\mathbf{f}}_X(\omega)$ of a function with bounded interval can be fully known provided it is known at discrete sampling points Cherubini *et al.* (2010).

2.6 Conclusion

In this chapter we have modelled asset returns as infinite activity Lévy processes due to the ability of the Lévy processes to adequately describe the empirical properties of asset-returns and, simultaneously, provide a reasonable fit to the implied volatility surfaces observed in the real financial markets, which shows the risk-neutral returns are not normally distributed and leptokurtic.

A great advantage of exponential Lévy models is their mathematical tractability due to the availability of their CFs, which makes it possible to perform many computations explicitly and to present deep results of modern mathematical finance in a simple format. We have presented some of these exponential Lévy models; the BS, NIG and VG models, and also discussed the numerical behaviour of the CFs of their distributions. Experimental results show the CFs of the distributions of BS and NIG models to be naturally continuous but the VG model is not. The CF of the distribution of the VG model is only continuous when the complex log is restricted to the principal branch, despite the presence of a multi-valued function in the CF. Thus, discontinuities can be avoided in option pricing by using numerical methods. Literature confirms that Fourier methods are preferred to other numerical methods in dealing with discontinuities in option pricing, Lord and Kahl (2010).

The risk-neutral technique is mainly used for option pricing. In all our models, we assume the underlying asset price is formulated under a risk-neutral measure. Although, pricing options especially options with early-exercise features in these models are far from trivial due to the presence of jumps. To determine the worth of European options in our financial models, we are going to solve equation 2.38, but this cannot be done analytically so we have to use numerical approximations. In the next Chapter, we will consider some Fourier methods. Before studying the Fourier methods in detail, we have introduced the fundamental concept of Fourier analysis in relation to option pricing.

Chapter 3

Fourier methods for option pricing

3.1 Introduction

Fourier methods are very effective and widely applied mathematical tools for solving technical problems. As far as we know, in mathematical finance, the Fourier transform method was firstly used to determine the distribution of an underlying asset price under the stochastic volatility model by the inversion method, Stein *et al.* (1991). Since then, these methods have been widely applied in option pricing in different financial models, Scott (1997), Carr and Madan (1999), Raible (2000), Reiner (2001), Dempster and Hong (2000), Lewis (2001), Benhamou (2002), Borovkov and Novikov (2002), Sepp (2003), Attari (2003), Chourdakis (2004), Lee (2004), Sullivan (2005), Ju and Zhong (2006), Gutierrez (2007), Jackson. *et al.* (2008), Lord *et al.* (2008), M.Minenna and Verzella (2008), Cerny (2008), Fang and Oosterlee (2008), Surkov (2009), Dufrense *et al.* (2009), Fang and Oosterlee (2009b), Hurd and Zhou (2009), Chiarella *et al.* (2009), Cherubini *et al.* (2010), Eberlein. *et al.* (2010), Pascucci (2011), Fang and Oosterlee (2011) and many more. Fourier methods have been widely applied in the valuation of commodity derivatives, Jaimungal and Surkov (2008), electricity derivatives, Deng (2000), value-at-risk for portfolios with derivatives, and for models where the CF of the distribution is assumed to be unknown explicitly Albanese *et al.* (2004), and for valuation in Insurance Mathematics Dufrense *et al.* (2009). These methods are diversified in their application.

The discounted expected payoff approach to pricing vanilla-European options requires the availability of the density function of the underlying assets' returns under the risk-neutral measure as discussed in Section 2.4. Knowing that the analytic expression for the CFs of exponential Lévy models are readily available, we evaluate the expectation integral in terms of the CF. The one-to-one relationship between the CF and the density function, and the Parseval formula enhances the application of Fourier analysis to option-pricing theory.

Different approaches have been developed under the exponential Lévy model to compute option prices as an integral in the Fourier domain, using Fourier methods. Carr and Madan (1999) initiate the idea of pricing and analysing European option prices using Fourier transform-based methods with the help of the FFT algorithm.

The Fourier transform in Carr and Madan (1999) is taken with respect to the log-strike price. Raible (2000) and Lewis (2001) develop a slightly more general approach by taking the transform with respect to the log of the forward price and the log of the asset price. Raible (2000) applies the FFT algorithm to evaluate the European option formula derived by the bilateral Laplace transform. Lewis (2001) derives a pricing formula using the residual calculus by separating the payoff function from the CF of the underlying process with the help of the Parseval theorem. Lee (2004) generalises the work of Carr and Madan (1999), from pricing plain-vanilla options to other options, in particular multi-asset options, and unified the approach with other known Fourier-pricing techniques in literature. To obtain an analytic expression for the conditional expectation of the continuation value (see Chapter 4), Reiner (2001) observes the continuation value can be expressed as a convolution of the option value with the transition density function, which can be implemented efficiently by the FFT algorithm, while Lord *et al.* (2008) extends the work of Lee (2004) and implements the idea of Carr and Madan (1999) and Reiner (2001) to price early-exercise options and to calculate the hedge parameters of these options. Borovkov and Novikov (2002) presents a different approach for calculating the expectation associated with the risk-neutral valuation formula. In the case of the European option, the expectation can be achieved by simply integrating the moment-generation function of the model with a certain weight. To the best of our knowledge, the approach of Borovkov and Novikov (2002) is the first to price discretely-monitored exotic options of underlying assets driven by Lévy models.

Attari (2003) discusses a simple approach that reduces the two main numerical integrations involved in option pricing by a Fourier inversion into one numerical integration without using any numerical techniques for the integration. This method reduces the number of computations of the CF required to achieve a given accuracy. It is interesting to record that the computational speed of the Attari (2003) algorithm is not affected even when a *time-saving technique* (e.g FFT) is implemented to improve its computational efficiency. Chourdakis (2004) presents a similar approach to Carr and Madan (1999), but uses the fractional FFT (FRFFT) algorithm instead of the FFT algorithm approach initiated by Carr and Madan (1999). Fang and Oosterlee (2008) propose a method that substitutes the probability density function in the risk-neutral valuation formula with the Fourier-cosine series expansion, and approximates the infinite interval to finite interval, having in mind that a density function tends to be continuous and converges rapidly to zero. They extend the method to price early-exercise and discrete Barrier options, Fang and Oosterlee (2009b). The method of Fang and Oosterlee (2008) can also be used to recover the density function of the model and to calculate the hedge parameters. Jackson. *et al.* (2008) presents an algorithm that switches between the real space and the Fourier space. This method is based on solving the PIDE pricing formula associated with an underlying asset driven by Lévy models and can be extended to pricing options in regime-switching Lévy models, Jackson *et al.* (2007), Jaimungal and Surkov (2009), mean-reverting models Surkov (2009) and for hedging purpose Davison and Surkov (2010). Sullivan (2005) develop a method that combines the quadratic-pricing techniques with the FFT algorithm. This method is widely applicable for pricing plain-

vanilla options and exotic options. The article of Chiarella *et al.* (2009) considers the *Jamshidian method* and $Mckean\hat{a}^{TM}s$ incomplete Fourier method for solving the PIDE problems to obtain the American call price, early-exercise boundary and the hedging parameters. The *Jamshidian method* transforms the homogeneous PIDE on a bounded domain to inhomogeneous PIDE on an unbounded domain, and then solves the inhomogeneous PIDE problem by the Fourier transform method. Eberlein. *et al.* (2010) thoroughly investigate and analyse the necessary conditions for the existence of option-pricing formulas derived by Fourier transform methods in a more general framework for pricing exotic options. The recent work of Wong and Guan (2011) presents a simple network technique for pricing exotic options under Lévy dynamics using the FFT algorithm. This technique generalized the forward shooting grid method of lattice method to expand the FFT network to accumulate a path-dependent quantity, and the evaluation of the early-exercise boundary, and the option prices are similar to that of the lattice approach. The article of M.Schmelzle (2010) gives an introductory note on the properties of Fourier methods and CFs; he investigates the computational efficiency of the commonly-used Fourier pricing algorithms and numerical quadrature techniques for evaluating the density functions and for pricing options. Furthermore, F.Hubalek *et al.* (2006) determines the variance-optimal hedge using the Fourier transform methods. The books by Boyarchenko and Levendorskii (2002), Schoutens (2003), Cont and Tankov (2004), Cherubini *et al.* (2010), and Pascucci (2011), also explain the applications of Fourier methods to option pricing.

In this dissertation, we discuss some Fourier methods: The Carr-Madan approach Carr and Madan (1999), because it provides a kind of benchmark, being the most popular of the early Fourier method for pricing options; the convolution method (CONV method), Lord *et al.* (2008), the Fourier-cosine series expansion method (COS method), Fang and Oosterlee (2008), and the Fourier space time-stepping method (FST method), Jackson. *et al.* (2008), because of their remarkable computational efficiency and general applicability. To give more insight into the applications of these numerical methods to option pricing, we shall apply these methods to pricing European call options under the BS model, NIG model and VG model.

The density function of many underlying asset-price models can be efficiently recovered by Fourier methods. Option pricing and density calculations are then, as will be explained later, a matter of numerical integration for the Fourier inversion, either by using direct integration (COS method) or the FFT algorithm (Carr-Madan, CONV method and the FST method). The numerical implementation should be thoroughly investigated since the semi-infinite integral in the Fourier space might exhibit variation, which can introduce truncation and discretisation error into the result.

In Fourier pricing formulas, the two sources of error arise from transforming the infinite integral to a finite domain (*truncation error*), and discretising the finite domain (*discretisation error*). The truncation error can be avoided by ensuring the CF of the distribution of the underlying asset is continuous (see Section 2.3), Kahl

and Lord (2007). Truncating the infinite integral by this approach excludes the effect or use of FFT completely. Thus, the source of error is reduced to one; only left with a discretisation error that has to do with the selection of the grid size. In methods where FFT is implemented, a uniform grid size is required, which is not easy to achieve even in calibration of the model to observed option prices because few strike prices and maturities are often provided. Thus, the use of FFT introduces interpolation error. To avoid aliasing in the implementation of FFT, the Nyquist relation must be satisfied.

Using Fourier methods, the prices of vanilla-European options with a large range of strikes can be derived in a single time-step computation using the CF of the distribution of the underlying asset. These methods often implement the Fast-Fourier algorithm in their computation that improves the computational efficiency. Although, some think that direct integration is sometimes better, Kahl and Jäckel (2005). In subsequent Chapters, these methods are extended to determine the value of the early-exercise options by modifying the pricing formulas for vanilla-European options.

In the remainder of this Chapter, we introduce and discuss four Fourier methods for pricing European options. Section 3.2 explains the Carr-Madan method in connection with the derivation of the formula for pricing vanilla-European calls in a continuous exponential Lévy model. The CONV method relative to Carr-Madan method for pricing European options, is discussed in Section 3.3. Section 3.4 explains the COS method with an extension to the derivation of the general pricing formula for vanilla-European options in exponential Lévy models, while Section 3.5 illustrates the implementation of the Fourier space time-stepping method in detail. In Section 3.6, we shall compare the approximated results obtained from these methods with the exact value derived from the closed-form solution where the prices of the options are known analytically, or else with reference prices taken from Kéllezi and Webber (2004), Sullivan (2005), Lord *et al.* (2008) and Fang and Oosterlee (2008), and also compare the speed and the accuracy of the Fourier methods.

3.2 Carr-Madan method

In this section we present the Fourier transform approach to option pricing by Carr and Madan (1999). The method requires the convolution of the pay-off function and the risk-neutral density with respect to the log of the strike price, as shown in Theorem 2.5.2. To illustrate the Carr-Madan method, we present the Black-Scholes model with Fourier transform pricing methodology.

An algorithm for the efficient pricing of options with a large range of simultaneous strikes simultaneously is developed. This approach implements the FFT algorithm in pricing options. The use of FFT for pricing options involves different numerical methods of integral evaluation. These numerical methods are often termed the quadrature method. Numerical results show that the QUAD-FFT method is more complicated compared to the Carr-Madan and the CONV methods which will be discussed later. The aim of the FFT in Carr-Madan method is to speed up the

computation of the Fourier transform by developing an analytic expression for the Fourier transform of the option price and calculate the option price by Fourier Inversion. The numerical behaviour of this method is discussed in detail in this section.

Let K be the strike price and T be the maturity of a vanilla-European option. The call C_0 and the put P_0 option prices are computed as discounted risk-neutral conditional expectations of the terminal payoffs, as stated in equation 2.38.

$$\Psi := \begin{cases} (S_T - K)^+ & \text{for a call,} \\ (K - S_T)^+ & \text{for a put .} \end{cases} \tag{3.1}$$

Introducing a change of variable in equation 3.1, let s be a log-terminal asset price and k be a log-strike price such that $s = \ln S$ and $k = \ln K$. Then,

$$\begin{aligned} C(K) &:= e^{-rT}\mathbb{E}^{\mathbb{Q}}[(e^{\ln S} - e^{\ln K})^+], \\ P(K) &:= e^{-rT}\mathbb{E}^{\mathbb{Q}}[(e^{\ln K} - e^{\ln S})^+]. \end{aligned} \tag{3.2}$$

As equation 3.2 is an expectation, it can be evaluated using numerical integration once the density function of the distribution is known or can be calculated. Thus, the expression for the vanilla-call value is given by

$$V(k) := C(k) = e^{-rT}\int_k^{\infty}(e^s - e^k)\mathbf{f}(s)ds \tag{3.3}$$

where $\mathbf{f}(s)$ is a risk-neutral density of s. Recall from equation 2.42, the CF of s is the Fourier transform of its density function $\mathbf{f}(s)$;

$$\Phi(\omega) := \mathcal{F}(\mathbf{f}(s))(\omega) = \int_{-\infty}^{\infty} e^{i\omega s}\mathbf{f}(s)ds,$$

$\omega \in \mathbb{R}$ appear as the argument of a Fourier transform. Recall the CF of the log-stock price in the BS model,

$$\Phi(\omega) := e^{(i\omega(r-\frac{1}{2}\sigma^2)t - \frac{1}{2}\omega^2\sigma^2 t)}. \tag{3.4}$$

To calculate the initial call price, we need to take the Fourier transform of equation 3.3. To do this, $V_0(k)$ must satisfy equation 2.43 in k to avoid oscillation in the payoff function which might lead to a discretisation error and truncation error. However,

$$\lim_{k\to-\infty} V(k) := S_0 \neq 0 \tag{3.5}$$

because $V(k) \to S_0$ as $k \to -\infty$. Thus, $V(k)$ is not square-integrable. For equation 3.3 to be square-integrable, Carr and Madan (1999) propose $\alpha > 0$ (damped variable) such that the modified price $V(k, \alpha)$;

$$V(k, \alpha) := e^{\alpha k}V(k)$$

is a square-integrable function. That is,

$$\int |V(k, \alpha)|^2 dk < \infty.$$

Based on Lee (2004) observation, there is no restriction on α, for the choice of α depends on the type of option and the density function of the distribution of the model. He noted that for pricing options with many strikes, a choice of any $\alpha > 1$ works well.

3.2.1 Evaluating the Fourier transform of the call price.

Firstly, we develop an analytical expression for the Fourier transform of the modified call price $V(k,\alpha)$ in terms of the CF of the distribution of the underlying asset. Secondly, we obtain the call price by using a Fourier inversion numerically. Let

$$\psi(\omega,\alpha) := \mathcal{F}\left[V(k,\alpha)\right] = \int_{-\infty}^{\infty} e^{i\omega k} e^{\alpha k} V(k) dk \tag{3.6}$$

$$= \int_{-\infty}^{\infty} e^{i\omega k} e^{\alpha k} \int_{k}^{\infty} e^{-rT}(e^{s}-e^{k})\mathbf{f}(s)\, dsdk. \tag{3.7}$$

For direct computation of the integrals, we change the order of integration, that is

$$\begin{aligned}
\psi(\omega,\alpha) &= e^{-rT}\int_{-\infty}^{\infty}\mathbf{f}(s)\int_{k}^{\infty}(e^{s}-e^{k})e^{\alpha k}e^{i\omega k}\, dsdk \\
&= e^{-rT}\int_{-\infty}^{\infty}\mathbf{f}(s)\int_{-\infty}^{s} e^{i\omega k}(e^{s+\alpha k}-e^{(1+\alpha)k})\, dkds \\
&= e^{-rT}\int_{-\infty}^{\infty}\mathbf{f}(s)\left[\frac{e^{(i\omega+\alpha+1)s}}{i\omega+\alpha}-\frac{e^{(i\omega+1+\alpha)s}}{i\omega+\alpha+1}\right] ds \\
&= \frac{e^{-rT}}{(i\omega+\alpha)(i\omega+\alpha+1)}\int_{-\infty}^{\infty}\mathbf{f}(s)e^{i(\omega-i(\alpha+1))s}ds.
\end{aligned} \tag{3.8}$$

Carr and Madan (1999) assume the distribution of the underlying asset process has a distribution moment of order $\alpha+1$ for some $\alpha>0$, such that

$$\int e^{(\alpha+1)s}\mathbf{f}(s)ds < \infty, \tag{3.9}$$

in terms of model with a Lévy density, equation 3.9 becomes

$$\int_{|y|\geq 1} e^{(1+\alpha)y}\nu(dy) < \infty \tag{3.10}$$

where $\nu(dy)$ is the Lévy measure of the Lévy process. Knowing the CF, we can write the integral in equation 3.8 as

$$\int_{-\infty}^{\infty}\mathbf{f}(s)e^{i(\omega-i(\alpha+1))s}ds := \Phi(\omega-i(\alpha+1)).$$

Hence, equation 3.8 becomes

$$\psi(\omega,\alpha) := \frac{e^{-rT}\Phi_T(\omega-i(\alpha+1))}{(i\omega+\alpha)(i\omega+\alpha+1)}. \tag{3.11}$$

From equation 3.11, we notice if $\alpha=0$ and $\omega=0$, the denominator vanishes so that there is a singularity in the integrand. Since the FFT algorithm evaluates the integrand at $\omega=0$, the use of the damping factor $e^{\alpha k}$ or something similar is required.

Now, we want to obtain the call-pricing function from equation 3.6 using the Fourier inversion numerically:

$$V(k) := \frac{e^{-\alpha k}}{2\pi} \int_{-\infty}^{\infty} e^{-i\omega k} \psi(\omega, \alpha) d\omega. \tag{3.12}$$

Since the call price is always real, we can say that $\psi(\omega, \alpha)$ is even in its real part and odd in its imaginary part. Then,

$$V(k) := \frac{e^{-\alpha k}}{\pi} \int_{0}^{\infty} e^{-i\omega k} \psi(\omega, \alpha) d\omega. \tag{3.13}$$

Applying the *FFT* algorithm:

We want to express equation 3.13 in terms of the DFT in equation 2.49. Applying the trapezoidal rule, we set

$$\omega_j := \beta(j-1). \tag{3.14}$$

Then equation 3.13 becomes

$$V(k) \approx \frac{e^{-\alpha k}}{\pi} \sum_{j=0}^{N-1} e^{-i\beta(j-1)k} \psi(\omega_j)\beta \tag{3.15}$$

where β is the step size of the numerical integration, and $j = 0, \cdots, N-1$.
Equation 3.15 proposes we calculate the call values using the FFT algorithm:

$$\mathcal{W}(u) = \sum_{j=0}^{N-1} e^{-i\frac{2\pi}{N}(j-1)(u-1)} xj, \tag{3.16}$$

for $j = 0 \leq j, u \leq N-1$.
Let $\lambda > 0$ be the regular spacing between values of the log strikes, such that

$$k_u := -c + \lambda(u-1), \quad \text{for } u = 0, \cdots, N-1 \tag{3.17}$$

and

$$c := \frac{N\lambda}{2}.$$

Substituting equation 3.17 into 3.15 yields:

$$\begin{aligned} V(k_u) &\approx \frac{e^{-\alpha k_u}}{\pi} \sum_{j=0}^{N-1} e^{-i\beta(j-1)(-\frac{N\lambda}{2}+\lambda(u-1))} \psi(\omega_j)\beta \\ &= \frac{e^{-\alpha k_u}}{\pi} \sum_{j=0}^{N-1} e^{-i\lambda\beta(j-1)(u-1)} e^{i\frac{1}{2}(j-1)N\lambda\beta} \psi(\omega_j)\beta. \end{aligned} \tag{3.18}$$

In order to apply the FFT algorithm to compute equation 3.18, we shall express equation 3.18 in form of equation 3.16. That is, we let

$$\lambda\beta := \frac{2\pi}{N}. \tag{3.19}$$

Then,

$$V(k_u) \approx \frac{e^{-\alpha k_u}}{\pi} \sum_{j=0}^{N-1} e^{-i\frac{2\pi}{N}(j-1)(u-1)} e^{i(j-1)\pi} \psi(\omega_j)\beta$$
$$= \frac{e^{-\alpha k_u}}{\pi} \sum_{j=0}^{N-1} e^{-i\frac{2\pi}{N}(j-1)(u-1)} (-1)^{j-1} \psi(\omega_j)\beta. \tag{3.20}$$

For further simplification of β, we choose the strikes near the initial underlying asset price, S_0. In that regard, the prices should be arranged such that S_0 appears in the interval of the strikes. Thus, λ should be chosen to be small in order to have many strikes around it. This implies a large value of β which would give a large grid for the integration. To obtain an accurate integration with large values of β, Carr and Madan (1999) implemented Simpson's rule weightings into the summation in equation 3.20 since the values of k are regularly spaced. Based on Simpson's rule weightings, and the restriction on equation 3.19, equation 3.20 becomes

$$V(k) \approx \frac{e^{-\alpha k}}{\pi} \sum_{j=0}^{N-1} e^{-i\frac{2\pi}{N}(j-1)(u-1)} (-1)^{j-1} \psi(\omega_j) \frac{\beta}{3} (3 + (-1)^j - \delta_{j-1}) \tag{3.21}$$

where δ_n is the kronecker delta function, defined as:

$$\delta_n = \begin{cases} 1 & \text{for } n = 0, \\ 0 & \text{, otherwise.} \end{cases}$$

The summation term in equation 3.21 is equal to the FFT algorithm in equation 3.16 where,

$$x_j = (-1)^{j-1} \psi(\omega_j) \frac{\beta}{3} (3 + (-1)^j - \delta_{j-1}). \tag{3.22}$$

Hence,

$$V(k) := \frac{e^{-\alpha k}}{\pi} \sum_{j=0}^{N-1} e^{-i\frac{2\pi}{N}(j-1)(u-1)} x_j. \tag{3.23}$$

In most Lévy models, $\mathbf{f}(s)$ is not known. Therefore, we cannot price plain-vanilla options directly using equation 3.3. Since there is a one-to-one relationship between the probability density and the CF, we can rewrite equation 3.3 in terms of ψ in equation 3.21. Then, we will be able to price options in general exponential Lévy models with the FFT algorithm by using equation 3.23.

3.2.2 Implementation details

Studying equation 3.23, there are some unknown parameters. Experimenting with equation 3.23 shows that the α, N, T and λ play an important role in the accuracy of the Carr-Madan method. The smaller the value of α, the more the deviation in the results compared with the analytic solution. The larger the value of N, the more accurate the results are. The effect of increasing T depends on the model. If the choice of β is small in order to obtain a finer grid for the integration, then the call prices at strike spacings that are relatively large have few strikes lying in the desired region near the underlying asset price. The challenge here is the choice of these parameters.

Effect of maturity date T:

An increase in the value of T introduces smoothness into the return densities which thins the tails of the CF of the distribution of some models, for example, the VG model.
Reference prices are given by the analytic solution. We observe that under the BS model, short-dated and one-year European calls are in agreement with the reference prices when the strikes are bounded between half and double of the initial stock price, which is mostly the case in the financial market.

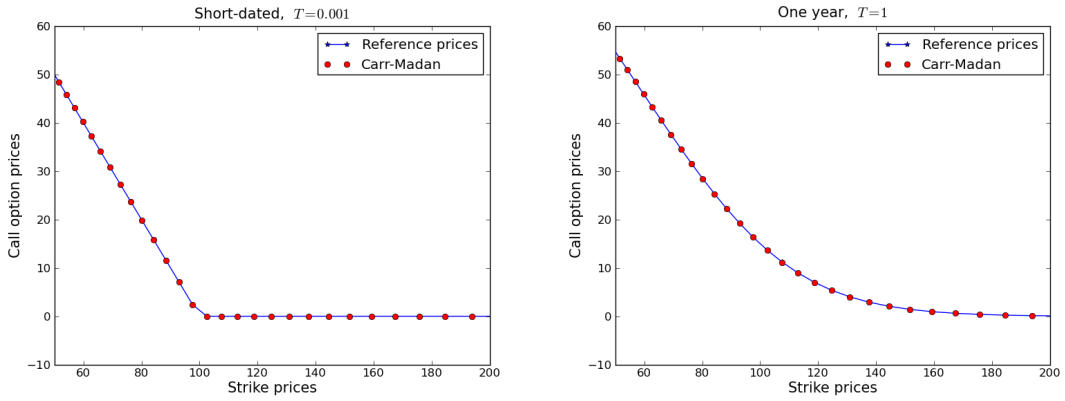

Figure 3.1: European calls under BS model. Parameters used: $K = [50, 200]$, $S_0 = 100$, $\sigma = 0.25$, $r = 0.1$, $N = 2^9$, $\beta = 0.25$ and $\alpha = 2.00$.

Spacing size (λ):

The value for the λ is calculated from equation 3.19;

$$\lambda\beta = \frac{2\pi}{N}. \tag{3.24}$$

For a constant value of N, a decrease in the value of β leads to an increase in the value λ because of the reciprocal rule in equation 3.24. Carr and Madan (1999) suggest $\beta = 0.25$. Lee (2004) proposes $\beta > 0$, but the optimal value depends on the model. In subsequent results, $\beta = 0.25$ is used.

Choosing the damping factor α (decay rate parameter):

The damping parameter α ensures that the damped call price is square-integrable, which is a sufficient condition for the Fourier transform to exist. We need to know the optimal value of α to avoid highly-peaked and oscillatory integrals, especially for short maturities, and for strikes that are far from the money. Different values for α have been discussed in literature. Raible (2000) proposes $\alpha = 25$ for exponential Lévy models. Lee (2004) suggests five possible different value of α i.e. $\alpha < -1$, $\alpha = -1$, $\alpha \in [-1, 0]$, $\alpha = 0$ and $\alpha > 0$, but the optimal values of α depends on

the model, the position of the option, that is, the value of the strike, the value of N and the spacing parameter β. Schoutens *et al.* (2004) recommend $\alpha = 0.75$. Carr and Madan (1999) observe that positive values of α make the damped call price in equation 3.13 to be integrable over the negative log-price k-axis, but worsen the condition on the positive axis. He suggests for equation 3.13 to be integrable over the log price k, $\psi(0, \alpha)$ must be finite provided $\Phi(-(\alpha+1)i)$ is finite. Thus, equation 3.9 holds. That is,

$$\mathbb{E}[S_T^{\alpha+1}] < \infty.$$

Definitely, there exists a range of α that results in an integrand that has no peak and does not oscillate. Kahl and Lord (2007) give a clear explanation on the range of α.

Optimal α: The variation of a function $g : \mathbb{R} \to \mathbb{R}$ on a definite range $[-1, 1]$ can be determined by the total variation, Kahl and Lord (2007):

$$\mathbf{TV}(g) = \int_{-1}^{1} \left| \frac{\partial g}{\partial x}(x) \right| dx.$$

The integral in equation 3.8 should be adjusted in order to compare the total variation for different values of α, and α should be chosen to minimize the total variation, Kahl and Lord (2007), in order to reduce the approximation error in the integral, Förster and Petras (1991). The optimal α parameter can be obtained by solving for the roots of the derivative of the option value with respect to α. Thus,

$$\alpha_{op} = \underset{\alpha \in \{\alpha_{\min}, \alpha_{\max}\}}{\operatorname{argmin}} \left| e^{-\alpha k} \int_0^{\infty} \frac{\partial \psi(\omega, \alpha)}{\partial \alpha} \right| d\omega, \tag{3.25}$$

where $\left[\underset{x}{\operatorname{argmin}} f(x) \right]$ implies the value of x for which $f(x)$ attains its smallest value, and $\{a, b\}$ is the set containing just a and b. An efficient way to evaluate equation 3.25 is to minimise the maximum value of the integral of $\psi(\omega, \alpha)$ when $\omega = 0$. Then equation 3.25 becomes

$$\alpha_{op} = \underset{\alpha \in \{\alpha_{\min}, \alpha_{\max}\}}{\operatorname{argmin}} \left| e^{-\alpha k} [\psi(-(\alpha + 1)i)] \right|.$$

Thus,

$$\alpha_{op} = \underset{\alpha \in \{\alpha_{\min}, \alpha_{\max}\}}{\operatorname{argmin}} \Psi(\alpha, k), \quad \Psi(\alpha, k) = -\alpha k + \frac{1}{2} \ln[\psi(-(\alpha + 1)i)^2]. \tag{3.26}$$

Solution to equation 3.26 shows that Ψ will have a local minimum in three ranges: $\alpha \in (\alpha_{\min}, -1), \alpha \in (-1, 0)$ and $\alpha \in (0, \alpha_{\max})$, since ψ is not always positive. To derive the optimal alpha, α_{op}, demands to know the minimum Ψ. Thus,

$$\frac{\partial \Psi(\alpha, k)}{\partial \alpha} = 0.$$

Note Ψ is not finite when $\alpha = -1$ and $\alpha = 0$.

Result 3.2.1 (Effect of α (damping parameter) on Carr-Madan for pricing European calls)**.** Reference prices are given by the analytic solution. Investigating the effect of α on the Carr-Madn method, Figure 3.2 shows for $K = 80$, $\alpha = 2.25$ gives a more accurate result. Moreover, for $K = 100$, $\alpha > 1.25$ we also obtain an accurate result. Table 3.1 also explains the choice of α.

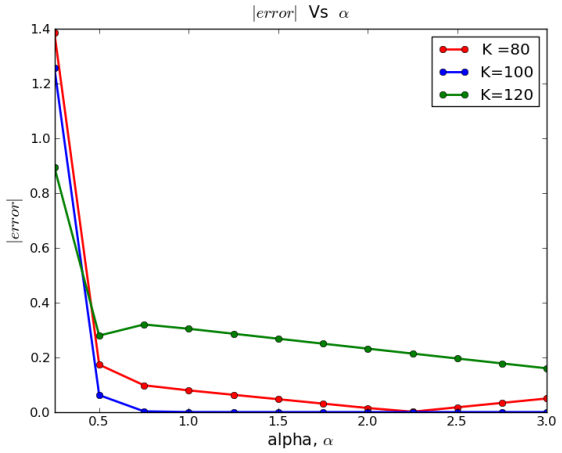

Figure 3.2: The absolute differences between the references prices and Carr-Madan method for pricing European calls under the BS model with respect to alpha (α). Parameters used: $S_0 = 100$, $K = [80, 100, 120]$, $\sigma = 0.25$, $r = 0.1$, $N = 2^{10}$ and $\beta = 0.25$.

$K\|\alpha$	0.25	0.50	0.75	1.00	1.25	1.50
80	1.38	0.17	9.77×10^{-2}	7.91×10^{-2}	6.30×10^{-2}	4.69×10^{-2}
100	1.25	6.18×10^{-2}	2.68×10^{-3}	1.16×10^{-4}	4.76×10^{-6}	9.54×10^{-7}
120	8.93×10^{-1}	2.79×10^{-1}	3.19×10^{-1}	3.04×10^{-1}	2.85×10^{-1}	2.77×10^{-1}

Table 3.1: Error convergence ($\log_{10}$ of the absolute error) of Carr-Madan method for pricing European calls under the BS model with respect to alpha (α). Parameters used: $S_0 = 100$, $K = [80, 100, 120]$, $\alpha = [0.25, 1.5]$, $\sigma = 0.25$, $r = 0.1$, $N = 2^{10}$ and $\beta = 0.25$.

Effect of N:

The choice of N depends on the model and the maturity of the option. For each model and maturity date, we choose the number of N large enough to capture the discretisation and the truncation error. The value of λ depends on N.

Result 3.2.2 (The Effect of N on the Carr-Madan method for pricing European calls under the BS model)**.** The reference price is given by the analytic solution. We notice for one-year European calls, the method requires $N > 1000$ to achieve an error of order $\mathcal{O}(10^{-3})$. Thus, the convergence is slow.

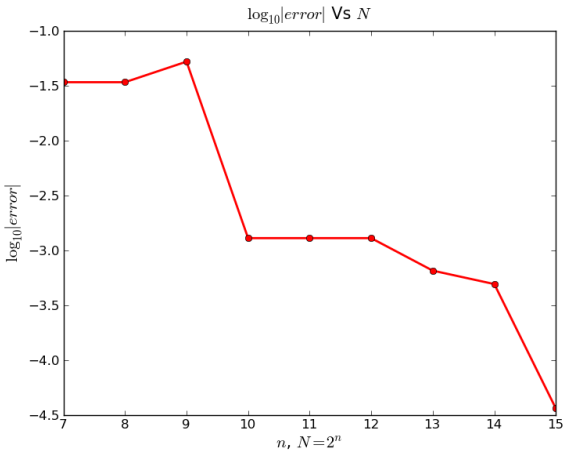

Figure 3.3: Error convergence of Carr-Madan method for pricing European call under the BS model with respect to N. Parameters used: $S_0 = 100$, $K = 80$, $T = 1$, $\sigma = 0.25$, $r = 0.1$, $\alpha = 2.25$ and $\beta = 0.25$.

3.2.3 Summary

Algorithm 3.2.1: **Carr-Madan method**

1: Declare the initial variables: S_0, T, α, N, β;
2: Compute the CF of log-asset returns of the distribution of the model, that is, $\Phi(\cdot)$;
3: Compute $\psi(\cdot)$ according to equation 3.11;
4: Discretize the transformed domain by defining ω_j according to equation 3.14 (for $0 \leq j \leq N-1$);
5: Discretize the spatial domain using equation 3.17 (for $0 \leq u \leq N-1$);
6: Compute x_j according to equation 3.22;
7: Compute V_0 via FFT using equation 3.23.

In this section we have presented the Carr-Madan method. Algorithm 3.2.1 presents a summary of the implementation of the Carr-Madan algorithm for pricing European option under the BS model. This method provides a benchmark for pricing options with Fourier transform methods using FFT algorithm. For efficient calibration of the model using the Carr-Madan method, the optimal choice of α is crucial. After experimenting with different values of α, we suggest for pricing European calls with $T \in [0.01, 10]$ under the BS model, $\alpha \in [1.5, 3]$ could be a good choice for the damping variable. As the number of steps in the numerical integration increases, error convergence smoothness increases. The order of error convergence is algebraic. In Section 3.3, we present another Fourier transform-based method that improves on the Carr-Madan approach.

3.3 The Convolution method: Extension of Carr-Madan

Similar to the spirit of Carr and Madan (1999) and Reiner (2001), Lord *et al.* (2008) presents a Fourier transform-based method primarily developed for pricing early-exercise options. The main insight of this method is based on Fourier convolution (see Theorem 2.5.2). The Fourier convolution method was first introduced in option pricing by Carverhill and Clewlow (1990). They represent the density of the sum of random variables as a convolution of each density using FFT, and then integrate the payoff function against the density function. Since then, the convolution method has been widely applied in the valuation of options. In this section, we discuss the Convolution method Lord *et al.* (2008). Before pricing early-exercise options with the CONV method, the prices of the European counterpart of the options must be known because the implementation of the early-exercise option is based on the successive application of the risk-neutral valuation formula for European options using dynamic programming, Lord *et al.* (2008). Thus, we will discuss the pricing of European options by the CONV method before extending it to early-exercise options in Chapter 4. For details on the application of the CONV method and the implementation see Section 4.2. The main idea of Reiner (2001) and Lord *et al.* (2008), is based on the stationary independent increments of a Lévy process which allows the the probability density function of the underlying process to be written as the transition density. Recall the risk-neutral valuation formula can be written as

$$V_0(x) := e^{-r\Delta t}\mathbb{E}^{\mathbb{Q}}[\Psi(y)] \tag{3.27}$$

where $\Psi(\cdot)$ is the pay-off function. Since equation 3.27 is an expectation and the process of the underlying variables is Markovian in nature, we represent equation 3.27 as

$$V_0(x) := e^{-r\Delta t}\int_{-\infty}^{\infty}\Psi(y)\mathbf{f}(y|x;\Delta t)dy \tag{3.28}$$

where $\Delta t = T - t_0$ and $\mathbf{f}(y|x;\Delta t)$ is the conditional probability density function representing the transition of x at time t_0 to y at time T. Assuming x is a log-asset price, $\left(\ln\frac{S_0}{S_0}\right) = 0$ at t_0 and the log-asset price of y is $\left(\ln\frac{S_T}{S_0}\right)$ at T. If the model of the underlying process is a BS model, then, y is normally-distributed. It is important to note the probability density function $\mathbf{f}(y|x;\Delta t)$ governing the change in log-asset price over Δt can be written as

$$\mathbf{f}(y|x;\Delta t) = \mathbf{f}(y-x;\Delta t) = \mathbf{f}(z;\Delta t). \tag{3.29}$$

This means the conditional transition density is a function that depends only on the size of the transition, or change in log-asset price. The function $\mathbf{f}(z)$ which satisfies equation 3.29 will be referred to as unconditional transition density function hereafter. To obtain the analytic formula for equation 3.28, Reiner (2001) suggests equation 3.28 can be expressed as a convolution of the discounted payoff function with the transition density function which can be approximated efficiently by the FFT algorithm. The CONV method is developed based on the Reiner (2001) suggestion, and the FFT implementation is the Carr and Madan (1999) initiative. Next, we discuss the Fourier transform of equation 3.28. Recall the product of Fourier transforms of two functions being convolved is the same as a Fourier transform of a convolution.

3.3.1 Fourier transform of the option value

In the same manner to the Carr and Madan (1999) method discussed in Section 3.2, to ensure the Fourier and inverse Fourier transform of option values exist, i.e, satisfy equation 2.43, a damping variable α is applied. Although with respect to log-asset price not strike price as in Carr and Madan (1999). Recall, the restriction placed on α depends on the option pay-off. Let the damping option value be written as $v(x, t_m)$ so that

$$v_0(x) := e^{\alpha x} V_0. \tag{3.30}$$

Recall from equation 2.40, the Fourier transform of $v_0(x)$ is given by:

$$\begin{aligned} \mathcal{F}\{v_0(x)\}(\omega) &:= \int_{-\infty}^{\infty} e^{i\omega x} v_0(x) dx \\ &= \int_{-\infty}^{\infty} e^{i\omega x} e^{\alpha x} V_0 dx \end{aligned} \tag{3.31}$$

where $\omega \in \mathbb{R}$ is the argument of the Fourier transform. Substitute equations 3.28 and 3.29 into equation 3.31, then:

$$\mathcal{F}\{v_0(x)\}(\omega) := \int_{-\infty}^{\infty} e^{i\omega x} \left(e^{\alpha x} e^{-r\Delta t} \int_{-\infty}^{\infty} \Psi(x+z) \mathbf{f}(z; \Delta t) dz \right) dx. \tag{3.32}$$

Note the damping quantity $v_0(x+z) := e^{\alpha(x+y)} V_0$. To express equation 3.32 in term of $V(\cdot)$ the option price, un-damped the equation such that;

$$\begin{aligned} \mathcal{F}\{V_0(x)\}(\omega) &:= e^{-r\Delta t} \int_{-\infty}^{\infty} e^{i\omega x} e^{\alpha x} \int_{-\infty}^{\infty} \Psi(x+z) \mathbf{f}(z; \Delta t) e^{-\alpha(x+z)} dz dx \\ \mathcal{F}\{V_0(x)\}(\omega) &:= e^{-r\Delta t} \int_{-\infty}^{\infty} \int_{-\infty}^{\infty} e^{i\omega(x+z)} \Psi(x+z) \mathbf{f}(z; \Delta t) e^{-i\omega z - \alpha z} dz dx \\ &= e^{-r\Delta t} \int_{-\infty}^{\infty} \int_{-\infty}^{\infty} e^{i\omega(x+z)} \Psi(x+z) \mathbf{f}(z; \Delta t) e^{-i(\omega - i\alpha)z} dz dx. \end{aligned}$$

Recall $y - x = z$, changing the order of integration, $dx = dy$:

$$\mathcal{F}\{V_0(x)\}(\omega) := e^{-r\Delta t} \int_{-\infty}^{\infty} \int_{-\infty}^{\infty} e^{i\omega(y)} \Psi(y) dy \ \mathbf{f}\ (z; \Delta t) e^{-i(\omega - i\alpha)z} dz. \tag{3.33}$$

Using the fact that the Fourier transform of a density function is the CF;

$$\Phi_X(\omega) := \int_{\mathbb{R}} e^{i\omega t} \mathbf{f}_X(t) dt \quad \text{and} \quad \mathbf{f}_X(t) := \frac{1}{2\pi} \int_{\mathbb{R}} e^{-i\omega t} \Phi_X(\omega) d\omega,$$

equation 3.33 becomes;

$$\begin{aligned} \mathcal{F}\{V_0(x)\}(\omega) &:= e^{-r\Delta t} \mathcal{F}\{\Psi(\cdot)\}(\omega) \Phi_h(-(\omega - i\alpha); \Delta t) \\ &= e^{-r\Delta t} \mathcal{F}\{\Psi(\cdot)\}(\omega) \Phi_h((i\alpha - \omega); \Delta t). \end{aligned} \tag{3.34}$$

Taking the inverse Fourier transform of equation 3.34, the option value is given by;

$$V_0 := e^{-r\Delta t}\mathcal{F}^{-1}\{\mathcal{F}\{\Psi(\cdot)\}(\omega)\Phi_h((i\alpha-\omega);\Delta t)\}. \tag{3.35}$$

To calculate equation 3.35, we compute the inverse Fourier transform of the product of the Fourier transform of $\Psi(\cdot)$ and the quantity $\Phi(\cdot)$. Studying equation 3.35, the damping coefficient only appears in the CF and the transition probability density function is always bounded. i.e, $\Phi(i\alpha) < \infty$. Thus, we ignore the damping variable in the numerical implementation.

3.3.2 Implementation details

Considering the expression given in equation 3.35, we noticed that the simplification of $V(\cdot)$ is not going to be trivial. Thus, we propose to approximate the equation by discrete sums so that FFT can be used for the computation. This motivates the use of uniform grids for the state variable y and the angular frequency ω. Recall: If x is a log-asset price at time t_0, $x = \log(S_0/S_0) = 0$. For consistency, the grids $\bar{y}$ and $\bar{\omega}$ are given by

$$\bar{y} := [y_{\min}, y_{\max}],$$
$$\bar{\omega} := [\omega_{\min}, \omega_{\max}].$$

To avoid the effects of aliasing caused by the use of the DFT that resulted into a distorted overlapped approximation of the Fourier transform, it is important that the Nyquist relation is satisfied. We could implement the FRFFT algorithm Bailey *et al.* (1991) without satisfying the Nyquist relation but numerical results show FFT is more efficient than the FRFFT algorithm, Lord *et al.* (2008).

Selecting the discretisation grid:

In order to reduce the errors in approximating the Fourier integral by a discrete Fourier transform, the grids need to be wisely chosen to control and reduce oscillation. Lord *et al.* (2008) propose $[-\frac{L}{2}, \frac{L}{2}]$ to replace the infinite range of integration on the Fourier series, for $L > 0$. It is important to ensure the underlying asset price lies on the $\bar{y}$ grid to avoid discontinuity.

Deriving L: To derive the length of the truncation range L such that the mass of the density outside $\left[-\frac{L}{2}, \frac{L}{2}\right]$ is negligible to avoid aliasing, Lord *et al.* (2008) propose a principle that has a wide application but is not strictly accurate or reliable in every situation. That is,

$$L \propto \mathcal{S}(\cdot)$$

where

$$L = \mathcal{K}\mathcal{S}(\cdot), \tag{3.36}$$

$\mathcal{K}$ is the proportionality constant and $\mathcal{S}(\cdot)$ is the standard deviation of the log-asset price S at time T conditional on the initial time 0. The rule of thumb is implemented

similar to the suggestion by Andricopoulos *et al.* (2003). In their observation, they set $\bar{y}$ to

$$\bar{y} := [x - L, x - L + \Delta y, \cdots, x + L]$$

where Δy is the difference between two steps and N is the number of steps in the integration. This implies the probability density function should be calculated as a $\mathcal{K}$ standard deviation on the negative and positive side of x on the y grid. Recall $x = 0$. For the BS model, $\mathcal{S}(\Delta t) = \sigma\sqrt{T}$. Thus, $L = \mathcal{K} \cdot \sigma\sqrt{T}$ where $\mathcal{K} = 10$ is expected to give satisfactory result because the probability that an underlying asset driven by geometric Brownian motion where we have more than 10 standard deviation at a given time interval, is insignificant Andricopoulos *et al.* (2003). However, larger values for L reduce the truncation errors on the y grid, and cause the size of the ω grid to be smaller, whereby the truncation error in the ω-domain increases Lord *et al.* (2008). Sullivan (2005) proposes $\mathcal{K} = 20$ for $N = 512$ and 1024. Lord *et al.* (2008) validates $\mathcal{K} = 20$ for the BS model, and $\mathcal{K} = 40$ for Lévy models which have fatter tails. The selection of the ω-grid and y-grid is trivial when pricing an European option, because the option is time independent. Recall $\bar{y} = [y_{\min}, y_{\max}]$. In order to have a smooth convergence, it is important to avoid any source of discontinuity in the domain. For a European call (V), $S_T > K$ so that $\frac{\partial V}{\partial S} = 1$ (the option is valued). But for $S_T < K$, $\frac{\partial V}{\partial S} = 0$ (the option is worthless). Thus, there is discontinuity on the y-grid when $y = 0$. To avoid discontinuity, we tend to ignore a region with worthless prices. We split the $\bar{y}$ into two regions, with the discontinuity point $y = 0$ on the boundary such that

$$\bar{y} := [y_{\min}, y_{\max}] = [[y_{\min}, 0], [0, y_{\max}]]. \tag{3.37}$$

Then,

$$\bar{y} := [0, y_{\max}]$$

and

$$\frac{N}{2} := \frac{y_{\max} - 0}{\Delta y}.$$

Recall $\bar{y} := \left[-\frac{L}{2}, \frac{L}{2}\right]$, then

$$y_0 := -\frac{L}{2}, \qquad \Delta y := \frac{L}{N}. \tag{3.38}$$

Using the Nyquist relation;

$$\Delta\omega\Delta y := \frac{2\pi}{N}$$

and

$$\Delta\omega := \frac{2\pi}{L}.$$

Then;

$$[y_0, y_{N-1}] := \left[-\frac{L}{2}, \frac{L}{2} - \Delta y\right]$$

and

$$[\omega_0, \omega_{N-1}] := \left[-\frac{N\pi}{L}, \left(N-1-\frac{N}{2}\right)\frac{2\pi}{L}\right].$$

Thus, we can say;

$$y_j = \left[j - \frac{N}{2}\Delta y\right] \tag{3.39}$$

and

$$\omega_j = \left[j - \frac{N}{2}\Delta\omega\right]. \tag{3.40}$$

Effect of T:

Result 3.3.1 (Effect of T on the CONV method for pricing European calls under the BS model)**.** Reference prices are given by the analytic solution. We observe that under the BS model, short-dated and one-year European calls are in agreement with the reference prices when the strikes are bounded between half and double of the initial stock-price.

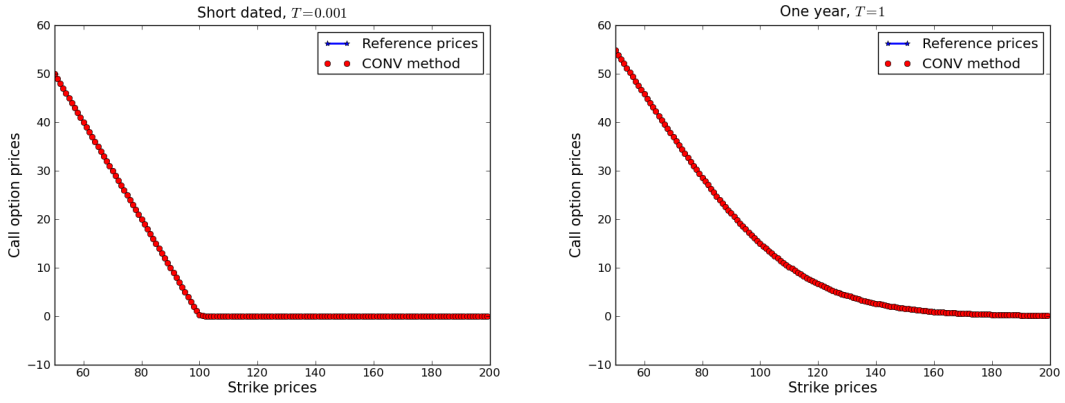

Figure 3.4: European calls under BS model. Parameters used: $K = [50, 200]$, $S_0 = 100$, $\sigma = 0.25$, $r = 0.1$, $N = 2^6$ and $\mathcal{K} = 10$.

Role of $\mathcal{K}$:

Result 3.3.2 (Effect of $\mathcal{K}$ (the proportional constant) on the CONV method for pricing European calls)**.** Reference prices for the BS model are given by the analytic solution. For the NIG model, we used the CONV method by setting $N = 2^{20}$, and the reference price for the VG model is taken from Sullivan (2005). Investigating the effect of $\mathcal{K}$ on the CONV method, Figure 3.5 shows at $\mathcal{K} = 10$, the prices of the European calls gives more accurate results under the BS model. This is in agreement with the suggestion by Andricopoulos *et al.* (2003). In Figure 3.6, we observe for at-the-money call under the BS, NIG, VG models, $\mathcal{K} = 10$ gives a more accurate

result when $N = 64$. Experiments show that the optimal choice of $\mathcal{K}$ for a particular model is not trivial, for optimal values of $\mathcal{K}$ for each model for different values of K and N changes over time. In all our numerical results, we set $\mathcal{K} \in [10, 40]$.

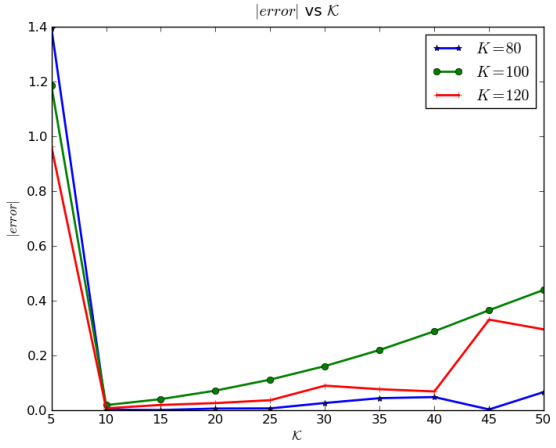

Figure 3.5: The absolute differences between the references prices and CONV method for pricing European calls under the BS model with respect to $\mathcal{K}$. Parameters used: $S_0 = 100$, $K = [80, 100, 120]$, $\sigma = 0.25$, $r = 0.1$ and $N = 2^6$.

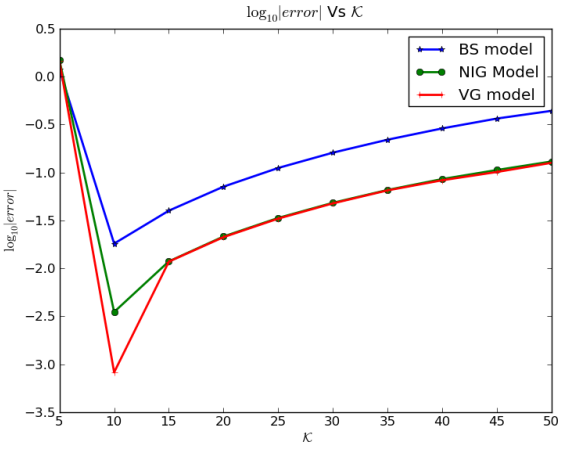

Figure 3.6: Error convergence of the CONV method for pricing European calls under the BS, NIG and VG models with respect to $\mathcal{K}$: Parameters used: $T = 1$, $N = 2^6$, $S_0 = 100$, $K = 100$, $\sigma_{BS} = 0.25$, $\sigma_{NIG} = 0.12$, $\sigma_{VG} = 0.12$, $\theta_{VG} = -0.14$, $\kappa = 0.2$, $\alpha = 28.42141$, $\beta = -15.086$ and $\delta = 0.31694$.

3.3.3 Summary

Algorithm 3.3.1: **Convolution method.**

1: Declare the initial variables: S_0, T, K, N, $\mathcal{K}$;
2: Compute L according to equation 3.36;
3: Discretize the spatial domain using equation 3.39 (for $0 \leq j \leq N-1$);
4: Discretize the frequency domain according to equation 3.40, based on Nyquist relation;
5: Compute the payoff function $\Psi(\cdot)$ (for $0 \leq j \leq N-1$);
6: Compute the CF of log-asset returns of the distribution of the model, that is, $\Phi(\cdot)$;
7: Compute the option value V_0 via FFT according to equation 3.35 (for $0 \leq j \leq N-1$).

We have discussed the CONV method. Algorithm 3.3.1 summarises the implementation of the CONV algorithm for pricing European options under different models. The method is based on the insight of Carr and Madan (1999) and Reiner (2001). The CONV method is widely applicable to any process with stationary and independent increments and to any monotonic functions of asset price, not necessarily the log-asset price. The implementation details are similar to the method of Andricopoulos *et al.* (2003). The optimal choice of L for discretizing the infinite integral wholly depends on the model and the type of option to be priced. To price European options, the CONV method gives satisfactory results without any dependence on the damping variable, unlike Carr and Madan (1999) method.

3.4 Fourier-cosine series expansion

Fourier series are well-known for representing periodic functions by the coefficients of the function in an expansion, as a sum of sine and cosine functions. The main aim of this section is to reconstruct the integral in the risk-neutral pricing formula, equation 2.38 from its Fourier-cosine series expansion and factorizing out the series coefficient directly from the integrand. Let us introduce the Fourier series expansion. Fourier series can be described as the trigonometric representation of a periodic function in terms of cosine and sine waves. Recall from Boyd (2000), the basics of a Fourier series expansion. Let $\mathbf{f}(\theta)$ be a function defined and integrable on the interval $(-\pi, \pi)$, the Fourier series of $\mathbf{f}(\theta)$ is given by

$$\mathbf{f}(\theta) := \frac{A_0}{2} + \sum_{n=1}^{\infty}(A_n \cos(n\theta) + B_n \sin(n\theta)) \tag{3.41}$$

where

$$\begin{aligned} A_0 &:= \frac{1}{2\pi}\int_{-\pi}^{\pi} \mathbf{f}(\theta)d\theta \\ A_n &:= \frac{1}{\pi}\int_{-\pi}^{\pi} \mathbf{f}(\theta)\cos(n\theta)d\theta \\ B_n &:= \frac{1}{\pi}\int_{-\pi}^{\pi} \mathbf{f}(\theta)\sin(n\theta)d\theta, \end{aligned}$$

for $1 \leq n$, A_0, A_n and B_n are called the Fourier-coefficients. If $\mathbf{f}(\theta)$ is defined on a finite interval $[a, b] \in \mathbb{R}$, the Fourier series expansion can be easily obtained by a change of variable approach. Let

$$\theta := \frac{(y-a)\pi}{b-a}, \qquad y := \theta + a. \tag{3.42}$$

Substitute equation 3.42 into 3.41. Thus, equation 3.41 becomes

$$\mathbf{f}(y) := \frac{A_0}{2} + \sum_{n=1}^{\infty}\left[A_n \cos\left(n\pi\frac{y-a}{b-a}\right) + B_n \sin\left(n\pi\frac{y-a}{b-a}\right)\right]. \tag{3.43}$$

If $\mathbf{f}$ is even, $\mathbf{f}(y) = \mathbf{f}(-y)$, then

$$A_n := \frac{2}{b-a}\int_0^b \mathbf{f}(y)\cos\left(n\pi\frac{y-a}{b-a}\right)dy, \tag{3.44}$$

and $B_n = 0$.
If $\mathbf{f}$ is odd, $\mathbf{f}(-y) = -\mathbf{f}(y)$, then

$$B_n := \frac{2}{b-a}\int_0^b \mathbf{f}(y)\sin\left(n\pi\frac{y-a}{b-a}\right)dy, \tag{3.45}$$

and $A_n = 0$. For $1 \leq n < \infty$ and $a \leq 0 \leq b$.
Thus, if a function $\mathbf{f}$ is defined on an interval $[0, b]$, for $a \leq 0 \leq b$, it can be made even by extending its domain:

$$\mathbf{f} : [a, b] \to \mathbb{R} : y \to \begin{cases} \mathbf{f}(y) & y \in [0, b] \\ \\ \mathbf{f}(-y) & y \in [a, 0]. \end{cases}$$

Recall the risk-neutral pricing formula, equation 2.38;

$$V(x,t) := e^{-r\Delta t}\int_{\mathbb{R}} \Psi(y,T)\mathbf{f}(y|x)dy \tag{3.46}$$

where

$$\mathbf{f}(y|x) := \frac{1}{2\pi}\int_{-\infty}^{\infty} e^{-i\omega y}\Phi(\omega)d\omega \tag{3.47}$$

and $V(x,t)$ is the option price, $\Delta t = T - t$, for $t \in [0,T]$, $\Psi(y,T)$ is the pay-off function, x and y are state variables at time t and T, and $\mathbf{f}(y|x)$ is the conditional probability density function. Knowing the function $\mathbf{f}(y)$ in equation 3.43 is square-integrable, we want to express the density function $\mathbf{f}(y|x)$ in terms of $\mathbf{f}(y)$.

As $V(x,t)$ is always a real number, $V(x,t) = \overline{V(x,t)}$. Thus changing the variable x into $-x$ in $V(x,t)$ is the same, and this implies the real part of $\Psi(\cdot)$ is even and the imaginary part is odd. Recall the Fourier series of a periodic even-function includes only the Fourier-cosine series part. Hence,

$$\mathbf{f}(y) := \frac{A_0}{2} + \sum_{n=1}^{\infty}\left[A_n \cos\left(n\pi\frac{y-a}{b-a}\right)\right], \quad \text{for } B_n = 0. \tag{3.48}$$

In this section, the COS formula for pricing vanilla-European options is established, following the idea implemented in Fang and Oosterlee (2008). We discuss a different method in solving the inverse Fourier integral in equation 2.38. We take advantage of the fact that only a few terms in the expansion may be needed to give a good approximation, due to the fact that a density function tends to be continuously differentiable. It follows from the analysis of Fang and Oosterlee (2008) that when dealing with transition densities for which there are no singularities on $[a,b]$, the cosine series expansion of $\mathbf{f}(y|x;\Delta t)$ will exhibit an exponential convergence.

In this method, the density function in the risk-neutral pricing formula is computed from the CF of the distribution by Fourier cosine expansion. As a consequence of the integrability condition of existence of a Fourier transform, the infinite range of integration of the density functions have to decay to zero at $\pm\infty$. Then, we can truncate the infinite integration range to a finite range without losing significant accuracy. Let $[a,b] \in \mathbb{R}$ such that:

$$\int_{\mathbb{R}\setminus[a,b]} \mathbf{f}(y|x)dx < \delta \tag{3.49}$$

for some tolerance level δ. Equation 3.49 implies that for $[a,b] \notin \mathbb{R}$, the value of the integral of the density function is negligible. Therefore, equation 3.46 can be written as follows:

$$V(x,t_0) := e^{-r\Delta t}\int_a^b \Psi(y,T)\mathbf{f}(y|x)dy + \varepsilon, \tag{3.50}$$

where ε is the error due to the truncation of interval $[a,b]$. Now, we want to reconstruct the whole integral by extracting the series coefficient directly from the

integrand. The density function in equation 3.50 can be written in form of the cosine expansion of $f(y)$, that is, by substitute equation 3.43 into 3.50, then,

$$V(x,t_0) := e^{-r\Delta t}\int_a^b \Psi(y,T)\sum_{n=0}^{\infty}{}' \left[A_n \cos\left(n\pi\frac{y-a}{b-a}\right)\right] dy + \varepsilon. \tag{3.51}$$

where $\sum'$ means the first term of the summation of the series is weighted by half. Let

$$\mathcal{V}_n := \frac{2}{b-a}\int_a^b \Psi(y,T)\cos\left(n\pi\frac{y-a}{b-a}\right) dy \tag{3.52}$$

be the coefficient of the Fourier cosine expansion of price function. Thus, equation 3.51 becomes;

$$V(x,t_0) := \frac{b-a}{2}\cdot e^{-r\Delta t}\sum_{n=0}^{\infty}{}' A_n\mathcal{V}_n. \tag{3.53}$$

Assuming we have successively chosen $[a,b] \in \mathbb{R}$ such that the truncated interval is approximately the infinite integral, then we can say that

$$\Phi^*(\omega) := \int_a^b \mathbf{f}(y|x)e^{i\omega y}d\omega \approx \int_{\mathbb{R}} \mathbf{f}(y|x)e^{i\omega y}d\omega = \Phi(\omega). \tag{3.54}$$

where $\Phi(\cdot)$ is the CF of the conditional density $\mathbf{f}(y|x)$ under the risk-neutral measure.

3.4.1 Density recovery: Deriving A_n

Recall from the Euler identity,

$$e^{iA} := \cos A + i\sin A, \quad \mathcal{R}\{e^{iA}\} := \cos A \quad \text{and} \quad \mathcal{I}\{e^{iA}\} := \sin A$$

then,

$$\mathcal{R}\left\{e^{in\pi\frac{y-a}{b-a}}\right\} := \cos\left(n\pi\frac{y-a}{b-a}\right) \quad \text{and} \quad \mathcal{I}\left\{e^{in\pi\frac{y-a}{b-a}}\right\} = \sin\left(n\pi\frac{y-a}{b-a}\right).$$

Thus, A_n in equation 3.43 can be expressed as:

$$A_n := \frac{2}{b-a}\int_a^b \mathbf{f}(y|x)\mathcal{R}\left\{e^{in\pi\frac{y-a}{b-a}}\right\} dy \approx \frac{2}{b-a}\mathcal{R}\left\{e^{-in\pi\frac{a}{b-a}}\Phi^*\left(\frac{n\pi}{b-a},x\right)\right\}. \tag{3.55}$$

It follows from equation 3.54 that $A_n \approx H_n$ in the series expansion of $\mathbf{f}(y)$ with

$$H_n := \frac{2}{b-a}\mathcal{R}\left\{e^{-in\pi\frac{a}{b-a}}\Phi\left(\frac{n\pi}{b-a},x\right)\right\}. \tag{3.56}$$

Hence, we substitute equation 3.56 into the cosine expansion in equation 3.48 to obtain,

$$h_1(x) := \sum_{n=0}^{\infty}{}' H_n \cos\left(n\pi\frac{x-a}{b-a}\right). \tag{3.57}$$

To approximate the infinite series of summation in equation 3.57, we truncate the series such that equation 3.57 becomes,

$$h_2(x) := \sum_{n=0}^{N-1}{}' H_n \cos\left(n\pi \frac{x-a}{b-a}\right). \tag{3.58}$$

The resulting error in equation 3.58 consists of two parts: An error generating from approximating $An \approx Hn$ due to truncating the range of integration to $[a, b]$ and a series truncation error from equation 3.57 to 3.58 Fang and Oosterlee (2008).

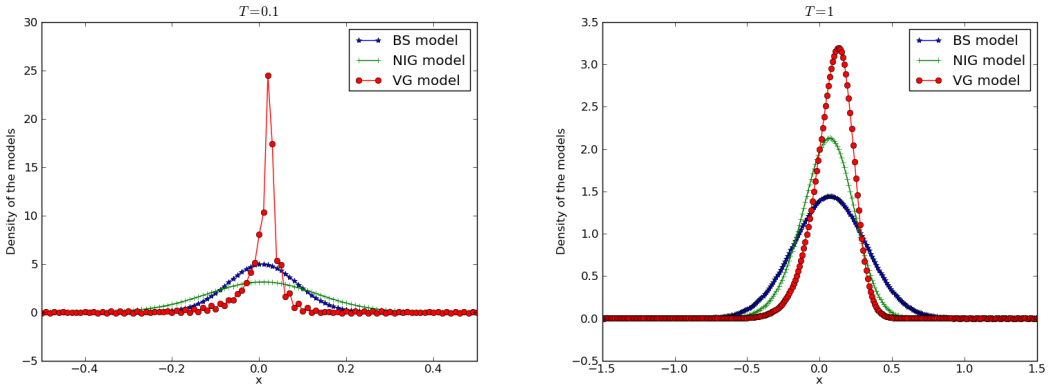

Figure 3.7: Recovered density functions of BS, NIG and VG models. Parameters used: $L = 10$, $N = 2^7$, $\sigma_{BS} = 0.25$, $\sigma_{NIG} = 0.12$, $\sigma_{VG} = 0.12$, $r = 0.1$, $\alpha = 28.42$, $\beta = -15.08$, $\delta = 0.31$, $\theta_{VG} = -0.14$ and $\kappa = 0.2$.

Figure 3.7 shows the difference in shape of recovered density functions for three different models at two maturities. For $T = 0.1$; in the BS model, we observe the distribution does not have fat tails as we have when $T = 1$, which is predominant to the CF of a normal distribution; the NIG model retains its shape at both maturities; in the VG model, the density has a sharp peak. The sharp-peakedness originates from the discontinuous part of the CF due to the fact that $\Delta t(0.1) < \kappa(0.2)$, κ is the variance in the VG model. Sharp peakedness in the density function causes difficulties in numerical integration.

Remark 3.4.1. Direct numerical integration can price European options successfully when T is sufficiently large without loosing significant accuracy. Difficulties are encountered if T is too small. For small maturity dates, the density becomes unpredictably large near the origin as the maturity date decreases.

3.4.2 Deriving $\mathcal{V}_n$

Let us assume that the CF of a log-asset price is known, and represents the pay-off as a function of the log-asset price normalized by the strike price. Thus, the log-asset price is given by

$$x := \ln(S_0/K), \qquad y := \ln(S_T/K). \tag{3.59}$$

The pay-off of the European option follows:

$$\Psi(y,T) := (\iota \cdot K(e^y - 1))^+, \text{ with } \quad \iota = \begin{cases} 1 & \text{for a call option,} \\ -1 & \text{for a put option.} \end{cases}$$

Substitute $(\iota \cdot K(e^y - 1))^+$ into 3.52, then equation 3.52 becomes

$$\mathcal{V}_n := \frac{2}{b-a}\int_a^b \Psi(y,T)\cos\left(n\pi\frac{y-a}{b-a}\right)dy = \frac{2\iota.K}{b-a}\int_a^b (e^y-1)^+\cos\left(n\pi\frac{y-a}{b-a}\right)dy. \tag{3.60}$$

Now, split the integral part of equation 3.60 into two on $[c,d] \subset [a,b]$. For a call, we integrate from $c = 0$ to $d = b$ since the pay-off $\Psi(y,T)$ is positive when $\ln\left(\frac{S_T}{K}\right) > 0$. For a put, we integrate from $c = a$ to $d = 0$. The first integral part with $[e^y]$, i.e, the cosine series coefficient β_n on $[c,d] \subset [a,b]$ is given by

$$\beta_n(c,d) := \int_c^d e^y \cos\left(n\pi\frac{y-a}{b-a}\right)dy \tag{3.61}$$

and the second part [1] with cosine series coefficient γ_n on $[c,d] \subset [a,b]$ is given by

$$\gamma_n(c,d) := \int_c^d \cos\left(n\pi\frac{y-a}{b-a}\right)dy. \tag{3.62}$$

Using the basic calculus integration of the trigonometry function;

$$\int_a^b e^{ms}\cos(mt)dm := \left(\frac{e^{bs}}{s^2+t^2}(s\cos(bt)+t\sin(bt)) - \frac{e^{as}}{s^2+t^2}(s\cos(at)+t\sin(at))\right)$$

and

$$\int_a^b \cos(mt)dm := \{\sin(bt) - \sin(at)\}.$$

Thus, equation 3.61 and 3.62 becomes

$$\begin{aligned}\beta_n(c,d) :=& \frac{1}{1+\left(\frac{n\pi}{b-a}\right)^2}\left[\cos\left(k\pi\frac{d-a}{b-a}\right)e^d - \cos\left(n\pi\frac{c-a}{b-a}\right)e^c\right] \\ &+ \frac{n\pi}{b-a}\sin\left(n\pi\frac{d-a}{b-a}\right)e^d - \frac{n\pi}{b-a}\sin\left(n\pi\frac{c-a}{b-a}\right)e^c\end{aligned}$$

and

$$\gamma_n(c,d) := \begin{cases} \left[\sin\left(n\pi\frac{d-a}{b-a}\right) - \sin\left(n\pi\frac{c-a}{b-a}\right)\right]\frac{b-a}{n\pi} & n \neq 0, \\ (d-c) & n = 0. \end{cases}$$

Assuming $(a \leq 0 \leq b)$, the pay-off function for a European call and put with a constant value $\frac{2}{b-a}$ is given by

$$\mathcal{V}_n^c := \frac{2}{b-a}\int_a^b [K(e^y-1)]^+ = \frac{2}{b-a}K[\beta_n(0,b) - \gamma_n(0,b)] \tag{3.63}$$

and

$$\mathcal{V}_n^p := \frac{2}{b-a}\int_a^b [K(1-e^y)]^+ = \frac{2}{b-a}K[-\beta_n(a,0)+\gamma_n(a,0)]. \tag{3.64}$$

Thus, the approximated formula for the option value $V(x,t_0)$ from equation 3.53 is given by

$$V(x,t_0) \approx \frac{b-a}{2}e^{-r\Delta t}\sum_{n=0}^{N-1}{}'\mathcal{R}\left\{e^{-in\pi\frac{a}{b-a}}\Phi\left(\frac{n\pi}{b-a};x\right)\right\}\cdot\mathcal{V}_n. \tag{3.65}$$

This is the *COS formula for general underlying processes.* In order to price the contracts with the COS formula, the analytic solution of $\mathcal{V}_n$ is required. Substituting equation 3.63 into equation 3.65, the *COS formula for pricing European call option* is written as

$$V(x,t_0) \approx \frac{2K\cdot e^{-r\Delta t}}{b-a}\sum_{n=0}^{N-1}{}'\mathcal{R}\left\{e^{-in\pi\frac{a}{b-a}}\Phi\left(\frac{n\pi}{b-a};x\right)\right\}.(\beta_n(0,b)-\gamma_n(0,b)). \tag{3.66}$$

To price options with a range of strikes at a single time step, $\mathcal{V}_n$ in equation 3.65 can be written as

$$\mathbf{V}_n := \begin{cases} \frac{2}{b-a}\mathbf{K}[\beta_n(0,b)-\gamma_n(0,b)], & \text{for a call option} \\ \frac{2}{b-a}\mathbf{K}[-\beta_n(a,0)+\gamma_n(a,0)], & \text{for a put option} \end{cases}.$$

where $\mathbf{K}$ is the range of strikes. The COS formula for pricing vanilla European call options with many strikes $\mathbf{K}$ is

$$V_{\mathbf{K}} \approx \frac{2\mathbf{K}\cdot e^{-r\Delta t}}{b-a}\sum_{n=0}^{N-1}{}'\mathcal{R}\left\{e^{in\pi\frac{\mathbf{x}-a}{b-a}}\Phi\left(\frac{n\pi}{b-a}\right)\right\}\cdot(\beta_n(0,b)-\gamma_n(0,b)) \tag{3.67}$$

where the summation can be written as a matrix-vector product if $\mathbf{K}$ is a list of values. The COS method is applicable to calculate the hedge parameter with less modification to the original formula.

3.4.3 Implementation details

Studying equation 3.63 we notice there are some undetermined parameters. These parameters are the range of integration, $[a,b]$, and the number of steps in the sum, N. The next question is: "How do we choose these parameters, especially the range of integration?"

In order to avoid a truncation error while truncating the infinite interval to finite interval, Fang and Oosterlee (2008) propose the following expression for truncating the range of the integration in the COS method:

$$[a,b] := \left[c_1 - L\sqrt{c_2+\sqrt{c_4}}, c_1 + L\sqrt{c_2+\sqrt{c_4}}\right] \qquad \text{with } L=10. \tag{3.68}$$

c_n represents the n-th cumulant of the log-asset price of the model. Recall the cumulants in the BS model. Thus, $c_1 = (r - \frac{\sigma^2}{2})$, $c_2 = \sigma^2$, $c_3 = 0$ and $c_4 = 0$. At time T, the truncated range of integration is

$$[a, b] := \left[(r - \frac{\sigma^2}{2})T - L\sqrt{\sigma^2 T}, (r - \frac{\sigma^2}{2})T + L\sqrt{\sigma^2 T}\right]. \tag{3.69}$$

Choosing the value of L:

The choice of L is very sensitive in pricing a call option because of the unbounded behaviour of the call pay-off by the strike value unlike the valuation of a put option. The payoff function of a call grows exponentially with the log-asset price and exhibits a scaling truncation error in the pay-off. Thus, Fang and Oosterlee (2008) propose that $L \in [7.5, 10]$ in equation 3.69 for valuing the call option when $T \in [0.1, 10]$. To avoid the restrictions placed on the range of L. Fang and Oosterlee (2008) propose to use put-call parity.

Put Call Parity:

Put-call parity is a vital tool in finance due to its flexibility and wide range application in practice. It establishes the relationship between a European call and put option with the same strike price and maturity time T. This assume the underlying asset is liquid[1] with no assumption on any financial models. Practitioners prefer to know the value of their options in-the-money to out-of-the-money, i.e to know the value of a call option out-of-the-money, they would rather find the value of a put option in-the-money which is equivalent. In our case, since the pricing of a put option is less sensitive to the value of L because the payoff is bounded by the value of K, we can successfully price the call option with the put-call parity. The put-call parity relation is given by

$$V_c(S) = V_p(S) + S_0 - Ke^{-rT}, \tag{3.70}$$

where $V_c(\cdot)$ is the pricing function for a European call option, $V_p(\cdot)$ is for the put option and r is the interest rate, Hull (2007). The importance of the put-call parity is presented in Result 3.4.4 and in subsequent experiments, the put-call parity is used.

Effect of L on T:

Result 3.4.2 (Effect of T on the COS method for pricing European calls under BS model)**.** As shown in Figure 3.8, for a short-dated ($T = 0.01$) span of European calls, $L = 10$ when $N = 64$ works accurately for prices in-the-money, at-the-money and out-of-the-money. For few prices deeply in-the-money and deeply out-of-the-money, this choice of L seems to be inaccurate. Larger values of L with larger values of N give a better result, see Figure 3.8. For a one-year span, $L = 10$ gives a satisfactory result (see Figure 3.9).

[1] market liquidity is an asset's ability to be sold without causing a significant movement in the price and with minimum loss of value

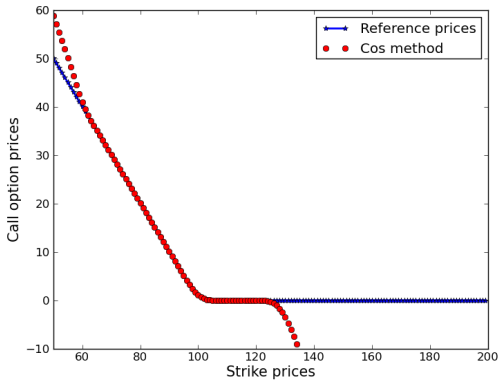

(a) Parameters used: $N = 2^6$ and $L = 10$.

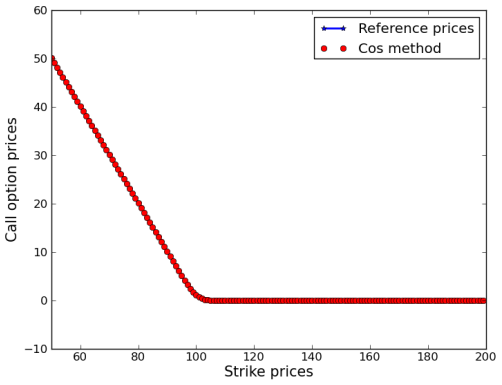

(b) Parameters used: $N = 2^{10}$ and $L = 30$.

Figure 3.8: Effect of T on the COS method for pricing short-dated ($T = 0.01$) European calls under BS model. Parameters used: $S_0 = 100$, $K = [50, 200]$, $\sigma = 0.25$ and $r = 0.1$.

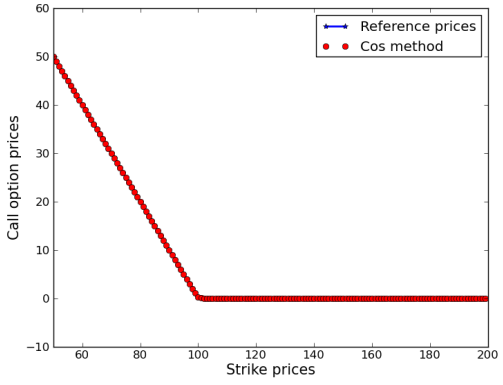

(a) Parameters used: $T = 0.001$, $N = 2^{10}$ and $L = 100$ and $N = 2^6$.

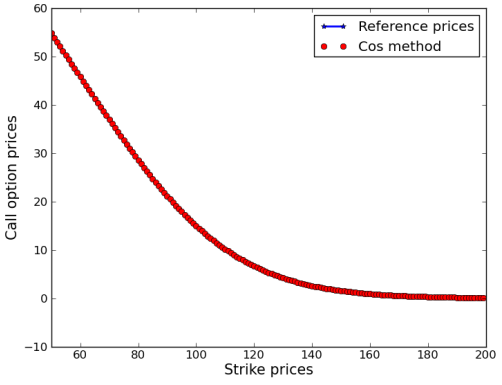

(b) Parameters used: $T = 1$, $N = 2^6$ and $L = 10$.

Figure 3.9: European calls under BS model. Parameters used: $S_0 = 100$, $K = [50, 200]$, $\sigma = 0.25$ and $r = 0.1$.

Result 3.4.3 (Effect of L (truncating parameter) on the COS method for pricing European calls under BS model)**.** We experiment with the effect of L and the put-call parity. Fang and Oosterlee (2008) suggest $L \in [7.5, 10]$. We notice for values deep in-the-money there is deviation from the reference prices but for some values in-the-money, at-the-money and out-of-money, $L \in [7.5, 10]$ works well. With the put-call parity, we can successfully price European calls by setting $L \in [5, 20]$.

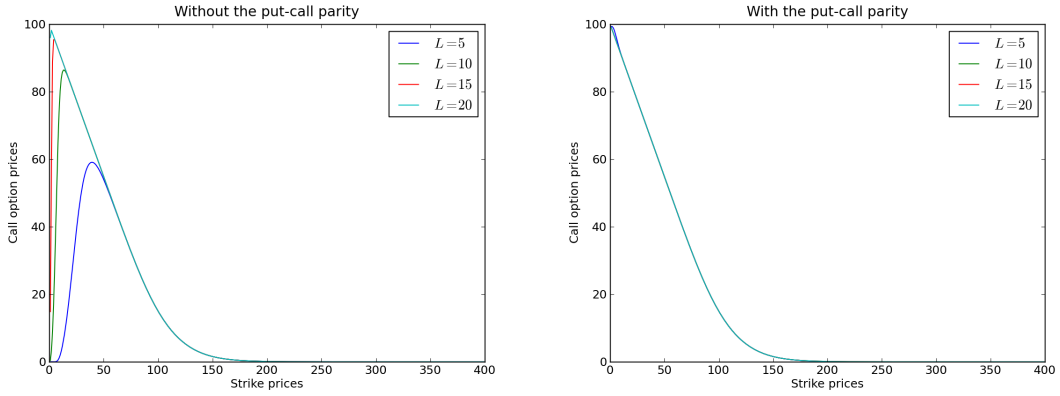

Figure 3.10: Effect of L on the COS method when pricing European calls under BS model with the put-call parity and without the put-call parity. Parameters used: S_0, $K = [0, 400]$, $\sigma = 0.25$, $r = 0.1$ and $N = 64$.

We experiment with Table 3.2 without the put-call parity approach. This shows for small value of N, the European calls converge faster when $L \in [8, 12]$. For $K = 80$, $L = 16$ takes 1000 points to reach the same level of accuracy with $L = 10$ when $N = 64$. Thus, we can say $L \in [8, 12]$ works well for pricing European calls under the BS model. Larger values of L require larger values of N to reach the same level of accuracy. We don't want to do this because its computationally expensive.

$K \vert L$	7	8	10	12	14	16
80	$2.13 \cdot 10^{-14}$	$7.10 \cdot 10^{-15}$	$2.13 \cdot 10^{-14}$	$7.11 \cdot 10^{-15}$	$7.81 \cdot 10^{-14}$	$1.36 \cdot 10^{-11}$
100	$1.47 \cdot 10^{-12}$	$7.10 \cdot 10^{-15}$	$7.10 \cdot 10^{-15}$	$7.10 \cdot 10^{-15}$	$9.23 \cdot 10^{-14}$	$1.92 \cdot 10^{-11}$
120	$2.76 \cdot 10^{-10}$	$1.84 \cdot 10^{-13}$	$7.10 \cdot 10^{-15}$	$7.10 \cdot 10^{-15}$	$1.42 \cdot 10^{-13}$	$7.70 \cdot 10^{-11}$

Table 3.2: Error convergence of the COS method for pricing European calls under BS model with respect to L. Parameters used: $S_0 = 100$, $K = [80, 100, 120]$, $\sigma = 0.25$, $r = 0.1$, $N = 64$ and $T = 1$.

The role of N:

Fang and Oosterlee (2008) observed that for the successful application of Fourier transformed integrals, a fine grid is required because of the high oscillatory behaviour of the integrand. The larger the value of N, the higher the computation cycle.

Result 3.4.4 (Effect of N on the COS method for pricing European calls under the BS model)**.** We experiment with this without the put-call parity approach. We observe the COS method retains the exponential order of convergence for larger values of N (a finer grid) across a range of strikes. The error convergence on the successive finer grids are the same for a one-year span of European calls with low volatility and high volatility. We observe the error convergence of the COS method is exponential and it clearly shows significant improvement over the Carr-Madan and CONV methods.

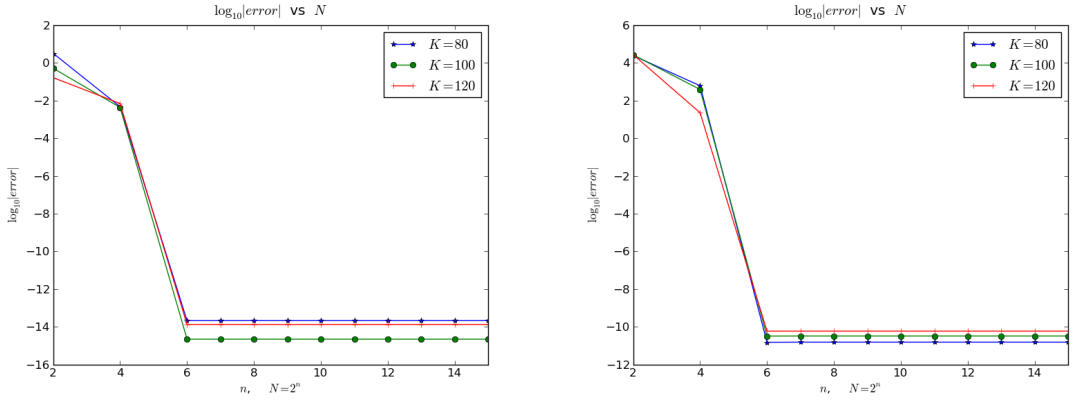

(a) One year with volatility ($\sigma = 0.2$). (b) One year with volatility ($\sigma = 0.7$)

Figure 3.11: Error convergence of COS method for pricing European calls under BS model with respect to N: Parameters used: $S_0 = 100$, $K = [80, 100, 120]$, $r = 0.1$, $T = 1$, $L = 10$.

3.4.4 Summary

Algorithm 3.4.1: **Fourier-cosine series method**

1: Declare the initial variables: S_0, T, K, N, L;
2: Compute a and b according to equation 3.68;
3: Compute $\mathcal{V}_n$ using equation 3.63 for a call and 3.64 for a put option (for $0 \leq n \leq N-1$);
4: Compute the CF of the log-asset price, that is, $\Phi(\cdot)$, (for $0 \leq n \leq N-1$);
5: Compute the option value V_0 according to equation 3.66 (for $0 \leq n \leq N-1$).

Algorithm 3.4.1 summarises the implementation of the COS algorithm for pricing European options under different models. The main idea in the derivation of the COS formula is built around the fact that the probability density function $\mathbf{f}(y|x)$ in the risk-neutral density function equation 2.38 can be substituted with the Fourier-cosine series expansion. The product of the probability density function and the pay-off function is transformed into a simple combination of the product of the pay-off function which can be derived analytically, and the cosine basis function. The Fourier-cosine series expansion of continuous function anywhere in the complex plane except at ∞ exhibits exponential convergence Boyd (2000). Thus, the COS method gives good approximations to density functions that have no discontinuities on interval $[a, b]$, with a small values of N. The efficiency of the COS method depends on the cosine series of the probability density function and not the pay-off function. The convergence, speed and accuracy of the COS method will be discussed in detail in Section 3.6.

3.5 Fourier space time-stepping method

When pricing options under the BS model, the pricing function is governed by PDE with independent variables being the underlying asset price and time. Under the Lévy model, the PDE is transformed to PIDE due to the presence of jump. Thus, the PIDE is solved in Lévy models. The PIDE is made up of the diffusion term and the integral term. The PDE can be solved directly to price many options by imposing the terminal conditions. The solution to the PIDE is non-trivial because of the integral part which are jump components. In this section we discuss the Fourier space time-stepping method, Jackson *et al.* (2007), Jaimungal and Surkov (2009), Surkov (2009). This method specialises in the pricing and hedging of options under exponential Lévy models by alternating between real space and Fourier space in order to solve the problems associated with the Fourier transform of the PIDE.

First, we introduce the PIDE for pricing options under the Lévy model. Recall the Feynman-Kač formula for Lévy processes. Let the option price function $V(s,t)$ be $C^{1,2}$, i.e. one is continuously differentiable in t and twice in s, $\forall\ t \in [0,T]$ such that

$$\begin{aligned} &\frac{\partial V(s,t)}{\partial t} + \gamma(s,t)\frac{\partial V(s,t)}{\partial s} + \frac{1}{2}\sigma^2(s,t)\frac{\partial^2 V(s,t)}{\partial s^2} \\ &+ \underbrace{\int_{\mathbb{R}} (V(s+y,t) - V(s,t) - \mathbb{I}_{|y|<1} y\frac{\partial V(s,t)}{\partial s})\nu(dy)}_{\text{jump component, } \nu(dy) \text{ is the Lévy measure}} = r(s,t)V(s,t) \end{aligned} \tag{3.71}$$

with the terminal condition

$$V(s,T) = \Psi(s),$$

where $\gamma(s,t)$, $\sigma(s,t)$ and $r(s,t)$ are known functions and $\nu(dy)$ is the Lévy measure of the risk-neutral distribution. Then,

$$V(s,t) := \mathbb{E}[e^{-\int_t^T r(s_\tau d\tau)}\Psi(S_T)|S_t = s], \tag{3.72}$$

and S is a Lévy process with fixed dynamics such that $S(0) = s$, Nualart and Schoutens (2001). Equation 3.72 is similar to the risk-neutral valuation formula in equation (2.38). Alternatively, the Feynman-Kăc formula can be used to derive the pricing formula in terms of equation (2.38). Thus, numerical methods can be used to approximate the option price.

Recall from equation 3.71, the expression for PIDE;

$$\begin{cases} [\partial_t + \mathcal{G}]V(s,t) &= 0 \\ V(s,T) &= \Psi(s) \end{cases} \tag{3.73}$$

where,

$$\mathcal{G}V(s) := \underbrace{\left(\gamma\partial_s + \frac{1}{2}\partial_s^2\sigma^2\right)V(s)}_{\text{diffusion term}} + \underbrace{\int_{\mathbb{R}^d/\{0\}} [V(s+y) - V(s) - \mathbb{I}_{|y|<1} y\partial_s V(s)]\nu(dy)}_{\text{integral term}} \tag{3.74}$$

and $\mathcal{G}$ is defined by the diffusion and integral component and works on $V(s)$. $V(s)$ is a twice-continuously differentiable function.

Various finite difference schemes have been implemented in literature to solve PIDE problems, equation 3.73, Andersen and Andreasen (2000), Cont and Tankov (2004), but are prone to problems of convergence and speed, Lord *et al.* (2008), Jackson. *et al.* (2008) and Surkov (2009). These schemes solve the PIDE in real space; the diffusion term and the integral term are often solved separately. The integral term is always solved explicitly in order to avoid solving a dense system of linear equations. Furthermore, the FFT algorithm is implemented to speed up the computation of the integral term by means of convolution or its inverse. Unfortunately, these methods demand quite a few approximations such as Jaimungal and Surkov (2009):

- Independent handling of the diffusion and the integral term demand that function values are extrapolated and interpolated between the integral domain and the diffusion part in order to evaluate the convolution term.
- In infinite activity processes, small-size jumps are approximated by a diffusion and are integrated into the diffusion component instead of the integral component.
- Larger jumps are truncated.
- The behaviour of the option price outside the solution domain must be assumed.

All these features aggravate the flaws of the finite difference methods for pricing options under jump models.

We present a method to value vanilla-European options, as first presented by Jackson. *et al.* (2008). The FST method is an efficient transform-based method that treats the diffusion and the integral term of the PIDE symmetrically, Jackson. *et al.* (2008), Surkov (2009) and Jaimungal and Surkov (2009), and avoids any definite assumptions on the activities of option prices outside the truncated domain. Unlike other Fourier methods, the FST method does not require the Fourier transform of the pay-off function of the option to be priced. Thus, it can price options with complex pay-off functions with ease. The FST method is applicable to pricing options defined on multiple underlying assets and pricing options with complexity (exotic options) such as early-exercise options and barrier options, and naturally extends to the regime-switching Lévy model. We continue this section by introducing the option-pricing formula in terms of ODE. Then, we transform the PIDE into ODE and solve the ODE with the FFT algorithm. The advantage of the FST method over other numerical methods is discussed.

3.5.1 Fourier transform of the PIDE

Diverse integral techniques have been applied in literature for solving PDEs. Here, we shall discuss solutions to the PIDE using Fourier transform-based method, and transform the solution to a solvable ordinary differential equation. Subsequently,

we shall apply the convolution theorem on the risk-neutral valuation formula as an alternative for deriving the option prices to solving the PIDE. The transform-based method solves the PIDE efficiently, without the additional difficulty related to the integral term. Recall from equation 2.40 and 2.41 the expression for the Fourier transform and inverse Fourier transform

$$\mathcal{F}[\mathbf{f}](\omega) := \int_{-\infty}^{\infty} e^{i\omega x}\mathbf{f}(x)dx \quad \text{and} \quad \mathcal{F}^{-1}[\hat{\mathbf{f}}](x) := \frac{1}{2\pi}\int_{-\infty}^{\infty} e^{-i\omega x}\hat{\mathbf{f}}(\omega)d\omega, \tag{3.75}$$

where $\mathbf{f}(x)$ is the space domain often referred to as the original space, $\hat{\mathbf{f}}(\omega)$ is the frequency domain that is the transformed space and ω is the frequency given in radians per second. The Fourier transform is continuously differentiable and maps derivatives on the space domain into multiplication in the frequency domain, Boyd (2000), that is;

$$\mathcal{F}\left[\frac{\partial \hat{\mathbf{f}}}{\partial x}\right](\omega) := i\omega\mathcal{F}[\hat{\mathbf{f}}] \quad \text{and} \quad \mathcal{F}\left[\frac{\partial^2 \hat{\mathbf{f}}}{\partial x^2}\right](\omega) := -\omega^2\mathcal{F}[\hat{\mathbf{f}}]. \tag{3.76}$$

Now, we take the Fourier transform of the PIDE, that is;

$$\begin{cases} \partial_t\mathcal{F}[V](\omega,t) + \mathcal{F}[\mathcal{G}(V)](\omega,t) & = 0 \\ \mathcal{F}[V](\omega,T) & = \mathcal{F}[\Psi](\omega). \end{cases} \tag{3.77}$$

Taking the Fourier transform of the equation 3.74, $\mathcal{F}[\mathcal{G}(V)](\omega)$ becomes

$$\begin{aligned} \mathcal{F}[\mathcal{G}(V)](\omega) := \gamma\mathcal{F}[\partial_s V] + \frac{1}{2}\mathcal{F}[\partial_s^2 V]\sigma^2 \\ + \int_{\mathbb{R}^d/\{0\}} (V(s+y,t) - V(s,t) - y\cdot\mathbb{I}_{|y|<1}\mathcal{F}[\partial_s V])\nu(dy). \end{aligned} \tag{3.78}$$

Substitute equation 3.76 into 3.78, then 3.78 becomes

$$\mathcal{F}[\mathcal{G}(\omega)] := \left[i\gamma\omega - \frac{1}{2}\omega^2\sigma^2 + \int_{\mathbb{R}^d}[e^{i\omega y} - 1 - y\cdot\mathbb{I}_{|y|<1}\cdot i\omega]\nu(dy)\right]\mathcal{F}[V](\omega,t). \tag{3.79}$$

Recall the Lévy exponent for exponential Lévy process;

$$\varrho(\omega) := i\gamma\omega - \frac{1}{2}\omega^2\sigma^2 + \int_{\mathbb{R}^d}(e^{i\omega y} - 1 - y\cdot\mathbb{I}_{|y|<1}\cdot i\omega)\nu(dy). \tag{3.80}$$

Thus, equation 3.79 becomes

$$\mathcal{F}[\mathcal{G}(\omega)] := \varrho(\omega)\mathcal{F}[V](\omega,t). \tag{3.81}$$

Substituting equation 3.81 into 3.77, equation 3.77 becomes;

$$\begin{cases} \partial_t\mathcal{F}[V](\omega,t) + \varrho(\omega)\mathcal{F}[V](\omega,t) & = 0 \\ \mathcal{F}[V](\omega,T) & = \mathcal{F}[\Psi](\omega). \end{cases} \tag{3.82}$$

Knowing the value of the Fourier transform of $V(\omega, t)$ at time $t_2 \leq T$, the PIDE can be written as the n-dimensional family of ODEs with functions defined on ω and t, and the system of ODE can be easily eliminated to find the value at time $t_1 \leq t_2$. Thus,

$$\begin{aligned} \partial_t \mathcal{F}[V](\omega, t) + \varrho(\omega)\mathcal{F}[V](\omega, t) = 0, \\ \frac{\partial F}{\partial t} + \varrho(\omega)(t) = 0, \qquad \text{for } F := \mathcal{F}[V](t, \omega). \end{aligned} \tag{3.83}$$

$$\begin{aligned} \frac{\partial F}{\partial t} &:= -\varrho(\omega)(t), \quad F_1 := \mathcal{A}e^{-\varrho(\omega)(t_1)}, \quad \mathcal{A} := F_2 e^{\varrho(\omega)(t_2)} \\ F_1 &:= F_2 e^{\varrho(\omega)(t_2 - t_1)}. \end{aligned} \tag{3.84}$$

Thus,

$$\mathcal{F}[V](\omega, t_1) := \mathcal{F}[V](\omega, t_2) e^{\varrho(\omega)(t_2 - t_1)}. \tag{3.85}$$

To derive the FST formula for pricing options, take the inverse Fourier transform of equation 3.85;

$$V(s, t_1) := \mathcal{F}^{-1}[\mathcal{F}[V](\omega, t_2).e^{\varrho(\omega)(t_2 - t_1)}](s). \tag{3.86}$$

3.5.2 Applying the FFT.

The selection of the grid points on the real space (stock price domain) and the Fourier space (frequency domain) is very crucial. The relationship between the spatial domain and the frequency domain is established with the help of FFT and its inverse. We consider a single-dimensional case with an extension to a multi-dimensional case. Here, we shall discuss some precautions for selecting the grid points on the real space and the frequency domain. In a similar fashion, we discuss the relationship between these spaces.

Selecting the grid points on the real space:

Let Ω denote the discretised sample domain on the real space[2]. Consider a breaking up of the time and the discretised real space $\Omega = [0, T] \times [x_{\min}, x_{\max}]$ into countable lattice of points $[t_m | m = 0, \ldots, M] \times [x_n | n = 0, \ldots, N-1]$, where

$$x_n = x_{\min} + n\Delta x, \quad \text{for } \Delta x = \frac{(x_{\max} - x_{\min})}{N} \quad \text{and } t_m = m\Delta t, \quad \text{for } \Delta t = \frac{T}{M}. \tag{3.87}$$

To ensure valid selection of the grid points, Jackson. *et al.* (2008), Surkov (2009), Jaimungal and Surkov (2009) suggest x should be transformed into a log variables

[2]The spatial variable x is in log-returns. i.e, $x = \log\left(\frac{S}{S_0}\right)$ where S is the underlying asset price at time T.

such that the valuing of the option prices lies in the neighbourhood of $x = 0$ to avoid interpolation error. Thus, x on the real space can be written as $\log\left(\frac{S_{t_m}}{S_0}\right)$, that is, $x = \log\left(\frac{S_{t_m}}{S_0}\right)$. If the valuing of the option prices is demanded around the strike price, the scaling $x = \log\left(\frac{S}{K}\right)$ can be used. Intuitively, the minimum value of x, $x_{\min}$ on the space grid is chosen to be the negative of the maximum value of x, i.e, $x_{\min} = -x_{\max}$. Then, the concentrated value of the option prices lies in the centre of the grid. The selection of correct grid points is very important to ensure accuracy. Although, a rigorous study on the optimal selection of grid points is yet to be established according to the literature, see Jackson. *et al.* (2008) and Surkov (2009).

Selecting the grid points on the Fourier space

In the same procedure to the selection of grid points on the real space, let $\hat{\Omega}$ denote the discretised sample domain on the Fourier space. Consider a breaking up of the time and the discretised frequency space $\hat{\Omega} = [0, T] \times [\omega_{\min}, \omega_{\max}]$ into a countable lattice of points $[t_m | m = 0, \ldots, M] \times [\omega_n | n = 0, \ldots, N/2]$, where

$$\omega_n = n\Delta\omega \quad \text{and} \quad \Delta\omega = \frac{2\omega_{\max}}{N}.$$

Based on the Nyquist rule, the maximum frequency on the Fourier space $w_{\max} = \frac{1}{2\Delta x}$. Thus;

$$\omega_{\max} = \frac{N}{2 \cdot (x_{\max} - x_{\min})}. \tag{3.88}$$

Keeping in mind that the option pricing function $V(x, t)$ at any time t is a real number, $\mathcal{F}[V](-\omega, t) = \overline{\mathcal{F}[V](\omega, t)}$. Therefore, the Fourier transform for frequencies on the negative line is negligible. Thus, $\omega \in [0, \omega_{\max}]$. $\omega_{\max}$ should be chosen large enough to avoid discontinuity in the CF, yet not too large to avoid distortion and overlapping on the frequency grid which might result in an inaccuracy in option prices. In the same manner, the real-space limit points $x_{\max}$ and $x_{-\max}$ should be selected large enough to capture the overall behaviour of the pricing function, yet not too large to keep the accuracy of the evaluated option-price in the domain of interest.

Equation 3.88 obviously spells out the relationship between the grid points on the Fourier space (frequency grid) and the real space (spatial grid). Substituting $x_{\min} = -x_{\max}$ into equation 3.88, we have

$$\omega_{\max} = \frac{N}{4 \cdot x_{\max}}. \tag{3.89}$$

The selection of different limit points on the real space will be experimented in Result 3.5.3. Jackson. *et al.* (2008), Surkov (2009), Jaimungal and Surkov (2009) suggest $x_{\max} \in [4, 8]$ is preferable for models with high volatility terms or a dominant jump component, and $x_{\max} \in [2, 5]$ works well for diffusion models with low-volatility and short maturity time.

Let $[V_m]_n := V(x_n, t_m)$ denote $V(s,t)$ at the node points of the partition on the entire space domain Ω, and $[\hat{V}_m]_n := \hat{V}(\omega_n, t_m)$ denote $\mathcal{F}[V](\omega, t)$ at the node points of $\hat{\Omega}$ at time t_m. The prices defined on the frequency domain can be derived by taking the Fourier transform of prices defined on the spatial domain, that is,

$$\hat{V}(\omega_n, t_m) := \int_{-\infty}^{\infty} e^{i\omega_n x_k} V(x_k, t_m) dx \tag{3.90}$$

where $x_k = x_{\min} + k\Delta x$, for $k \in [0, N-1]$. Discretising the Fourier transform function, equation 3.90 can be approximated and written in form DFT. Thus, equation 3.90 can be written as

$$\hat{V}(\omega_n, t_m) \approx \sum_{k=0}^{N-1} e^{i\omega_n x_k} V(x_k, t_m) \Delta x. \tag{3.91}$$

Substituting $x_k = x_{min} + k\Delta x$ into equation 3.91, equation 3.91 becomes

$$\begin{aligned}
[\hat{V}_m]_n = \mathcal{F}[V](\omega_n, t_m) &\approx \sum_{k=0}^{N-1} e^{i\omega_n (x_{\min} + k\Delta x)} [V_m]_k \Delta x \\
&= \beta_n \sum_{k=0}^{N-1} [V_m]_k e^{-ink/N} \qquad \text{for } \beta_n = e^{i\omega_n x_{\min}} \Delta x \\
&= \beta_n [FFT(V_m)]_n.
\end{aligned}$$

$[FFT(V_m)]_n$ can be computed accurately with less computational time with the help of FFT, and β_n contains information about the selection of the grid-point on the terminal of the space domain. β_n and $[FFT(V_m)]_n$ ($[.]_x$ means the x vector form of $[.]$) represents the nth component of FFT of the vector V_m. In a similar manner, the prices on the spatial domain can be derived by taking the inverse of prices defined on the frequency domain:

$$\begin{aligned}
[\hat{V}_m]_n = \mathcal{F}[V](\omega_n, t_m) &= \beta_n [FFT(V_m)]_n \\
[V_m]_n &= [FFT^{-1}(\beta^{-1}.\hat{V}_m)]_n.
\end{aligned} \tag{3.92}$$

A time-step backward of $[V_m]_n$ in equation 3.92 is given by

$$\begin{aligned}
[V_{m-1}]_n &= [FFT^{-1}(\beta^{-1}.\hat{V}_{m-1})]_n \\
V_{m-1} &= FFT^{-1}(\beta^{-1}\hat{V}_{m-1}).
\end{aligned} \tag{3.93}$$

Note $[V_m]_n$ is defined on the space domain and $[\hat{V}_m]_n$ is defined on the frequency domain, and V_m is the vector with the nth component $[V_m]_n$. Studying equation 3.86, that is the Fourier transform of the PIDE,

$$V_{m-1} = FFT^{-1}[FFT[V_m](\omega).e^{\varrho(\omega)(t_m - t_{m-1})}](x), \tag{3.94}$$

we discover a time step t_m in the frequency domain requires a step backward in time (t_{m-1}) on the space domain. Initiating the idea of the time step in the spatial and

frequency domain of the Fourier transform of the PIDE in equation 3.94 on equation 3.93, equation 3.93 can be written as:

$$\begin{aligned} V_{m-1} &= FFT^{-1}[\beta^{-1} \cdot \hat{V}_m \cdot e^{\varrho(\cdot)\Delta t_m}] \\ &= FFT^{-1}[\beta_n^{-1} \cdot \beta_n \cdot FFT[V_m] \cdot e^{\varrho(\cdot)\Delta t_m}] \\ &= FFT^{-1}[FFT[V_m] \cdot e^{\varrho(\cdot)\Delta t_m}]. \end{aligned} \tag{3.95}$$

It is worth mentioning that β, which contains information about the limiting condition on the space domain, cancels out in equation 3.95. Thus, β is negligible during the numerical implementation of the FST algorithm. The one-dimensional FST method in 3.95 can be extended to a universal multi-dimensional FST method, where a step backward time is calculated by

$$\begin{aligned} V_{m-1} &= FFT^{-1}[\beta^{-1} \cdot \hat{V}_m \cdot e^{\varrho(\cdot)\Delta t_m}] \\ &= FFT^{-1}[\beta_n^{-1} \cdot \beta_n \cdot FFT[V_m] \cdot e^{\varrho(\cdot)\Delta t_m}] \\ &= FFT^{-1}[FFT[V_m] \cdot e^{\varrho(\cdot)\Delta t_m}]. \end{aligned} \tag{3.96}$$

In equation 3.96, the FFT is the multi-dimensional FFT transform and V_m is the d-dimensional matrix of option prices at time t_m.

Another approach for deriving equation 3.95 that does not involve solving the PIDE is the representation of the risk-neutral valuation formula:

$$V(X(t_m), t_m) = \mathbb{E}_{t_1}^{\mathbb{Q}}[V(X(t_{m+1}), t_{m+1})], \tag{3.97}$$

where $X(t)$ is a stochastic process characterized with stationary and independent increments and $V(\cdot)$ is a $\mathbb{Q}$ martingale. Thus, $X(t_{m+1}) = X(t_m) + x$.

$$\begin{aligned} V(X(t_m), t_m) &= \int_{-\infty}^{\infty} V(X(t_m) + x, t_{m+1}) f_{X(t_{m+1}) - X(t_m)}(x) dx \\ &= \int_{-\infty}^{\infty} V(X(t_m) + x), t_{m+1}) f_{X(t_{m+1} - t_m)}(x) dx, \end{aligned} \tag{3.98}$$

and $\mathbf{f}_{X(t)}(x)$ is the probability density function of the stochastic process $X(t)$. Transforming equation 3.98 from the space domain x into a frequency domain ω (taking the Fourier transform), equation 3.98 becomes

$$\mathcal{F}[V](\omega, t_m) = \mathcal{F}[V](\omega, t_{m+1}) \mathcal{F}[f_{X(t_{m+1} - t_m)}](\omega).$$

Note, a convolution in the space domain corresponds to product in the frequency domain and $\mathcal{F}[f_{X(t)}](\omega) = e^{t\varrho(-\omega)}$. Then,

$$\mathcal{F}[V](\omega, t_m) = \mathcal{F}[V](\omega, t_{m+1}) e^{\varrho(\omega)(t_{m+1} - t_m)}.$$

Hence,

$$V(\omega, t_m) = \mathcal{F}^{-1}[\mathcal{F}[V](\omega, t_{m+1}) e^{\varrho(\omega)(t_{m+1} - t_m)}].$$

If $m = 1$, then;

$$V(\omega, t_1) = \mathcal{F}^{-1}[\mathcal{F}[V](\omega, t_2) e^{\varrho(\omega)(t_2 - t_1)}]. \tag{3.99}$$

3.5.3 Pricing European options using FST method.

Options that can be exercised only at the maturity date (European options) can be valued at a single-time step, since equation 3.96 is a justifiable approximation for any time size (Δt), with only truncation on the real space and Fourier space adding to the level of inaccuracy. Our interest is a single time step, say $m = 1$ for a single asset. To solve for V_0 in equation 3.95, the discounted pay-off function;

$$V_1 = e^{-r\Delta t}\Psi(\mathbf{s}) \tag{3.100}$$

must be known ($\mathbf{s} = S_0 e^{x_n}$). Recall the pay-off function for a vanilla-European call and put option, the FST formula, equation 3.96 for pricing a European-call option is given by

$$V_0 = FFT^{-1}[FFT(e^{-r\Delta t} \cdot [\mathbf{s} - K]^+) \cdot e^{\varrho(\cdot)\Delta t}]. \tag{3.101}$$

In view of the fact that the analytic solution of the Fourier transform of the payoff function is not required, this method is distinct in pricing options with complex pay-off function.

3.5.4 Implementation details.

The implementation depends on the selection of the grids' size and interpolation. Equation 3.99 generates a finite number of values with respect to the number of points on the real space (the independent variable). To derive the approximated value of our option, it is required to estimate the value of equation 3.99 for an intermediate value of the independent variable. This is often achieved by curve fitting. A good example of a curve fitting method is the interpolation method. The existence of interpolation is built around the fact that to approximate a continuous function $f(x)$ define on $[a, b]$ by a polynomial $g(x)$, for each $\epsilon > 0$, such that $|f(x) - g(x)| < \epsilon \quad \forall x \in [a, b]$. The linear interpolation formula $g(x^*)$ for $x^* \in [a, b]$ is given as:

$$g(x^*) = g(b) - \frac{(g(a) - g(b))(b - x^*)}{b - a}. \tag{3.102}$$

Effect of T:

Result 3.5.1 (Effect of T on FST method for pricing European calls under the BS model)**.** For both short-dated and one-year span of European calls with $x = 1.5$ (i.e $x_{\min} = -1.5$ and $x_{\max} = 1.5$) and $N = 64$, the FST method works well. The call prices computed with the FST method fit perfectly on the reference prices.

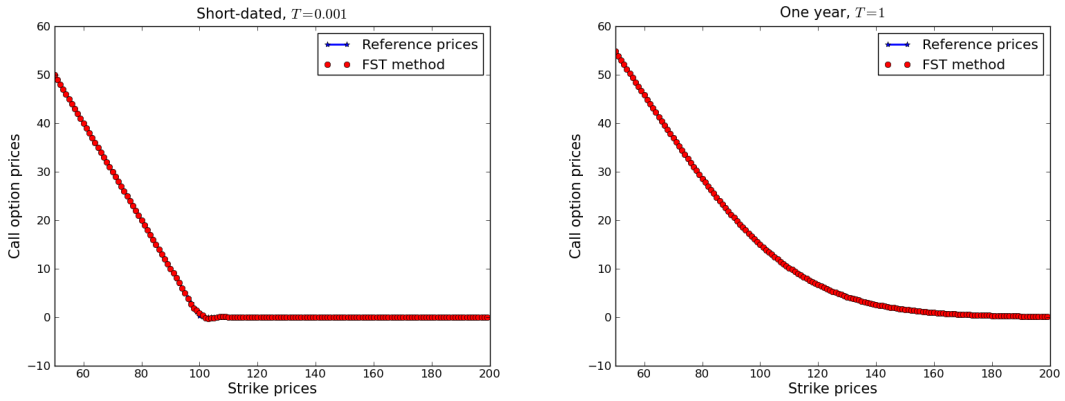

Figure 3.12: Effect of T on the FST method for pricing European calls under BS model. Parameters used: $S_0 = 100$, $K = [50, 200]$, $\sigma = 0.25$, $r = 0.1$, $N = 64$ and $x = 1.5$.

The role of N:

Result 3.5.2 (Effect of N (the number of points in the truncating interval) on the convergence of the FST method for pricing European calls)**.** We set $x = 1.5$ due to the fast convergence of the option prices at this point, for some values of N. The results presented in Table 3.3 suggest the convergence of the FST method is algebraic (second-order convergence).

$K \vert N$	32	64	128	256	512	1024
80	$1.11 \cdot 10^{-03}$	$1.55 \cdot 10^{-03}$	$1.86 \cdot 10^{-03}$	$3.29 \cdot 10^{-04}$	$8.22 \cdot 10^{-05}$	$1.71 \cdot 10^{-05}$
100	$5.49 \cdot 10^{-02}$	$1.31 \cdot 10^{-02}$	$3.23 \cdot 10^{-03}$	$8.00 \cdot 10^{-04}$	$1.98 \cdot 10^{-04}$	$4.82 \cdot 10^{-05}$
120	$5.05 \cdot 10^{-02}$	$9.34 \cdot 10^{-03}$	$1.29 \cdot 10^{-04}$	$1.77 \cdot 10^{-04}$	$2.14 \cdot 10^{-04}$	$3.47 \cdot 10^{-05}$

Table 3.3: Error convergence of the FST method for pricing European calls under BS model with respect to N. Parameters used: $S_0 = 100$, $K = [80, 100, 120]$, $\sigma = 0.25$, $r = 0.1$ and $x = 1.5$

Effect of x:

Result 3.5.3 (Effect of x, the limit point on the real space)**.** Reference prices for the BS model are given by an analytic solution. For NIG model, we used the CONV method by setting $N = 2^{20}$, and the reference price for VG model is taken from Lord *et al.* (2008). Studying Figure 3.13, we observe how the parameters T and σ play a vital role in the choice of x. For short-dated European calls with low volatility, $x \in [1.5, 5.5]$ works well, and for high volatility, $x \in [0.5, 2.5]$ gives more accurate results. We observe for $x > 5.5$ under low volatility and $x > 2.5$ under high volatility, there is deviation from the reference prices when $K \in [80, 120]$ because there is discontinuity on the x-grid when we are pricing in the neighbourhood of

$x = 0$. For a one-year span of options with low volatility, $x \in [1.5, 7.5]$ works well, and for high volatility, $x \in [3.5, 9.5]$ gives more accurate results. Thus, the choice of x depend on the volatility of the model, maturity time of the option, and the value of N. Table 3.4 summarises the effect of x-gird on European calls bounded on $K = [80, 100, 120]$. Figure 3.14 shows the best choice of x under the BS, NIG and VG models is 1.5.

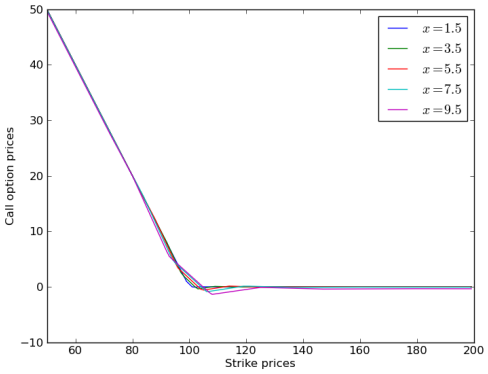

(a) $T = 0.001$ and $\sigma = 0.25$.

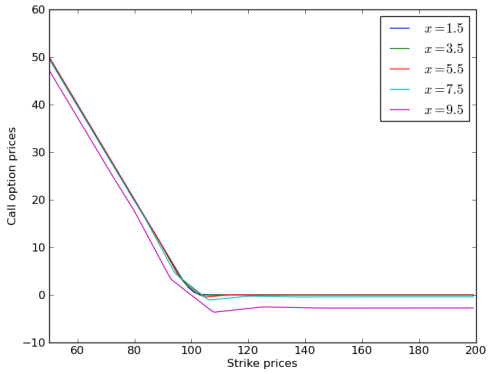

(b) $T = 0.001$ and $\sigma = 0.75$.

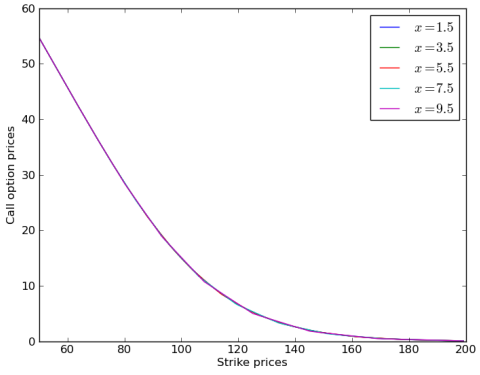

(c) $T = 1$ and $\sigma = 0.25$.

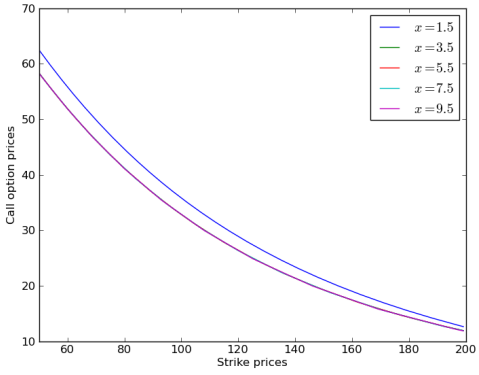

(d) $T = 1$ and $\sigma = 0.75$.

Figure 3.13: Effect of x on European call prices in the BS model using FST. Parameters used: $S_0 = 100$, $r = 0.1$, $N = 128$.

$K\|x$	0.5	1.5	3.5	4.5	6.5	7.5
80	3.17	$8.22 \cdot 10^{-05}$	$9.73 \cdot 10^{-06}$	$2.60 \cdot 10^{-04}$	$5.08 \cdot 10^{-04}$	$1.91 \cdot 10^{-03}$
100	2.63	$1.98 \cdot 10^{-04}$	$1.08 \cdot 10^{-03}$	$1.79 \cdot 10^{-04}$	$3.75 \cdot 10^{-03}$	$4.90 \cdot 10^{-03}$
120	2.07	$2.14 \cdot 10^{-04}$	$1.73 \cdot 10^{-04}$	$9.60 \cdot 10^{-04}$	$2.85 \cdot 10^{-03}$	$2.69 \cdot 10^{-03}$

Table 3.4: Error convergence of the FST method for pricing European calls under the BS model with respect to x: Parameters used: $T = 1$, $\sigma = 0.25$, $r = 0.1$ and $N = 128$.

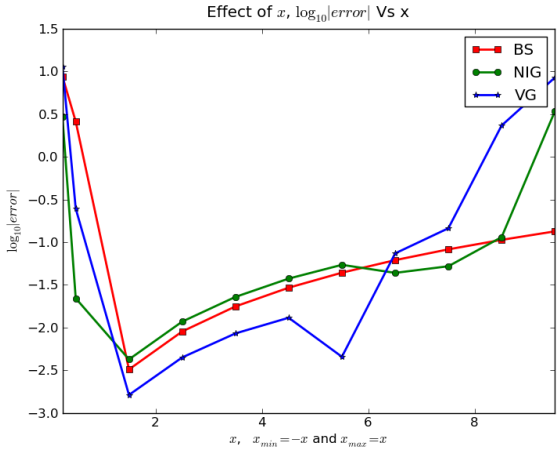

Figure 3.14: Error convergence of the FST method for pricing European calls under the BS, NIG and VG models with respect to (x). Parameters used: $T = 1$, $N = 128$, $S_0 = 100$, $K_{BS} = 100$, $K_{NIG} = 100$, $K_{VG} = 100$, $\sigma_{BS} = 0.25$, $\sigma_{NIG} = 0.12$, $\sigma_{VG} = 0.12$, $\theta_{VG} = -0.14$, $\kappa = 0.2$, $\alpha = 28.42141$, $\beta = -15.086$ and $\delta = 0.31694$.

3.5.5 Summary

Algorithm 3.5.1: **Fourier space time-stepping method**

1: Declare the initial variables: S_0, T, x, N;
2: Compute the Lévy exponent of the distribution of the underlying asset, that is, $\varrho(\cdot)$;
3: Discretize the spatial domain $[0, T] \times (x_{\min}, x_{\max})$ using equation 3.87 (for $0 \leq n \leq N-1$);
4: Discretize the frequency domain $[0, T] \times (\omega_{\min}, \omega_{\max})$ according to equation 3.88 (for $0 \leq n \leq N-1$);
5: Compute V_1 according to equation 3.100;
6: Compute V_0 via FFT using equation 3.101.

Algorithm 3.5.1 summarises the implementation of the COS algorithm for pricing European options under different models. The main advantage of the FST method is that the PIDE problems in an exponential Lévy model can be solved efficiently with this method, neglecting the additional complexity associated with the integral term. The key steps in the algorithm are the transformation of the PIDE into ODE, applying the FFT algorithm on the solvable ODE and interpolating the result to derive the desired option prices. This is applicable to price a large range of strike prices at a single goal of computation, and to derive the hedge parameters of different options with less modification to the original algorithm of the option of its counterpart. The option-pricing formula defined in terms of PDE (PDE formula for European option in Black-Scholes) can be priced using equation 3.96, similar to the equation for solving the PIDE except that the integral term of the characteristic factor, equation 3.80, is zero.

3.6 Numerical results

In this section we present numerical results to demonstrate the convergence properties of Fourier methods by pricing European calls under the BS model, NIG model and VG model. It is important to note that we report as the reference price, the most precise result reported in literature. For the NIG model where the reported result is only approximated to 4 decimal places, we include our computed reference price obtained by setting $N = 2^{20}$ using the CONV method.

Error convergence: The error function is the absolute difference between the result obtained from the analytical solution or the given reference price and the Fourier method:

$$\text{error} := |\text{ref}_{price} - \text{approx}_{price}(2^n)|. \tag{3.103}$$

And, the error convergence is the log 10 of the error function. The ref_{price} represents the benchmark option price against which approximations are calculated. In all numerical results the number of grid points is defined by $N = 2^n$, other parameters are taken from Table 3.5. The cumulants and the CFs are given in Table 2.1 and 2.2, respectively. To achieve exponential convergence, we define a ratio,

$$\text{Ratio} := \frac{\log_{10}|\text{error}(2^{n+1})|}{\log_{10}|\text{error}(2^n)|}, \quad n \in \mathbb{Z}^+. \tag{3.104}$$

If

$$\text{error}(2^n) \approx P_1 e^{(-Q_1 N)}$$

where P_1 and Q_1 are convergence constants, equation 3.104 should equal to 2. Thus, the error convergence is exponential. If

$$\text{error(N)}: = P_2 N^{-Q_2}$$

where P_2 and Q_2 are convergence constants,

$$\text{Ratio} \leq \frac{n+1}{n},$$

then we can say the convergence is algebraic.

In all our numerical results involving the CONV method, we set $\mathcal{K} = 10$ ($\mathcal{K}$-the proportionality constant in equation 3.36) in the BS, $\mathcal{K} = 20$ in NIG model and $\mathcal{K} = 40$ in VG model. For the COS method, we set $L = 10$ (L-the constant in the formula for the truncated range of integration, see equation 3.68), and for FST method we set $x = 1.5$ (the grid size on the spatial domain, i.e. $x_{\min} = -1.5$ and $x_{\max} = 1.5$) for the three models.

BS	$\sigma_{BS} = 0.25$	$r = 0.1$	$S_0 = 100$	$q = 0$			
VG	$\sigma_{VG} = 0.12$	$r = 0.1$	$S_0 = 100$	$q = 0$	$\theta_{VG} = -0.14$	$\kappa = 0.2$	$K = 90$
NIG	$\sigma_{NIG} = 0.12$	$r = 0.1$	$S_0 = 100$	$q = 0$	$\alpha = 28.42141$	$\beta = -15.08623$	$\delta = 0.31694$

Table 3.5: Parameters used for the implementation. Otherwise, stated.

3.6.1 Black-Scholes model

Result 3.6.1 (Error convergence for pricing short-dated European calls under the BS model using the CONV, COS and the FST methods)**.** [For $K = [80, 100, 120]$, the $\text{ref}_{price} = [20.79922620, 3.65996845, 0.04457726]$]. As shown in Figure 3.15, to price in-the-money ($K = 80$) European call, the CONV method needs $N < 256$ points for an error of order $\mathcal{O}(10^{-6})$ when $T = 0.1$. For an at-the-money ($K = 100$) European call, the CONV method needs $N < 1000$ points to achieve an error of order $\mathcal{O}(10^{-4})$, and $N < 256$ points to price an out-of-the-money European call to achieve the same level of accuracy when $T = 0.1$.

The results from the COS method are accurate up to an error of order $\mathcal{O}(10^{-12})$ for pricing in-the-money calls with $N = 64$ points, and an error of order $\mathcal{O}(10^{-14})$ is achieved in pricing at-the-money and out-of-the-money European calls, in less than 2 milliseconds. The COS method converges at a very high rate. The convergence is stable and similar for different strikes. The convergence of the COS method is superior.

In the case of FST method, for in-the-money European calls, the prices converges to an error of order $\mathcal{O}(10^{-4})$ with $N < 256$ points, at-the-money European calls, it takes $N < 1400$, and $N < 512$ for out-of-the-money European calls to reach the same level of accuracy as an in-the-money-option. Thus, we can say the CONV and FST methods converge in a similar manner.

Result 3.6.2 (Error convergence and the CPU-time comparing the CONV, COS and the FST methods for pricing one-year European calls under the BS model)**.** [For $K = [80, 100, 120]$, the $\text{ref}_{price} = [28.59149449, 14.97579077, 6.63830907]$.] Figure 3.16 presents the error convergence of the CONV method, COS method and the FST method. In term of accuracy, the numerical results from CONV are accurate up to an error of order $\mathcal{O}(10^{-3})$ with $N < 250$ points, in more than 2 milliseconds of CPU-time. The results from the FST method are accurate up to an error of order $\mathcal{O}(10^{-3})$ with $N < 250$ points, in less than 2 milliseconds. The results from the COS are accurate up to an error of order $\mathcal{O}(10^{-12})$ with $N = 64$ points, in less than 2 milliseconds, similar to short-dated European calls. The COS method uses less CPU-time and it converges faster than the other methods. This makes it outstanding when the required accuracy is high.

The error convergence of the COS method is exponential. For the CONV and FST methods, they exhibit algebraic convergence. For stability, we observe the behaviour of the COS method under the BS model to be stable across different strikes, the error convergence rate of the three strikes is exponential.

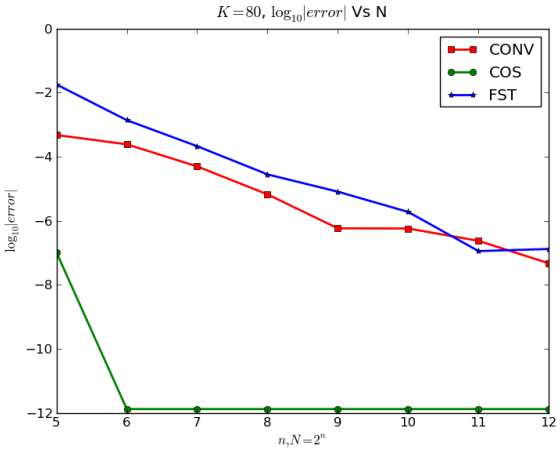

(a) Parameter used: $K = 80$ and $T = 0.1$

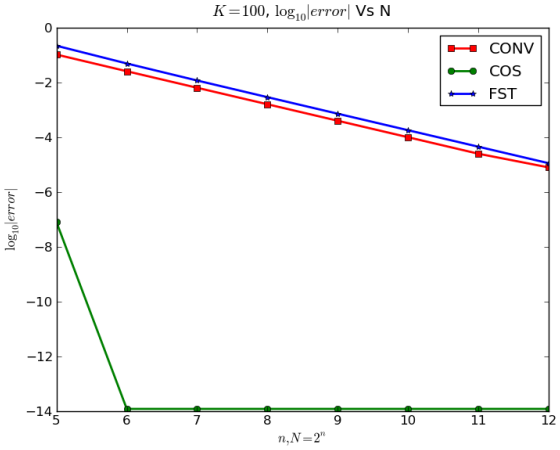

(b) Parameter used: $K = 100$ and $T = 0.1$.

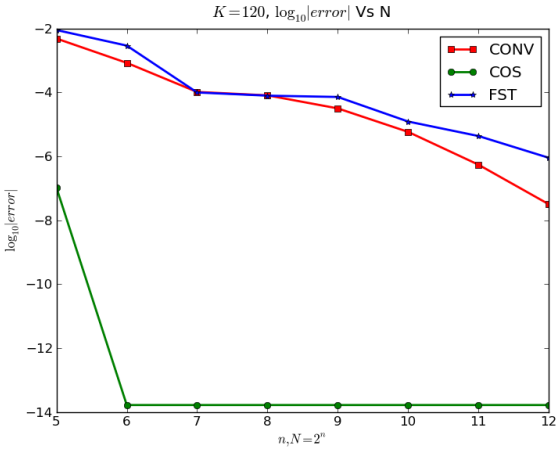

(c) Parameter used: $K = 120$ and $T = 0.1$.

Figure 3.15: Short-dated European calls under BS model with different strikes.

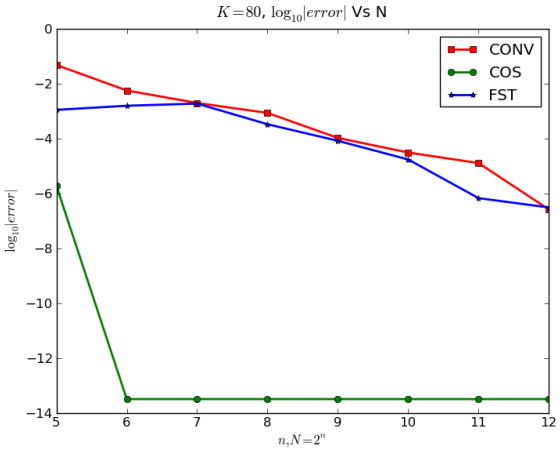

(a) Parameter used: $K = 80$ and $T = 1$.

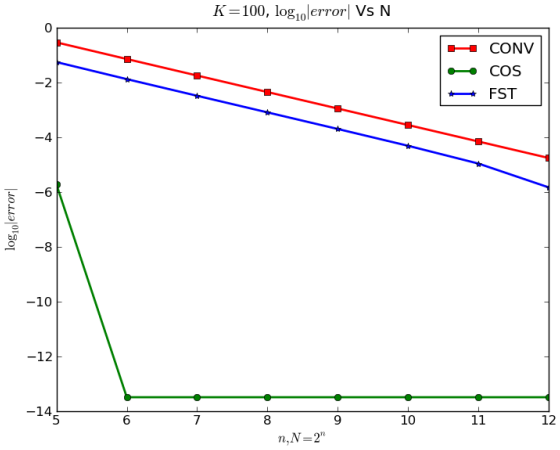

(b) Parameter used: $K = 100$ and $T = 1$.

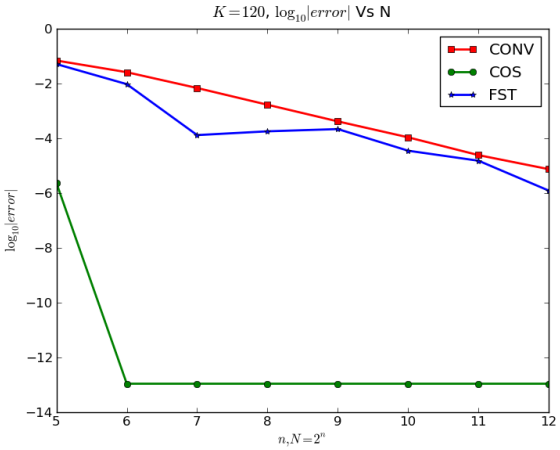

(c) Parameter used: $K = 120$ and $T = 1$.

Figure 3.16: One year European calls under BS model with different strikes.

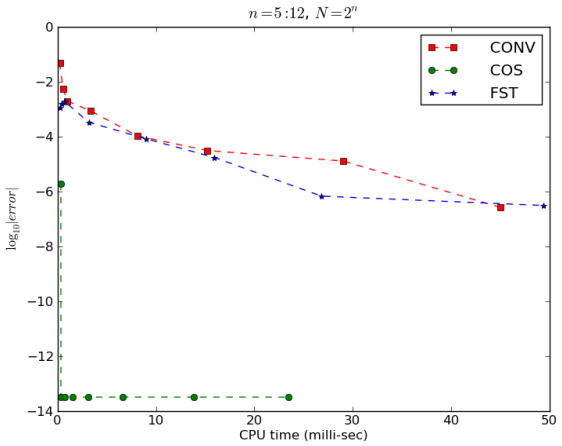

Figure 3.17: CPU-time for pricing one-year European calls under BS model, when $K = 100$.

	CONV		COS		FST	
n	**|error|**	**time**	**|error|**	**time**	**|error|**	**time**
5	0.28	0.23	$3.15e^{-06}$	0.35	$5.49e^{-02}$	0.28
6	$7.10e^{-02}$	0.56	$1.77e^{-13}$	0.37	$1.31e^{-02}$	0.39
7	$1.76e^{-02}$	1.10	$1.77e^{-13}$	0.76	$3.23e^{-03}$	0.75
8	$4.42e^{-03}$	3.37	$1.77e^{-13}$	1.52	$8.01e^{-04}$	3.17
9	$1.10e^{-03}$	8.11	$1.77e^{-13}$	3.15	$1.98e^{-04}$	8.98
10	$2.76e^{-04}$	15.21	$1.77e^{-13}$	6.59	$4.82e^{-05}$	15.94
11	$6.90e^{-05}$	29.05	$1.77e^{-13}$	13.82	$1.08e^{-05}$	26.88
12	$1.72e^{-05}$	45.01	$1.77e^{-13}$	23.46	$1.45e^{-06}$	49.37

Table 3.6: Error and CPU(time-milli-seconds) for pricing a one-year European call under BS model, K=100.

The CONV and FST methods work well for pricing short-dated in-the-money and out-of-the-money European calls compared to short-dated at the money European calls and long-span European calls.

The COS method requires less computational effort to converge to a highly accurate result compared to the CONV and COS methods. For it converges in less than 2 milliseconds to an error of order $\mathcal{O}(10^{-12})$. Thus, the COS method is superior to the CONV and the FST methods.

The numerical results from the Carr-Madan method is excluded in our analysis for the convergence of the method is fourth order. This is as a result of the fat tails exhibited in the CF of the BS model. For the Carr-Madan to achieve the same level of accuracy with the other Fourier methods, the truncation range N has to

be relatively large. The Carr-Madan needs $N > 4000$ points for an error of order $\mathcal{O}(10^{-3})$.

3.6.2 Normal Inverse Gaussian model

Here, we present the convergence results for pricing European calls under the NIG model using the Fourier transform-based methods. Reference prices of 11.3599 when $K = 100$, 1.9435 when $K = 120$ and parameters, are taken from Kéllezi and Webber (2004). Our computed reference prices are: 27.72853203 when $K = 80$; 11.35992896 when $K = 100$; and 1.94357695 when $K = 120$. These prices are obtained when $N = 2^{20}$ using the CONV method.

Result 3.6.3 (Error and CPU-time for pricing one-year European calls under the NIG model)**.** The convergence of the CONV and FST methods in Figure 3.19 are similar to that of the BS model but these methods converge faster in the NIG model as compared to the BS model. The convergence of the CONV and FST method are algebraic while COS method is exponential. For different strikes, the convergence of the COS and FST methods are stable and for pricing at-the-money European calls under the BS and NIG models, the convergence of the three methods are stable. The COS method uses less than 5 milliseconds of CPU-time to converge to an error of order $\mathcal{O}(10^{-12})$, while the CONV and FST methods converge to an error of order $\mathcal{O}(10^{-3})$ in more than 10 milliseconds of CPU-time.

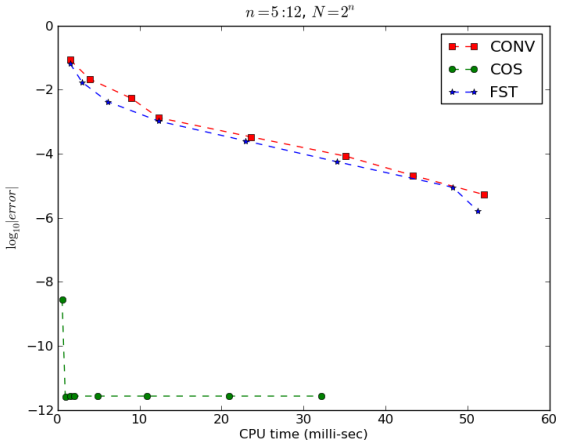

Figure 3.18: CPU-time for pricing one-year European calls under NIG model, when $K = 100$.

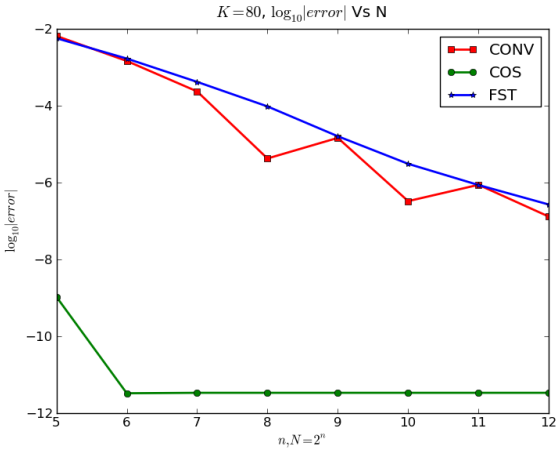

(a) Parameter used: $K = 80$ and $T = 1$.

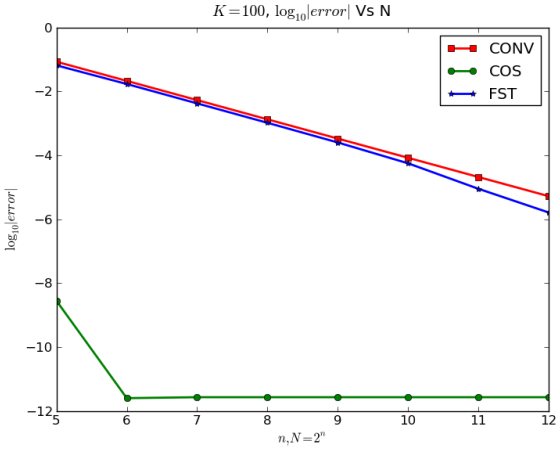

(b) Parameter used: $K = 100$ and $T = 1$.

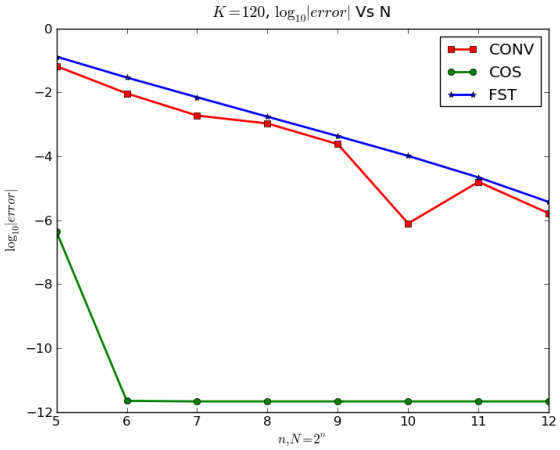

(c) Parameter used: $K = 120$ and $T = 1$

Figure 3.19: One year European calls under NIG model with different strikes.

	CONV		COS		FST	
n	**|error|**	**time**	**|error|**	**time**	**|error|**	**time**
5	$8.52e^{-02}$	1.55	$1.34e^{-04}$	0.57	$6.57e^{-02}$	1.55
6	$2.14e^{-02}$	3.93	$4.93e^{-09}$	0.94	$1.71e^{-02}$	3.01
7	$5.36e^{-03}$	9.02	$4.52e^{-11}$	1.54	$4.23e^{-03}$	6.13
8	$1.34e^{-03}$	12.31	$4.52e^{-11}$	2.09	$1.04e^{-03}$	12.33
9	$3.35e^{-04}$	23.59	$4.52e^{-11}$	4.90	$2.53e^{-04}$	22.91
10	$8.39e^{-05}$	35.12	$4.52e^{-11}$	10.84	$5.63e^{-05}$	34.04
11	$2.10e^{-05}$	43.32	$4.52e^{-11}$	20.91	$7.14e^{-06}$	48.17
12	$5.27e^{-06}$	52.01	$4.52e^{-11}$	32.13	$5.14e^{-06}$	51.25

Table 3.7: Error and CPU(time-milli-seconds) for pricing a one-year European call under NIG model, K=100.

3.6.3 Variance Gamma model

For pricing European calls under the VG model, we will narrow our experiment to when $K = 90$ for both short-dated and one-year span of European calls. For short-dated call, the reference price is 10.99370318, and for a one-year span of a European call, the reference price is 19.09935472. These are taken from Lord *et al.* (2008) and Kéllezi and Webber (2004).

Result 3.6.4 (Error and CPU-time for pricing European calls under VG model)**.** As shown in Figure 3.20, the CONV and FST methods converge faster for short-dated span of in-the-money European calls under the VG model than a one-year span of calls. In the case of the COS method for a short-dated span of European calls, the convergence is algebraic due to the presence of discontinuity in the CF of the model, as a result of the fact that $\Delta t(0.1) < \kappa(0.2)$. Thus, for short-dated European calls, the error convergence of the Fourier methods is algebraic, although the convergence of the COS method remains superior.

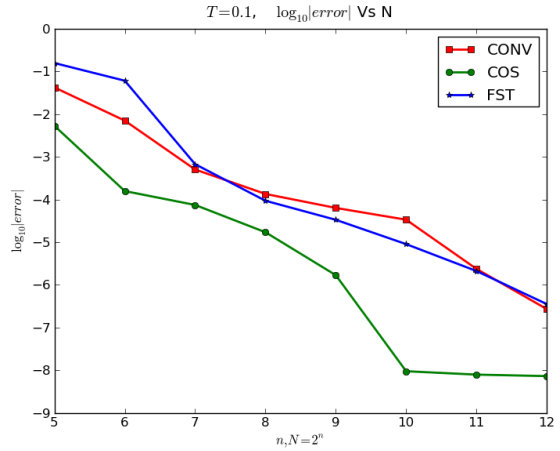

(a) Parameter used: $T = 0.1$.

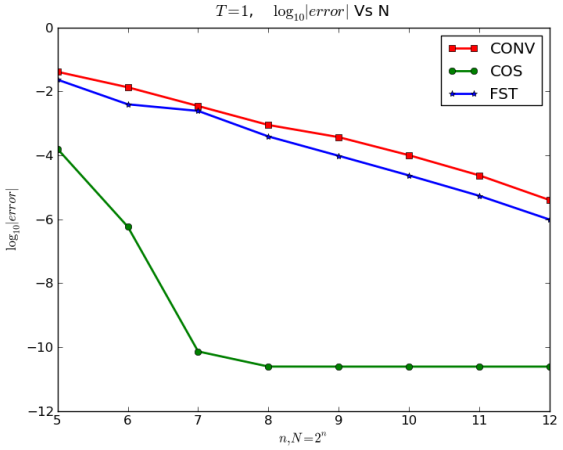

(b) Parameter used: $T = 1$.

Figure 3.20: European calls under VG model with different maturities.

For one-year European calls under the VG model, the CONV and FST methods needs $N > 120$ points to achieve an error of order $\mathcal{O}(10^{-3})$. The convergence of these methods are stable and algebraic for one-year European calls under the VG model while the convergence of the COS method is exponential since $\Delta t(1) > \kappa(0.2)$. The COS method still converges faster than the CONV and FST methods.

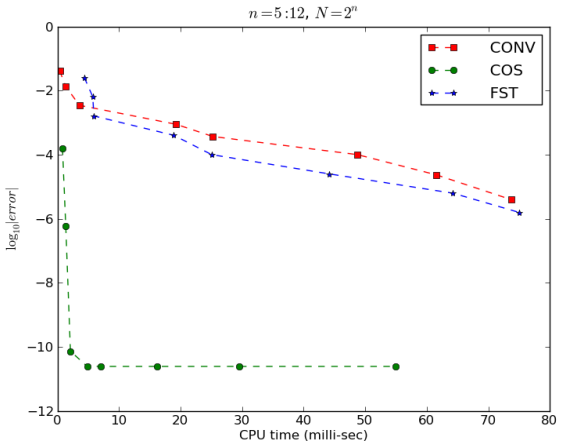

Figure 3.21: CPU-time for pricing a one-year European call under VG model, when $K = 90$.

	CONV		COS		FST	
n	**|error|**	**time**	**|error|**	**time**	**|error|**	**time**
5	$4.12e^{-02}$	0.37	$1.60e^{-04}$	0.82	$2.55e^{-02}$	4.37
6	$1.35e^{-02}$	1.34	$5.87e^{-07}$	1.35	$6.47e^{-03}$	5.73
7	$3.50e^{-05}$	3.57	$7.34e^{-11}$	2.11	$1.62e^{-03}$	5.92
8	$8.93e^{-04}$	19.27	$2.46e^{-11}$	4.83	$4.04e^{-04}$	18.81
9	$3.71e^{-05}$	25.24	$2.46e^{-11}$	7.10	$1.00e^{-04}$	25.06
10	$6.37e^{-05}$	48.72	$2.46e^{-11}$	16.19	$2.51e^{-05}$	44.20
11	$2.35e^{-05}$	61.55	$2.46e^{-11}$	29.47	$6.28e^{-06}$	64.24
12	$3.98e^{-06}$	73.70	$2.46e^{-11}$	54.99	$1.57e^{-06}$	75.03

Table 3.8: Error and CPU-time (milliseconds) for pricing a one-year European call under VG model, K=90.

3.6.4 Speed

In cases considered here, the parameters used for implementation are the same as in Table 3.5, unless otherwise stated. $K = 100$ under the BS model and the NIG model, and $K = 90$ under the VG model.

Result 3.6.5 (CPU-time taken to achieve a $\mathcal{O}(10^{-6})$ accuracy across the BS, NIG and VG models using the CONV, COS and FST methods)**.** Comparing the speed to accuracy across different models, the COS method is good for pricing a European call, for it converge faster than the CONV method and the FST method.

Method	BS model	NIG model	VG model
CONV	52.00	52.01	73.70
COS	0.35	0.65	0.94
FST	49.37	49.66	64.03

Table 3.9: CPU-time (milliseconds) for pricing a one-year European call that converges to an error of order $\mathcal{O}(10^{-6})$ under the BS, NIG and VG models using the CONV, COS and FST methods.

3.7 Conclusion

In this chapter we have presented the Carr-Madan method, CONV method, the COS method and the FST method for pricing European-style options. We introduced the Carr-Madan method with an extension to the CONV method that is less restricted to the choice of a damping variable which plays a vital role in the convergence of the Carr-Madan method. The implementation of the CONV and the FST methods are similar although, the approach taken in deriving the algorithm is different. The CONV method utilises the convolution representation to derive the option-pricing formula while the FST method solve the PIDE option-pricing equation.

The stable performance of the Carr-Madan method to price European options depends on the choice of α (damping factor). The optimal value of α depends on the CF of the distribution of the model, the position of the option, the value of N and the spacing parameter β. Large values of T introduce smoothness into the return densities which thins the tails of the CF of the distribution of some models.

The CONV method is highly efficient compared to the Carr-Madan method with a possible extension to early-exercise options in exponential Lévy models. Recall $\mathcal{K}$ is the proportional constant in the equation for the length of the truncation range L. In all numerical results involving the CONV method in this Chapter, $\mathcal{K} = 10$ gives more accurate results in the BS model, $\mathcal{K} = 20$ in the NIG model and $\mathcal{K} = 40$ works well in the VG model. The optimal value of L wholly depends on the choice of $\mathcal{K}$. The optimal choice of $\mathcal{K} = 20$ is yet unavailable in literature. The convergence of option prices using the CONV method is algebraic.

The FST method treats the integral and diffusion term in pricing of PIDE symmetrically. The method is more efficient in pricing European-style options compared to other PIDE finite-difference schemes for it does not require a time-stepping procedure. More so, the algorithm is more pleasing than other Fourier transform-based methods for it does not require the Fourier transform of the payoff function. In our numerical results involving the FST method, $x = 1.5$ (i.e $x_{\min} = -x$ and $x_{\max} = x$) gives more accurate results. The convergence of the method is stable for pricing at-the-money European calls across different models. The convergence is algebraic and in most cases similar to the CONV method.

The convergence behaviour of the COS method can be estimated by recovering the density function. In all numerical results applying the COS method to price European options, we observe the highest computational speed related to linear computational complexity, which means that the computational time grows only linearly with respect to an increasing number of the grid points N. Multiplying N by factor of 2, performing the computations, and checking the changes in subsequent timings, we can deduce the linear computational complexity. In most numerical results, the convergence of the COS method is exponential except when the density function of the underlying process has discontinuity in one of its derivatives, for example, the VG model, then algebraic convergence is expected when $\Delta t < \kappa$. With $N < 80$, all numerical results achieve an error of order $\mathcal{O}(10^{-12})$, in milliseconds of CPU-time except the VG model. The error convergence rate of the COS method is basically the same for different strikes. Thus the COS method is stable and superior to other Fourier methods.

In the next chapter, we will extend the Fourier methods to pricing options with early-exercise features.

Chapter 4

Pricing early-exercise options using the Fourier methods

4.1 Introduction

Early-exercise options, Bermudan and American options, are the most popularly-traded options in financial markets and are often used for fitting parameters[1]. The pricing of these options provides the basis for pricing more sophisticated exotic options. Therefore, it is very important to be able to price these options accurately so that arbitrage opportunities are avoided.

Geographically, Bermuda Island is located between Europe and America. In a similar manner, we can say that Bermudan options are 'in between' European options and American options, Schweizer (2002). Bermudan options are vanilla early-exercise options that give the holder the opportunity to purchase or sell a specific underlying asset on a finite set of specific exercise dates before, or on the maturity date of the option, at a predetermined price. At each exercise date, the option holder has the right to decide to receive the payoff or to wait until the next exercise date, at which time she/he has the same right. At maturity, the holder either exercises the option or the option expires worthless. Let $\mathcal{T} := \{t_0, t_1, \ldots, t_M\}$ be the set of possible exercise dates. An optimal exercise time is a stopping time (i.e. a *random variable*) whose values are in $\mathcal{T}$. Let $\mathbf{\Gamma}$ be the set of all stopping times with values in $\mathcal{T}$. Then a stopping time $\tau \in \mathbf{\Gamma}$ is optimal precisely when

$$\mathbb{E}^{\mathcal{Q}}[e^{-r\tau}\Psi(S_T)] = \sup_{\tau\in\mathbf{\Gamma}} \mathbb{E}^{\mathcal{Q}}[e^{-r\tau}\Psi(S_\tau)], \tag{4.1}$$

i.e. precisely when τ attains the supremum over all stopping times, Peskir and Shiryaev (2006). Not every stopping time is optimal. $\Psi(\cdot)$ is the payoff function, $e^{-rt}S_t$ is the discounted asset price that is a $\mathcal{Q}$-martingale, $\mathcal{Q}$ is a risk-neutral measure. In the case of an American option, $\mathcal{T}$ is the continuum of dates of dates between $t = 0$ and the maturity date. The pricing of American options is much harder than Bermudan options because more exercise dates are required. In Section 4.5, we will discuss American options.

[1] That is, obtaining model parameters from quoted or observed prices from financial markets.

Options with early-exercise features, the Bermudan and American options are worth more, or equal to European options since they give the holder all the rights of a European option with additional early exercise rights. In the case of a Bermudan put, assuming at time t where $t < T$ and S_t^* is the early-exercise boundary, i.e. the value of S for which the holder should exercise a put if $S_t \leq S_t^*$, but should hold (not exercise) if $S_t \geq S_t^*$. At the maturity date T, the option will only be exercised if $S_T \leq S_T^*$, provided the option has not be exercised beforehand. This implies S_t^* is a unique value which results in an early-exercise. The price of a Bermudan option is the discounted expected value of all future cash flow, Geske and Johnson (1984). Thus, the discounted payoff is integrated over all stock prices smaller than S_t^*. However, if $S_t < K - Ke^{-r(T-t)}$ is invested at a risk-free rate, the holder will receive an amount greater than K at time T. Thus, the value of the option at time t will be more than holding it to maturity.

A simple closed-form formula for pricing a Bermudan put and an American put option is yet to be established in literature. Since it is never optimal to exercise a Bermudan call on a non-dividend paying asset before maturity, Bermudan calls on such are equivalent to European calls, Hull (2007), then we can price Bermudan calls using the same procedures discussed in Chapter 3, or price them analytically in financial models with closed-form formulas. For Bermudan puts, this is much harder to price as a result of the optimal exercise time that may occur before maturity. In Andricopoulos *et al.* (2003), the quadrature method (QUAD for short) is introduced to price early-exercise options. The QUAD method demands the closed-form availability of the transition density function, which applies to very few models e.g. the BS model and the Merton-jump diffusion model. Thus, the QUAD method is not applicable to all models. In Kéllezi and Webber (2004), the lattice method constructed from Lévy density is implemented to price Bermudan options in an exponential Lévy model with infinite activity processes. Sullivan (2005) introduces a more general method called the QUAD-FFT method. The QUAD-FFT implement quadrature methods into Fourier transform methods. This method involves inverting the CF of the desired model to produce the transition density. The work of Kyriakos (2005) shows how the QUAD method can be used for pricing early-exercise options. For Monte Carlo methods, the pricing of Bermudan options using these methods is not trivial due to the complexity associated with the model and the option style. PIDE-based methods solve the PIDE problems (see equation 3.71) associated with Lévy models. The solution of the reformulated PIDE in equation 3.73 is subject to the terminal conditions or early-exercise constraints. PIDE-based methods are mostly used to price early-exercise and exotic options because their features can be represented as special payoff functions or terminal conditions. Hirsa and Madan (2004) and Almendral and Oosterlee (2007) presents a numerical solution to the PIDE under the VG model using backward schemes and by solving iteratively. Almendral (2005) discusses a solution using the same approach under the CGMY model. They price American options, respectively. These methods are said to be computationally expensive for pricing options in Lévy models because of the integral term with a weakly singular kernel in the PIDE equation Hirsa and Madan (2004), Almendral and Oosterlee (2007), Wang *et al.* (2007).

In this dissertation, we focus on Bermudan and American put options on non-dividend paying assets. The exercise dates for the Bermudan put are equally spaced. Implementing the risk-neutral idea discussed in Chapter 2, the pricing strategy between two successive exercise dates can be linked to that of a plain vanilla option Fang and Oosterlee (2009b). However, the value of an early-exercise option at an exercise date is greater or equal to the pay-off at the exercise date; the pricing of the Bermudan option is built around this fact. The pricing formula for a Bermudan option with initial time t_0, for $0 = t_0 < t_1 < \cdots < t_M = T$ with M exercise dates, for $m = M, M-1, \cdots, 2$ and x_m the log-asset price reads;

$$v(x_m, t_m) := \begin{cases} \Psi(x_M, t_M), & \text{the pay-off function at maturity,} \\ \max(\Psi(x_m, t_m), c(x_m, t_m)) & \text{for } m = M-1, M-2, \cdots, 0, \end{cases} \tag{4.2}$$

and the continuation value is given by

$$c(x_m, t_m) := e^{-r\Delta t} \int_{\mathbb{R}} v(x_{m+1}, t_{m+1}) f(x_{m+1}|x_m) dx_{m+1}, \tag{4.3}$$

where the scaled log-asset price $x_m := \ln(S(t_m)/K)$ and $x_{m+1} := \ln(S(t_{m+1})/K)$ are state variables given in equation 3.59, and the conditional probability density function of the risk-neutral measure of x_{m+1} given x_m is defined as $f(x_{m+1}|x_m)$. For simplicity, we equate $x = x_m$ and $y = x_{m+1}$. This describes the transition of the log-asset price from x at time t_m to y at time t_{m+1}. To solve for equation 4.3, we use the Markov property of the process which describes the underlying dynamics of the model i.e. we assume the time-homogeneity of x_m, so that $f(y|x)$ depends only on x, y and not time. This follows from equation 3.29; the probability density function $\mathbf{f}(y|x; \Delta t)$ governing the change in log-asset price over Δt can be written as

$$\mathbf{f}(y|x; \Delta t) = h(y - x; \Delta t) = h(z; \Delta t) \tag{4.4}$$

for some function $h(\cdot)$. The pricing of the Bermudan option, $v(x, t_0)$, requires adequate knowledge of *dynamic programming*.

To solve equation 4.2, the value of the integral that evaluate the continuation value $c(x, t_m)$ in equation 4.3 on log-asset price x at each time t_m, given the option value at $v(y, t_{m+1})$, for various y at time t_{m+1} must be known. Thus, we need numerical methods to approximate $c(x, t_m)$ at each t_m and then solve for the option value in equation 4.2 until time $t = 0$, for $m = M-1, M-2, \cdots, 0$. This backward recursion is based on dynamic programming. In view of this, we introduce dynamic programming.

Dynamic Programming

The term dynamic programming was originally used in the 1940*s* by Richard Bellman to solve a sequential problem, Bellman (1957). The main idea of dynamic programming is to divide a system of problems into sub-problems, solve each sub-problem once, save the solution and look it up when needed for further processing. It is used for mathematical optimization in economics and finance. Dynamic programming

problems can be divided into sequential problem or a functional problems (Bellman equation). Here, we are confronted with a sequential problem. To determine the Bermudan put price at time t_0, we begin by computing the pay-off at maturity t_M. Then, we compute the continuation value $c(x, t_{M-1})$ as a function of log-asset price x at time t_{M-1}, and use a root-finder technique to determine the value x^* for which $c(x^*, t_{M-1})$ equals the pay-off $\Psi(x^*, t_{M-1})$. Repeat until time t_0 (or until t_1 if t_0 is not a possible exercise date as in Fang and Oosterlee (2009b), Lord *et al.* (2008).

Proposition 4.1.1 (Principle of Optimality)**.** *With respect to an optimal problem, any rule for making a decision which results in a permissible sequence of decisions and maximises a preassigned function of the final-state variables, has the property of that, irrespective of the initial state and initial decision: the decision must consist of an optimal policy with respect to the state resulting from the first decision Bellman (1957).*

The remainder of this chapter discusses the extension of the Fourier methods discussed in Chapter 3 to approximate the continuation value and solve for the option value. In Section 4.2, we discuss the convolution method, Lord *et al.* (2008), and its implementation based on Andricopoulos *et al.* (2003) and Sullivan (2005). The discussion is similar to that of Section 3.3, but with more computational complexity because early-exercise options are time-dependent. To calculate the continuation value, $c(x, t_m)$, we compute the Fourier transform of the damped option value at time t_{m+1} , $e^{\alpha y} v(y, t_{m+1})$, multiply the result with the CF which is readily available in exponential Lévy model, $\Phi(\cdot)$, take the inverse Fourier transform of the product, and then un-damped and discount the result. Thus, we derive the continuation value at time t_m and calculate $v(x, t_m)$ as the maximum of the continuation and exercise value at t_m . We repeat this recursively based on dynamic programming until we have derived $v(x, t_0)$ in equation 4.2, Lord *et al.* (2008). Section 4.3 discusses the Fourier-cosine series expansion, Fang and Oosterlee (2009b). The COS method is based on the close relationship between the Fourier-cosine series expansion and the CF (see Section 3.4). Since the density function, $\mathbf{f}(y|x)$, decays to zero rapidly as $y \to \pm\infty$, the infinite integral in the continuation value, $c(x, t_m)$, equation 4.3 can be truncated into a finite range without loosing significant accuracy, then the approximated $c(x, t_m)$ at each time t_m can be calculated by backward recursion using dynamic programming Fang and Oosterlee (2009b). The Fourier space time-stepping method is discussed in Section 4.4 Jaimungal and Surkov (2009), Surkov (2009). Under the FST method, there is less to do in extending the FST European formula to pricing early-exercise options because naturally, a time step t_{m+1} in the frequency domain requires a step backward in time t_m on the space domain. That is, the original algorithm is path-dependent and the implementation is naturally based on backward recursion. A number of times steps in the FST algorithm are the same as the number of exercise dates and only a single time-step of algorithm is required between exercise dates, which would require several time steps in the CONV and COS methods Jackson. *et al.* (2008), Surkov (2009). Thus, a root-finder technique is not used and the early-exercise points x^* cannot be known directly during the implementation. In Section 4.5, we approximate the prices of American puts by those of Bermudan puts. Section 4.6 presents the prices of Bermudan puts under

the BS and VG models using the Fourier methods, and the prices of American puts under the VG models using the Fourier methods. Lastly, we conclude.

4.2 Pricing Bermudan option using the Convolution method

This section explains in detail, the extension of the CONV method discussed in Section 3.2 to pricing an early-exercise option. To convolve, we observe Reiner (2001) work that signifies that the Fourier transform of the continuation value in equation 4.3 can be expressed as the Fourier transform of the product of the option value with transition density. To ensure that the Fourier transform of the continuation price exists, a damping variable α is again necessary especially in pricing Bermudan put where $v(x, t_{m+1})$ tends to a constant as $x \to -\infty$, and as such is not square integrable. Thus, we have to choose α and need to know the singularities of the transformed pay-off function in order to apply Cauchy's residue theorem (see Iseger (2006)) to avoid discontinuity. The derivation of optimal-damping coefficients in pricing Bermudan options (as we have discussed under the Carr-Madan method for pricing European options) becomes problematic, for we need to find different values of α at each possible exercise date. Recall from Section 3.3, the application of a damping coefficient in deriving the CF is not significant as the transition probability density function is bounded. Let the damped continuation value and the damped option value be denoted as $\mathbb{C}(x, t_m)$ and $\mathbb{V}(x, t_m)$ respectively, so that

$$\mathbb{C}(x, t_m) := e^{\alpha x} c(x, t_m) \tag{4.5}$$

and

$$\mathbb{V}(x, t_m) := e^{\alpha x} v(x, t_m). \tag{4.6}$$

In this section we will use many notations. In order to avoid difficulty in keeping track of these notations, we present them and their meaning in the table below.

- v: the option value.
- $\mathbb{V}$: the damped option value.
- $\bar{\mathbb{V}}$: the Fourier transform of the damped option value.
- $\bar{\mathcal{V}}$: the discrete Fourier transform (DFT) approximation of $\bar{\mathbb{V}}$.
- c: the continuation value of Bermudan option.
- $\mathbb{C}$: the damped continuation value.
- $\bar{\mathcal{C}}$: approximation of the damped continuation value.

4.2.1 Applying the FFT

Now, we want to solve equation 4.3 based on a suggestion of Reiner (2001). Recall from equation 2.40 that the Fourier transform of the $\mathbb{C}(x,t_m)$ is given by

$$\begin{aligned}\mathcal{F}\{\mathbb{C}(x,t_m)\}(\omega) &:= \int_{-\infty}^{\infty} e^{i\omega x}\mathbb{C}(x,t_m)dx \\ &= \int_{-\infty}^{\infty} e^{i\omega x}e^{\alpha x}c(x,t_m)dx. \end{aligned} \tag{4.7}$$

where $\omega \in \mathbb{R}$ is the argument of a Fourier transform. Substitute equation 4.3 into equation 4.7, then,

$$\mathcal{F}\{\mathbb{C}(x,t_m)\}(\omega) := \int_{-\infty}^{\infty} e^{i\omega x}\left(e^{\alpha x}e^{-r\Delta t}\int_{-\infty}^{\infty} v(y,t_{m+1})\ \mathbf{f}(y|x)dy\right)\ dx. \tag{4.8}$$

From equation 4.4, $\mathbf{f}(y|x;\Delta t) = h(y-x;\Delta t) = h(z;\Delta t)$. Thus, equation 4.8 becomes

$$\mathcal{F}\{\mathbb{C}(x,t_m)\}(\omega) := \int_{-\infty}^{\infty} e^{i\omega x}\left(e^{\alpha x}e^{-r\Delta t}\int_{-\infty}^{\infty} v(x+z,t_{m+1})\ h(z;\Delta t)dz\right)\ dx.$$

Substitute $v(x+z,t_{m+1}) := e^{-\alpha(x+z)}\mathbb{V}(x+z,t_{m+1})$ into the above equation. Thus,

$$\begin{aligned}\mathcal{F}\{\mathbb{C}(x,t_m)\}(\omega) &:= e^{-r\Delta t}\int_{-\infty}^{\infty} e^{i\omega x}e^{\alpha x}\int_{-\infty}^{\infty}\mathbb{V}(x+z,t_{m+1})\ h(z;\Delta t)e^{-\alpha(x+z)}dz\ dx \\ &= e^{-r\Delta t}\int_{-\infty}^{\infty}\int_{-\infty}^{\infty} e^{i\omega(x+z)}\mathbb{V}(x+z,t_{m+1})\ h(z;\Delta t)e^{-i\omega z-\alpha z}dz\ dx \\ &= e^{-r\Delta t}\int_{-\infty}^{\infty}\int_{-\infty}^{\infty} e^{i\omega(x+z)}\mathbb{V}(x+z,t_{m+1})\ h(z;\Delta t)e^{-i(\omega-i\alpha)z}dz\ dx.\end{aligned}$$

Changing the ordering of integration,

$$\begin{aligned}\mathcal{F}\{\mathbb{C}(x,t_m)\}(\omega) &= e^{-r\Delta t}\int_{-\infty}^{\infty}\int_{-\infty}^{\infty} e^{i\omega(x+z)}\mathbb{V}(x+z,t_{m+1})dx\ h(z;\Delta t)e^{-i(\omega-i\alpha)z}\ dz \\ &= e^{-r\Delta t}\int_{-\infty}^{\infty}\int_{-\infty}^{\infty} e^{i\omega(y)}\mathbb{V}(y,t_{m+1})dy\ h(z;\Delta t)e^{-i(\omega-i\alpha)z}\ dz.\end{aligned} \tag{4.9}$$

Using the expression in equations 2.40 and 2.42, equation 4.9 becomes

$$\mathcal{F}\{\mathbb{C}(x,t_m)\}(\omega) = e^{-r\Delta t}\mathcal{F}\{\mathbb{V}(y,t_{m+1})(\omega)\}\Phi(-(\omega-i\alpha);\Delta t). \tag{4.10}$$

Thus, the continuation value can be derived by taking the inverse Fourier transform and un-damping equation 4.10, such that

$$\begin{aligned}c(x,t_m) &= e^{-\alpha x}\mathbb{C}(x,t_m) \\ &= e^{-r\Delta t-\alpha x}\mathcal{F}^{-1}\{\mathcal{F}\{e^{\alpha y}v(y,t_{m+1})(\omega)\}\Phi((i\alpha-\omega);\Delta t)\}(x)\end{aligned} \tag{4.11}$$

where $\Phi(\cdot)$ is the CF of the distribution of the model. To implement equation 4.11, we compute the Fourier transform of the damped option value at time t_{m+1}, $e^{\alpha y}v(y,t_{m+1})$, multiply the result with the CF which is readily available in the exponential Lévy model, $\Phi((i\alpha-\omega);\Delta t)$, take the inverse Fourier transform of the

product, and then undamped and discount the result at the same time. Thus, we derive the continuation value at time t_m and calculate $v(x, t_m)$ as the maximum of the continuation and exercise value at t_m. We repeat this recursively until we have derived $v(x, t_0)$ in equation 4.2.

Algorithm 4.2.1 presents the steps to value Bermudian option $v(x, t_0)$ as presented in Lord *et al.* (2008).

Algorithm 4.2.1:

1: $v(x_q, t_M) = \Psi(x_q)$ for $0 \leq q \leq N-1$;
2: For $m = M-1, M-2, \cdots, 0$

a. Compute $v(x_q, t_{m+1})$ and dampen it, then take the Fourier transform of the damped function for $0 \leq q \leq N-1$;

b. Compute the right-hand side of equation 4.10;

c. Compute $c(x_q, t_m)$ using equation 4.11 by taking the inverse Fourier transform of equation 4.10 and un-damping the result $0 \leq q \leq N-1$;

d. Set $v(x_q, t_m) = \max(\Psi(x_q), c(x_q, t_m))$ for $0 \leq q \leq N-1$;

Next, m;
3: Option value is given by $v(0, t_0) = c(0, t_0)$.

Approximating the discretised grid, for $\bar{\mathbb{V}}(\omega_j, t_{m+1}) \approx \bar{\mathcal{V}}(\omega_j, t_{m+1})$:

Let

$$\bar{\mathbb{V}}(\omega_j, t_{m+1}) = \int_{-\infty}^{\infty} e^{i\omega y} \mathbb{V}(y, t_{m+1}) dy \tag{4.12}$$

be the Fourier transform of $\mathbb{V}(y, t_{m+1})$. Studying equations 4.11 and 4.12, we observe the closed-form solution of these equations does not exist. Thus, we intend to approximate these equations by a discrete sum. Before we can approximate $\bar{\mathbb{V}}(\omega_j, t_{m+1}) \approx \bar{\mathcal{V}}(\omega_j, t_{m+1})$, it is necessary to find the discrete form of x, y and ω. To do this, we follow the implementation detail in Section 3.3, but in time-dependent structure, and assume

$$x_j = x_0 + \Delta x + 2\Delta x + \cdots + (N-1)\Delta x$$

is a uniform grid for a log-asset price on the spatial domain at time t_m;

$$y_j = y_0 + \Delta y + 2\Delta y + \cdots + (N-1)\Delta y$$

is a uniform grid for log-asset price on the spatial domain at time t_{m+1}; and

$$\omega_j = \omega_0 + \Delta\omega + 2\Delta\omega + \cdots + (N-1)\Delta\omega$$

is a uniform grid for the frequency domain, such that y_j's and ω_j's are equally spaced, and $\Delta x = \Delta y$. Since equations 4.11 and 4.12 are Fourier and inverse Fourier transforms, the use of uniform grids size on the spatial and frequency domain motivates

the use of special Fourier techniques (FFT) to improve the computational speed of the equations. In order to approximate $\bar{\mathbb{V}}(\omega_j)$, we use the trapezoidal rule. The difficulty in achieving smooth convergence with high-order Newton-Cotes rules was noted in Lord *et al.* (2008). Hence, the Fourier transform of the damped option value with reference to equation 4.12, corresponding to the j^{th} angular frequency sampling instant and time domain t_{m+1} in the angular frequency Fourier domain, is approximated by

$$\begin{aligned}
\bar{\mathbb{V}}(\omega_j, t_{m+1}) &\approx \Delta y \sum_{n=0}^{N-1} w_n e^{i\omega_j y_n} \mathbb{V}(y, t_{m+1}) \\
&\approx \Delta y \sum_{n=0}^{N-1} w_n e^{i[\omega_0 + j\Delta\omega][y_0 + n\Delta y]} \mathbb{V}(y, t_{m+1}) \\
&\approx e^{i[\omega_0 y_0 + j(\Delta\omega) y_0]} \Delta y \sum_{n=0}^{N-1} e^{i[\omega_0 n(\Delta y) + nj(\Delta\omega)(\Delta y)]} w_n \mathbb{V}(y, t_{m+1}) \\
&\approx e^{ijy_0(\Delta\omega)} e^{i\omega_0 y_0} \Delta y \sum_{n=0}^{N-1} e^{ijn\frac{2\pi}{N}} e^{i\omega_0 n(\Delta y)} w_n \mathbb{V}(y, t_{m+1}) \\
&\approx \bar{\mathcal{V}}(\omega_j)
\end{aligned} \tag{4.13}$$

where $w_{n\in[0,N-1]}$ are weights of the sampled points. The trapezoidal rule in the integral approximation is given by

$$w_n := \begin{cases} \frac{1}{2} & \text{for } j = 0 \text{ and } N-1, \\ 1 & \text{for others .} \end{cases} \tag{4.14}$$

Approximating the discretised grid, for $\mathbb{C}(x_q, t_m) \approx \bar{\mathcal{C}}(x_q, t_m)$:

We choose to approximate $\mathbb{C}(x_q, t_m)$ in equation 4.11 using the left-hand rule, as the error analysis in Lord *et al.* (2008). Note that the leading error term in approximating $\mathbb{C}(x_j, t_m)$ is determined by the Newton-Cotes rule used above to approximate $\bar{\mathbb{V}}(\omega_j, t_{m+1})$. Hence the damped continuation value corresponding to q^{th} vertex and time domain t_m in the log-asset structure is approximated by

$$\begin{aligned}
\bar{\mathcal{C}}(x_q, t_m) &= e^{-r\Delta_t} \frac{1}{2\pi} \Delta\omega \sum_{j=0}^{N-1} e^{-i\omega_j x_q} \bar{\mathcal{V}}(\omega_j, t_{m+1}) \Phi((i\alpha - \omega_j); \Delta_t) \\
&= e^{-r\Delta_t} \frac{1}{2\pi} \Delta\omega \sum_{j=0}^{N-1} e^{-i[\omega_0 + j(\Delta_\omega)][x_0 + q(\Delta y)]} \Phi((i\alpha - \omega_j); \Delta_t) \bar{\mathcal{V}}(\omega_j, t_{m+1}) \\
&= \frac{e^{-r\Delta t - i\omega_0[x_0 + q(\Delta y)]}}{2\pi} \Delta\omega \sum_{j=0}^{N-1} e^{-ij(\Delta\omega)[x_0 + q(\Delta y)]} \Phi((i\alpha - \omega_j); \Delta_t) \bar{\mathcal{V}}(\omega_j, t_{m+1}) \\
&= \frac{e^{-r\Delta t - i\omega_0[x_0 + q(\Delta y)]}}{2\pi} \Delta\omega \sum_{j=0}^{N-1} e^{-ijq\frac{2\pi}{N}} e^{-ijx_0(\Delta\omega)} \Phi((i\alpha - \omega_j); \Delta_t) \bar{\mathcal{V}}(\omega_j, t_{m+1}).
\end{aligned} \tag{4.15}$$

Let

$$\begin{aligned}\hat{v}(\omega_j, t_{m+1}) &:= e^{-ijy_0(\Delta\omega)}\bar{\mathcal{V}}(\omega_j, t_{m+1}) \\ &= e^{i\omega_0 y_0}\Delta y \sum_{n=0}^{N-1} w_n e^{ijn\frac{2\pi}{N}} e^{i\omega_0 n(\Delta y)}\mathbb{V}(y_n, t_{m+1}),\end{aligned}$$

then;

$$\bar{\mathcal{C}}(x_q, t_m) := \frac{e^{-r\Delta t - i\omega_0[x_0+q(\Delta y)]}}{2\pi}\Delta u \sum_{j=0}^{N-1} e^{-ijq\frac{2\pi}{N}} e^{ij(y_0-x_0)\Delta\omega}\Phi((i\alpha-\omega_j);\Delta_t)\hat{v}(\omega_j, t_{m+1}). \tag{4.16}$$

To represent $\bar{\mathcal{V}}(\omega_j, t_{m+1})$ and $\bar{\mathcal{C}}(x_q, t_m)$ in terms of the Discrete Fourier transform DFT, recall the expression for DFT and its inverse from equations 2.49 and 2.50. i.e,

$$DFT_j\{x_q\} := \sum_{q=0}^{N-1} e^{\frac{ijq2\pi}{N}} x_q \quad \text{and} \quad DFT_q^{-1}\{\hat{x}_j\} := \frac{1}{N}\sum_{j=0}^{N-1} e^{-\frac{ijq2\pi}{N}}\hat{x}_j, \tag{4.17}$$

for all $0 \leq q, j \leq N-1$. The computational complexity of $DFT_j\{\cdot\}$ or $DFT_q^{-1}\{\cdot\}$ in equation 4.17 using the usual approach of series summation is $\mathcal{O}(N^2)$. Substitute equation 4.17 into 4.16, 4.16 becomes

$$\bar{\mathcal{C}}(x_q, t_m) := \frac{e^{-r\Delta t - i\omega_0[x_0+q(\Delta y)]}}{2\pi} DFT_q^{-1}\{e^{ij(y_0-x_0)\Delta\omega}\Phi_h((i\alpha-\omega_j);\Delta_t)\hat{v}(\omega_j, t_{m+1})\}. \tag{4.18}$$

Assuming x_q and $\hat{x}_j$ have a uniform grid size, then FFT can be used to calculate equation 4.17 efficiently in order to reduce the complexity to $\mathcal{O}(N\log_2 N)$. Thus, we can approximate equation 4.18 by FFT since x_q and ω_j are equally spaced. Let

$$\omega_0 := -\frac{N}{2}(\Delta\omega), \quad \text{and} \quad \omega_0\Delta y := -\frac{N}{2}(\Delta\omega)(\Delta y). \tag{4.19}$$

Using equation 3.38,

$$y_0 = -\frac{L}{2}, \qquad \Delta y = \frac{L}{N}$$

and the Nyquist relation, equation 4.19 becomes

$$\omega_0 := -\frac{N}{2}\left(\frac{2\pi}{N}\right) = -\pi. \tag{4.20}$$

Then,

$$e^{i\omega_0 q(\Delta y)} := e^{-i\pi q} = (-1)^q. \tag{4.21}$$

Substituting equation 4.21 into equation 4.18 and expressing it in term of FFT, we get:

$$\begin{aligned}\bar{\mathcal{C}} := \frac{e^{-r\Delta t - i\omega_0 x_0}(-1)^q}{2\pi}\frac{2\pi}{N}(N)FFT_q^{-1}\left[e^{-ij(y_0-x_0)\Delta\omega}\phi_h((i\alpha-\omega_j);\Delta_t)\right] \\ .\left[FFT_j\left(e^{i\omega_0 y_0}(-1)^n w_n\mathbb{V}(y_n)\right)\right]\end{aligned} \tag{4.22}$$

Hence;

$$\bar{\mathcal{C}} := e^{-r\Delta t + i\omega_0(y_0 - x_0)}(-1)^q FFT_q^{-1}\left[e^{-ij(y_0-x_0)\Delta\omega}\phi_h((i\alpha - \omega_j);\Delta_t)FFT_j\left((-1)^n w_n \mathbb{V}(y_n)\right)\right].$$

Explicit inclusion of time dependency and undamping the approximated continuation value gives

$$c(t_m, x_q(t_m)) \approx e^{-r\Delta t - \alpha x_q(t_m) + i\omega_0(y_0(t_{m+1}) - x_0(t_m))}(-1)^q \\ FFT_q^{-1}\left[e^{-ij(y_0-x_0)\Delta\omega}\Phi_h((i\alpha - \omega_j);\Delta_t)FFT_j\left[(-1)^n w_n \mathbb{V}(y_n, t_{m+1})\right]\right]. \tag{4.23}$$

4.2.2 Implementation details.

The error analysis in Lord *et al.* (2008) shows that it is difficult to achieve stable convergence with the high-order Newton-Côtes Rule. Thus, we stick to the second-order trapezoidal rule. For detail on the error analysis, see Lord *et al.* (2008).

Similar to the pricing of European options using the CONV method discussed in Section 3.3, the optimal choice of $\mathcal{K}$ ($\mathcal{K}$ is the proportional constant in the equation for the length of the truncation range L, see equation 3.36) in $L = \mathcal{K}\mathcal{S}(\cdot)$ is not trivial and yet to be established in literature. Thus, we set $\mathcal{K} = 20$ under the BS model and $\mathcal{K} = 40$ under the VG model based on the Lord *et al.* (2008) recommendation.

Recall $m = M, M-1, \ldots, 1$, for our implementation is based on backward recursion. We begin by calculating the pay-off value at t_M, $\Psi(x, t_M)$, then the continuation value at t_{M-1}, $c(x_q, t_{M-1})$ since $c(x_q, t_{M-1})$ depends on $\Psi(x, t_M)$ for $0 \leq q \leq N-1$. For a Bermudan put option, it is clear that there will be discontinuity in $\Psi(x, t_M)$ on the y domain at $\ln(\frac{K}{S_0})$, i.e, at the point where $y = 0$, for $K = S_{t_m}$. Thus, it is certain that $c(x, t_{M-1})$ and $v(x, t_{M-1})$ will be discontinuous. Hence, it is important to shift the y-grid at time t_M such that the log-strike $\ln(\frac{K}{S_0})$ lies on it, and then calculate the $c(x, t_{M-1})$ using the new y-grid.

As we recurse backward from time t_{m+1} to t_m for $m = M-1, \cdots, 0$ there will, again, be a discontinuity to deal with at each time step but now in the Bermudan put function, $v(x, t_m)$, at some value of x. The point of discontinuity is called the early-exercise points and is denoted as x^*. x^* is the unique value of x where $c(x, t_m) = \Psi(x, t_m)$. Thus, there exists x^* in $v(x, t_m)$ at each t_m. The value of x^* is unique as the pay-off function of a plain vanilla option is a monotonic function.

The consequences of x^* are that at each t_m, it introduces discontinuity into the first derivative of $v(x, t_m)$, which leads to a non-stable convergence of the CONV method except we shift the x-grid such that x^* lies on it. Unlike the case of the y-grid, the location of x^* is hidden. Thus x^*_m must be estimated so that the x grid can be adjusted to have x^* lie on it.

Dealing with discontinuity

Recall the expression for y_j from equation 3.39. Assuming at time t_m, we place x^* on the x-grid and $\ln(\frac{K}{S_0})$ on the y-grid, then the grids can be shifted to approximate

$$x_j = \epsilon_{x,m} + \left(j - \frac{N}{2}\right)\Delta_y, \qquad \text{and} \quad y_j = \epsilon_y + \left(j - \frac{N}{2}\right)\Delta_y \tag{4.24}$$

where $\epsilon_{x,m} = x^*_m - \lceil x^*_m/\Delta x \rceil.\Delta x$ and $\epsilon_y = \ln(\frac{K}{S_0}) - \lceil \ln(\frac{K}{S_0})/\Delta y \rceil.\Delta y$. The ceiling function $\lceil g \rceil$ is given by $\min\{k \in \mathbb{Z} | k \geq g\}$. The challenge here is how to estimate x^*. Andricopoulos *et al.* (2003) determine x^* by equating the pay-off and continuation values, and solving numerically for the location of discontinuity. Lord *et al.* (2008) propose the following linear interpolation scheme to locate each x^*_m, for $m = M - 1, \ldots, 0$.

Algorithm 4.2.2:

1: Equate the x-grid at time t_m to the new y-grid at time t_{m+1}.
2: Evaluate $c(x, t_m)$ using equation 4.23.
3: Locate Δx, say $[x_l, x_{l+1}]$ between which the discontinuity is located.
4: Approximate x^*_m via the linear interpolation scheme:

$$x^*_m = \frac{x_{l+1}(c(x_l, t_m) - \Psi(x_l)) - x_l(c(x_{l+1}, t_m) - \Psi(x_{l+1}))}{(c(x_l, t_m) - \Psi(x_l)) - (c(x_{l+1}, t_m) - \Psi(x_{l+1}))} \tag{4.25}$$

5: Compute x_j in equation 4.24 using equation 4.25, and then recalculate $c(x_q, t_m)$ along the new x-grid.
6: Set the y-grid at time t_m with the new x-grid, and recurse backward to the previous exercise date, t_{m-1}, to evaluate $c(x_q, t_{m-1})$.
7: Finally, when $m = 0$, that is $t = 0$, we set $\epsilon_{x,0} = 0$ such that S_0 lies on the new x-grid, and then compute $v(x, t_0) = c(x, t_0)$ using equation 4.23.

4.2.3 Summary

Presented below is a pseudo-code that summarises the implementation of the CONV algorithm for pricing a Bermudan option.

Algorithm 4.2.3: **Convolution method**

1: Begin by shifting the y-grid at time t_M, equation 3.39, by ϵ_y to get y_j in equation 4.24 in order to avoid discontinuity on the y-grid since $\Psi(\cdot)$ is discontinuous at time t_M.
2: Compute the terminal pay-off, $\Psi(y_q, t_M)$, using the new y-grid, for $(0 \leq q \leq N-1)$.
3: Equate the $\bar{x}$ at time t_m to the new $\bar{y}$ at time t_{m+1}, for $(0 \leq q \leq N-1)$ and $m = M-1, M-2, \ldots, 1$. For now, we want to restrict our explanation to $m = M-1$.
4: Compute the continuation value, $c(x,t_{M-1})$, using equation 4.23. This is the part of the algorithm that requires the use of FFT and the damped variable,
5: Now, we can compute the early-exercise points x^*_{M-1} using equation 4.25. To determine the new x-grid, substitute x^*_{M-1} into ϵ and then compute x_j in equation 4.24.
6: Recompute the continuation value, $c(x_q, t_{M-1})$, at time t_{M-1} using the new $\bar{x}$-grid, for $(0 \leq q \leq N-1)$.
7: Then, we compute $v(x_q, t_{M-1}) = \max(c(x_q, t_{M-1}), \Psi(x_q, t_{M-1}))$ using equation 4.2, for $(0 \leq q \leq N-1)$.
8: Afterward, we reset the $\bar{y}$-grid at time t_{M-1} to the shifted $\bar{x}$-grid at time t_{M-1} such that at time t_{M-2}, the new y-grid will be the derived x-grid at time t_{M-1}. Then, we recompute the new x-grid at time t_{M-2} by deriving x^*_{M-2} at time t_{M-2}. We recompute the $c(x_q, t_{M-2})$, then $v(x_q, t_{M-2})$, and then reset the y-grid again. We repeat this procedure till we get to $m = 1$. i.e

$$v(x_q, t_1) = \max(c(x_q, t_1), \Psi(x_q, t_1)).$$

Now we can successfully proceed to the last stage since

$$c(x, t_0) = e^{-r\Delta t} \int_{\mathbb{R}} v(x, t_1) f(x|y) dx, \quad \text{for } (0 \leq q \leq N-1)$$

and we already know $\Psi(x_q, t_1)$.
9: Finally, when $m = 0$, that is at time t_0, we set $\epsilon_x = 0$ on the $\bar{x}$-grid, otherwise the price of the option will be available only as an interpolated approximation. Thus, we set the x-grid at time t_0 to the initial x_j in equation 3.39, and then computed equation 4.23.

Lord *et al.* (2008), present a detailed study on the error analysis of the CONV method when pricing Bermudan options in order to achieve a stable performance of the method, especially in models where the density function of the underlying process decays rapidly to zero and the time step between exercise dates is not too

small. For models where the density function of the underlying process decays slowly and the time step between the exercise dates is very small, the numerical results are prone to errors due to oscillations of the integrand Lord *et al.* (2008). Some of these errors can be avoided by using the appropriate (optimal) damping parameter (α), but means of deriving optimal α are yet to be established Lord *et al.* (2008).

4.3 Pricing Bermudan option using the COS method

This section is the extension of Fang and Oosterlee (2008) as discussed in Section 3.4. The pricing of Bermudan options using the COS method was first implemented by Fang and Oosterlee (2009b). Equation 4.3 can be approximated by the Fourier-cosine series expansion, as shown in equation 3.65 for European options. Thus, the approximated continuation value, $c(x,t_m)$, at each time t_m and log-asset price x, $\left(x := \log\left(\frac{S_{t_m}}{K}\right)\right)$, given the option value, $v(y,t_{m+1})$, for several y $\left(y := \log\left(\frac{S_{t_{m+1}}}{K}\right)\right)$ at time t_{m+1} (t is time-dependent) is given by

$$c(x,t_m) \approx \frac{b-a}{2} e^{-r\Delta_t} {\sum_{n=0}^{N-1}}' \mathcal{R}\left(e^{-in\pi\frac{a}{b-a}}\Phi\left(\frac{n\pi}{b-a};x\right)\right).\mathcal{V}_n(t_{m+1}) \tag{4.26}$$

and

$$\mathcal{V}_n(t_{m+1}) := \frac{2}{b-a}\int_a^b v(y,t_{m+1})\cos\left(n\pi\frac{y-a}{b-a}\right)dy, \quad \text{for } 0 \le n \le N-1 \tag{4.27}$$

where $\sum'$ means the first term of the summation of the series is weighted by half and the truncation range $[a,b]$ is given in equation 3.68 . The cosine series coefficients, $\mathcal{V}_n(t_{m+1})$, are now time-dependent and will be used to calculate the continuation value, equation 4.26, at each time t_m by backward recursion using dynamic programming.

4.3.1 Approximating the integral term in the continuation value.

At time t_m, the valuation of $\mathcal{V}_n(t_m)$ in equation 4.26 becomes non-trivial except at time t_M where $\mathcal{V}_n(t_M)$ is the same as equation 3.60. To compute $\mathcal{V}_n(t_m)$ for $m = M-1, M-2, \ldots, 1$ and $n = 0, 1, \ldots, N-1$ requires backward recursion in time. Substitute $v(\cdot)$ in equation 4.2 into 4.27 at time t_m, such that $\mathcal{V}_n(t_m)$ is given by

$$\mathcal{V}_n(t_m) := \frac{2}{b-a}\underbrace{\int_a^b \max(\Psi(x), c(x,t_m))\cos\left(n\pi\frac{x-a}{b-a}\right)dx}_{\text{integral part of the continuation value}}. \tag{4.28}$$

Our interest is to approximate the integral part of equation 4.28. Let's split the integral part into two parts, the continuation value $c(x,t_m)$, and the payoff $\Psi(x,t_m)$. The point x_m^*, (distinct value of the normalised log-asset price) where $c(x_m,t_m) = \Psi(x_m,t_m)$, is known as the early-exercise point, as discussed earlier in Section 4.2.2. The derivation of x_m^* requires a numerical method for deriving the root of a continuous function defined on a finite interval. Assuming for now that the method for finding x^* is known (it will be discussed later on), we can successfully split equation 4.28 into two finite intervals $[a,x^*]$ and $(x^*,b]$ for a put. Thus,

$$\begin{aligned}\mathcal{V}_n^{\text{put}}(t_m) := \frac{2}{b-a}\int_a^{x^*}\Psi(x)\cos\left(n\pi\frac{x-a}{b-a}\right)dx \\ + \frac{2}{b-a}\int_{x^*}^b c(x,t_m)\cos\left(n\pi\frac{x-a}{b-a}\right)dx.\end{aligned} \tag{4.29}$$

Define

$$\mathbb{X}_n(a, x^*) := \frac{2}{b-a}\int_a^{x^*} \Psi(x)\cos\left(n\pi\frac{x-a}{b-a}\right)dx \tag{4.30}$$

and

$$\mathcal{C}_n(x^*, b, t_m) := \frac{2}{b-a}\int_{x^*}^{b} c(x, t_m)\cos\left(n\pi\frac{x-a}{b-a}\right)dx, \tag{4.31}$$

for $1 \leq m \leq M-1$. Thus, equation 4.28 can be written as;

$$\mathcal{V}_n^{\text{put}}(t_m) := \mathbb{X}_n(a, x_m^*) + \mathcal{C}_n(x_m^*, b, t_m) \tag{4.32}$$

and

$$\mathcal{V}_n^{\text{put}}(t_M) := \mathbb{X}_n(a, 0), \quad \text{since, } x_M^* = 0. \tag{4.33}$$

Hence, we need to derive $\mathbb{X}_n(a, x^*)$ and $\mathcal{C}_n(x^*, b, t_m)$, for $1 \leq m \leq M-1$.

Deriving x^*:

Knowing that x^* is the unique value of a normalised log-asset price,

$$x^* := \ln\frac{S^*}{K}.$$

For a put, $(K-S)^+$, where $K > S^*$,

$$x^* := \ln\frac{S^*}{K} \leq 0,$$

If we define

$$g(x_m, t_m) := c(x_m, t_m) - \Psi(x),$$

for $1 \leq m \leq M-1$, then x^* is the unique solution of

$$g(x_m^*, t_m) = 0.$$

Fang and Oosterlee (2009b) propose the use of the Newton-Raphson method as an approach of approximating a solution of x^* since the semi-analytic expression for $c(x_m, t_m)$ is available and we can easily find the derivative of $g(x_m, t_m)$; (see Press *et al.* (2007) for detail on Newton-Raphson method.) Recall the initial root $x_M^* = 0$. Thus, at time t_{M-1}, the initial guess is the x^* at time t_M, $x_M^* = 0$.

Figure 4.3 shows that the early-exercise boundary decreases near the maturity date. The exercise points are a set of negative values; $x^* = \ln\frac{S^*}{K} \leq 0$, and the limits of points near the maturity date are below the strike. In calibration, the behaviour of the early-exercise point near the maturity date provides information on the particular Lévy process that can be used to model the dynamics of asset-log returns under a given risk-neutral measure. The nature of an underlying asset price in financial markets indicates there are upward and downward jumps under the real-world measure, therefore if the exercise point behaves in a standard manner, then one may conclude that a process of finite or infinite variation under a real-world measure must be the same as a process of finite or infinite variation under an equivalent martingale measure, Carr *et al.* (2002) and Levendorskiĭ (2004).

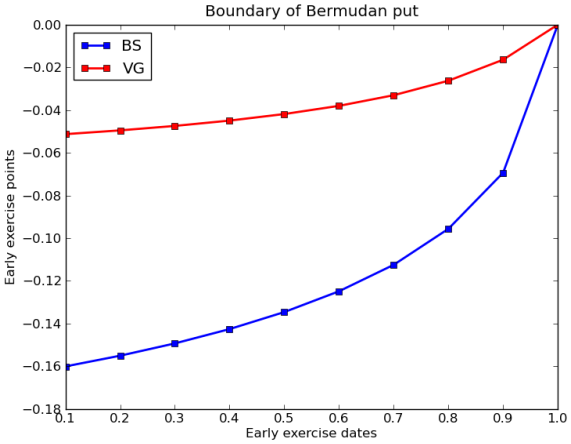

Figure 4.1: Early-exercise points x^*'s for pricing a one-year Bermudan put under the BS model and the VG model with $M = 10$, $T = 1$, $N = 64$, $r = 0.1$, $L = 12$, $\sigma_{BS} = 0.2$, $\sigma_{VG} = 0.12$, $\kappa = 0.2$ and $\theta = -0.14$.

Deriving $\mathbb{X}_n(a, x^*)$:

Recall from equation 3.60 in Section 3.4.2, $\mathbb{X}_n(a, x^*)$ can be determined numerically. Thus,

$$\begin{aligned}\mathbb{X}_n(a, x^*) &:= \frac{2}{b-a}\int_a^{x^*} [\iota.K(e^y - 1)]^+ \cos\left(n\pi\frac{x-a}{b-a}\right) dx \\ &= \frac{2\iota \cdot K}{b-a}(\beta_n(a, x^*) - \gamma_n(a, x^*)).\end{aligned} \tag{4.34}$$

Evaluating $\mathcal{C}_n(x^*, b, t_m)$:

Recall the expression for $\mathcal{C}_n(x^*, b, t_m)$ in equation 4.31. Substitute $c(\cdot)$ in equation 4.26 into 4.31. Then,

$$\begin{aligned}\mathcal{C}_n(x^*, b, t_m) := \frac{2}{b-a}\int_{x^*}^{b} \frac{b-a}{2} e^{-r\Delta_t} {\sum_{n=0}^{N-1}}' \mathcal{R}\left(e^{-ik\pi\frac{a}{b-a}}\Phi\left(\frac{k\pi}{b-a}; x\right)\right) \\ \cdot \mathcal{V}_k(t_{m+1}) \cos\left(n\pi\frac{x-a}{b-a}\right) dx.\end{aligned} \tag{4.35}$$

Let $\zeta_{n,k}(x^*, b)$ be defined as:

$$\zeta_{n,k}(x^*, b) := \frac{2}{b-a}\int_{x^*}^{b} e^{-ik\pi\frac{a}{b-a}} \cos\left(k\pi\frac{x-a}{b-a}\right) dx, \tag{4.36}$$

then, equation 4.35 can be written as:

$$\mathcal{C}_n(x^*,b,t_m) := e^{-r\Delta t}\sum_{n=0}^{N-1}{}'\mathcal{R}\left(\Phi\left(\frac{n\pi}{b-a};\Delta t\right)\hat{\mathcal{V}}_k(t_{m+1})\zeta_{n,k}(x^*,b)\right) \tag{4.37}$$

$$= \hat{\mathcal{C}}_n(x^*,b,t_m), \tag{4.38}$$

where the real parts of $\hat{\mathcal{V}}_k(\cdot)$ and $\zeta(\cdot)$ are taken; and $\hat{\mathcal{V}}_k(\cdot)$ is expressed as equation 4.33, for $m = M-1, M-2, \ldots, 1$ and $k = 0, \ldots, N-1$.

Evaluating $\zeta_{n,k}(\cdot)$

Recall the expression for $\zeta_{n,k}(x^*,b)$ from equation 4.36. Using the Euler identity as stated earlier, equation 4.36 becomes

$$\zeta_{n,k}(x^*,b) := \frac{2}{b-a}\int_{x^*}^{b}\left[\cos\frac{k\pi(x-a)}{b-a} + i\sin\frac{k\pi(x-a)}{b-a}\right]\cos\left(n\pi\frac{x-a}{b-a}\right)dx. \tag{4.39}$$

Let us introduce a change of variable $x^o_\beta = \frac{x_\beta - a}{b-a}$, and $v = \frac{x-a}{b-a}$, then,

$$\begin{aligned}\zeta_{n,k}(x^o_1,x^o_2) &:= 2\int_{x^o_1}^{x^o_2}[\cos(k\pi v) + i\sin(k\pi v)]\cos(n\pi v)dv \\ &= 2\int_{x^o_1}^{x^o_2}\cos(k\pi v)\cos(n\pi v)dv + 2i\int_{x^o_1}^{x^o_2}\sin(k\pi v)\cos(n\pi v)dv\end{aligned} \tag{4.40}$$

Using the basic calculus integrations of the trigonometry function,

$$\begin{aligned}\int_{c^o_1}^{c^o_2}\cos(xv)\cos(yv)dv &:= \left[\frac{\sin((x-y)v)}{2(x-y)} + \frac{\sin((x+y)v)}{2(x+y)}\right]_{v=c^o_2}^{v=c^o_1} \\ \int_{c^o_1}^{c^o_2}\sin(xv)\cos(yv)dv &:= \left[-\frac{\cos((x-y)v)}{2(x-y)} - \frac{\cos((x+y)v)}{2(x+y)}\right]_{v=c^o_2}^{v=c^o_1}.\end{aligned} \tag{4.41}$$

Applying equation 4.41 in 4.40 when $k+n \neq 0$ and $k-n \neq 0$. Then,

$$\begin{aligned}&\zeta_{n,k}(x^o_1,x^o_2) \\ &= 2\left[\frac{\sin((k\pi-n\pi)v)}{2(k\pi-n\pi)} + \frac{\sin((k\pi+n\pi)v)}{2(k\pi+n\pi)}\right]_{v=x^o_2}^{v=x^o_1} + 2i\left[-\frac{\cos(k\pi-n\pi)v}{2(k\pi-n\pi)} - \frac{\cos(k\pi+n\pi)v}{2(k\pi+n\pi)}\right]_{v=x^o_2}^{v=x^o_1} \\ &= \left[\frac{\sin((k-n)\pi v)}{(k-n)\pi} - \frac{i\cos((k-n)\pi v)}{(k-n)\pi}\right]_{v=x^o_2}^{v=x^o_1} + \left[\frac{\sin((k+n)\pi v)}{(k+n)\pi} - \frac{i\cos((k+n)\pi v)}{(k+n)\pi}\right]_{v=x^o_2}^{v=x^o_1} \\ &= -\frac{i}{\pi}\left[\frac{\cos((k-n)\pi v)}{(k-n)} + \frac{i\sin((k-n)\pi v)}{(k-n)}\right]_{v=x^o_2}^{v=x^o_1} - \frac{i}{\pi}\left[\frac{\cos((k+n)\pi v)}{(k+n)} + \frac{i\sin((k+n)\pi v)}{(k+n)}\right]_{v=x^o_2}^{v=x^o_1}\end{aligned}$$

Using the Euler formula,

$$\zeta_{n,k}(x^o_1,x^o_2) = -\frac{i}{\pi}\left[\frac{1}{k-n}\exp(i(k-n)\pi v) + \frac{1}{k+n}\exp(i(k+n)\pi v)\right]_{v=x^o_2}^{v=x^o_1} \tag{4.42}$$

and when $n = 0$ and $k = 0$, equation 4.40 can be written as:

$$\begin{aligned}\zeta_{0,0}(x^*, b) &:= 2\int_{x_1^o}^{x_2^o}[\cos^2(0) + 2i\sin(0)\cos(0)dv = 2\int_{x_1^o}^{x_2^o} 1dv \\ &= 2\cdot\frac{b-x^*}{b-a} = -\frac{i}{\pi}\left[i\pi\frac{b-x^*}{b-a} + i\pi\frac{b-x^*}{b-a}\right].\end{aligned} \tag{4.43}$$

Also, when $k = n$, $n \neq 0$ and $k \neq 0$, equation 4.40 can be written as:

$$\begin{aligned}\zeta_{n,k}(x^*, b) &= 2\int_{x_1^o}^{x_2^o}[\cos^2(n\pi v) + i\sin(n\pi v)\cos(n\pi v)]dv \\ &= 2\int_{x_1^o}^{x_2^o}\left[\frac{1+\cos(2n\pi v)}{2} + i\frac{\sin(2n\pi v)}{2}\right]dv \\ &= \int_{x_1^o}^{x_2^o}(1 + \exp(2n\pi vi))dv \\ &= \frac{b-x^*}{b-a} + \frac{1}{2n\pi i}[\exp(2in\pi v)]|_{v=x_1^o}^{v=x_2^o} \\ &= -\frac{i}{\pi}\left[i\pi\frac{b-x^*}{b-a} + \left[\frac{1}{k+n}\exp(i(k+n)\pi v)\right]_{v=x_1^o}^{v=x_2^o}\right].\end{aligned} \tag{4.44}$$

In summary;

$$\zeta_{n,k}(x^*, b) = -\frac{i}{\pi}[\zeta_{n,k}^c(x^*, b) + \zeta_{n,k}^s(x^*, b)] \tag{4.45}$$

where

$$\zeta_{n,k}^c(x^*, b) := \begin{cases} i\pi\frac{b-x^*}{b-a} & \text{for } n, k = 0 \\ \frac{1}{k+n}\left[\exp(i(k+n)\pi) - \exp(i(k+n)\frac{x^*-a}{b-a}\pi)\right] & \text{others} \end{cases} \tag{4.46}$$

and

$$\zeta_{n,k}^s(x^*, b) := \begin{cases} i\pi\frac{b-x^*}{b-a} & \text{for } n = j \\ \frac{1}{k-n}\left[\exp(i(k-n)\pi) - \exp(i(k-n)\frac{x^*-a}{b-a}\pi)\right] & \text{for } n \neq k. \end{cases} \tag{4.47}$$

Recall the expression $\hat{\mathcal{C}}_n(\cdot)$ in equation 4.37 and substitute equation 4.45 into 4.37. Then,

$$\begin{aligned}\hat{\mathcal{C}}_n(x^*, b, t_m) &= e^{-r\Delta t}\mathcal{R}\left(-\frac{i}{\pi}{\sum_{n=0}^{N-1}}'[\zeta_{n,k}^c(x^*, b) + \zeta_{n,k}^s(x^*, b)]\Phi\left(\frac{n\pi}{b-a}; \Delta t\right)\hat{\mathcal{V}}_k(t_{m+1})\right) \\ &= \frac{e^{-r\Delta t}}{\pi}\mathcal{I}\left({\sum_{n=0}^{N-1}}'[\zeta_{n,k}^c(x^*, b) + \zeta_{n,k}^s(x^*, b)]\Phi\left(\frac{n\pi}{b-a}; \Delta t\right)\hat{\mathcal{V}}_k(t_{m+1})\right).\end{aligned} \tag{4.48}$$

For $m = M-1, M-2, \cdots, 1$, let

$$w_k(t_{m+1}) := \begin{cases} \frac{1}{2}\Phi(0)\hat{\mathcal{V}}_0(t_{m+1}) & \text{for } k = 0 \\ \\ \Phi(\frac{k\pi}{b-a})\hat{\mathcal{V}}_k(t_{m+1}) & \text{for others,} \end{cases} \tag{4.49}$$

and the matrix-vector of $\hat{\mathcal{C}}_n(x^*, b, t_m)$, $\zeta^c_{n,k}(x^*, b)$ and $\zeta^s_{n,k}(x^*, b)$ can be written as:

$$\begin{aligned} \hat{\mathbf{C}}(x^*, b, t_m) &= [\hat{\mathcal{C}}_0(x^*, b, t_m), \ldots\ldots\ldots, \hat{\mathcal{C}}_{N-1}(x^*, b, t_m)]^{\mathbb{T}} \\ \underline{\zeta}^s(x^*, b) &= [\zeta^s_{n,k}(x^*, b)]^{N-1}_{n,k=0} \quad , \quad \underline{\zeta}^c(x^*, b) = [\zeta^c_{n,k}(x^*, b)]^{N-1}_{n,k=0} \\ \mathbf{w}(t_{m+1}) &= [w_0(t_{m+1}), \ldots\ldots\ldots\ldots, w_{N-1}(t_{m+1})]^{\mathbb{T}} \end{aligned}$$

where $[\ldots]^{\mathbb{T}}$ is the transpose of the input vector, for $m = M-1, M-2, \ldots, 1$. Then, equation 4.48 is given by

$$\hat{\mathbf{C}}(x^*, b, t_m) = \frac{e^{-r\Delta_t}}{\pi}\mathcal{I}\left([\underline{\zeta}^c(x^*, b) + \underline{\zeta}^s(x^*, b)]\mathbf{w}(t_{m+1})\right) \tag{4.50}$$

4.3.2 Improving computational efficiency.

The computation of each component of $\hat{\mathbf{C}}$ requires a computation of $\mathcal{O}(N^2)$, but the matrix $\zeta^c_{n,k}(\cdot)$ and $\zeta^s_{n,k}(\cdot)$ exhibit some special properties that stimulate the use of the FFT algorithm for efficient computation of matrix-vector products. Here, we discuss how the computational complexity can be reduced to $\mathcal{O}(N \log_2 N)$ by using the FFT algorithm.

A circular matrix is a special type of matrix in which each row is a rounded shift of a prior row. We note that $\underline{\zeta}^s(\cdot)$ and $\underline{\zeta}^c(\cdot)$ are special types of a circular matrix, i.e, the *Toeplitz* matrix and the *Hankel* matrix. Thus, $\underline{\zeta}^s(\cdot)$ can be written as:

$$\underline{\zeta}^s(x^*, b) = \begin{bmatrix} m_0 & m_1 & \ldots & m_{N-2} & m_{N-1} \\ m_{-1} & m_0 & \ldots & m_{N-3} & m_{N-2} \\ m_{-2} & m_{-1} & \ldots & \vdots & \vdots \\ \vdots & \vdots & \ddots & m_1 & \vdots \\ m_{2-N} & m_{3-N} & \ldots & m_0 & m_1 \\ m_{1-N} & m_{2-N} & \ldots & m_{-1} & m_0 \end{bmatrix} \tag{4.51}$$

and

$$\underline{\zeta}^c(x^*, b) = \begin{bmatrix} m_0 & m_1 & \ldots & m_{N-2} & m_{N-1} \\ m_1 & m_2 & \ldots & m_{N-1} & m_N \\ m_2 & m_3 & \ldots & \vdots & \vdots \\ \vdots & \vdots & \ddots & \vdots & \vdots \\ m_{N-2} & m_{N-1} & \ldots & m_{2N-4} & m_{2N-3} \\ m_{N-1} & m_N & \ldots & m_{2N-3} & m_{2N-2} \end{bmatrix} \tag{4.52}$$

where

$$m_k(x^*,b) := \begin{cases} i\pi\frac{x^*-b}{b-a} & \text{for } k=0 \\ \frac{\exp\left(ik\frac{b-a}{b-a}\right)-\exp\left(ik\frac{x^*-a}{b-a}\right)}{k} & \text{for } k\neq 0. \end{cases} \tag{4.53}$$

To improve the computational efficiency of $\underline{\zeta}^s(\cdot)$ and $\underline{\zeta}^c(\cdot)$, we begin by defining the following function with no dependence on (x^*,b) and t_{m+1}:

$$\mathbf{m}^s(x^*,b) = [m_0, m_{-1}, m_{-2}, \ldots, m_{1-N}, 0, m_{N-1}, m_{N-2}, m_{N-3}\ldots, m_1]^{\mathbb{T}} \tag{4.54}$$

$$\mathbf{w}^s(t_{m+1}) = [w_0, w_1, w_2, \ldots, w_{1-N}, \underbrace{0,\ldots,0}_{\text{N terms}}]^{\mathbb{T}} \tag{4.55}$$

$$\mathbf{m}^c(x^*,b) = [m_{2N-1}, m_{2N-2}, \ldots, m_1, m_0]^{\mathbb{T}} \tag{4.56}$$

$$\mathbf{w}^c(t_{m+1}) = [\underbrace{0,\ldots,0}_{\text{N terms}}, w_0, w_1, w_2, w_{N-1}]^{\mathbb{T}}. \tag{4.57}$$

Then it can be shown that (see Fang and Oosterlee (2009b) and Loan (1992) for detail of the proof);

$$\underline{\zeta}^s(x^*,b)\mathbf{w}(t_{m+1}) = \text{ first } N \text{ terms of } [\mathbf{m}^s(x^*,b) * \mathbf{w}^s(t_{m+1})] \tag{4.58}$$

$$\underline{\zeta}^c(x^*,b)\mathbf{w}(t_{m+1}) = \text{ first } N \text{ terms of } [\mathbf{m}^c(x^*,b) * \mathbf{w}^c(t_{m+1})], \text{ in reverse form.} \tag{4.59}$$

Recall from Fang and Oosterlee (2009b), a circular convolution of two vectors is equal to the inverse discrete Fourier transform of the products of the forward discrete Fourier transform:

$$\mathbf{p} * \mathbf{q} = DFT^{-1}[DFT[\mathbf{p}] \cdot DFT[\mathbf{q}]]. \tag{4.60}$$

Thus, the right-hand-side of equations 4.58 and 4.59 can be written as

$$\mathbf{m}^s(x^*,b) * \mathbf{w}^s(t_{m+1}) = DFT_j^{-1}[DFT_n[\mathbf{m}^s(x^*,b)] \cdot DFT_n[\mathbf{w}^s(t_{m+1})]] \tag{4.61}$$

and

$$\mathbf{m}^c(x^*,b) * \mathbf{w}^c(t_{m+1}) = DFT_j^{-1}[DFT_n[\mathbf{m}^c(x^*,b)] \cdot DFT_n[\mathbf{w}^c(t_{m+1})]], \tag{4.62}$$

for $j = 0,\cdots,2N-1$ and $n = 0,\cdots,2N-1$. Some observations made by Fang and Oosterlee (2009b), reveal ways of improving the computational efficiency of computing each vector in equation 4.50. Algorithm 4.3.1 summarises the efficient computation of $\hat{\mathbf{C}}(x^*,b,t_m)$.

4.3.3 Implementation details.

Result 4.3.1 (Effect of L in the convergence of the COS method for pricing Bermudan puts)**.** [For $K = 110$, the reference price:= [BS−11.98745352, VG−9.040646119]]. In Figure 4.2, we observe the performance of L across different values of N. Recall $N = 2^n$. For $n > 6$, the error convergence decreases as L increases. Under the BS model, for $n > 6$, $L \geq 10$ gives satisfactory results. Under the VG model, $L = 13$ gives satisfactory results across several values of N, for $L > 13$, the error convergence decreases as L increases when $n < 12$. In all experiments, we set $L = 10$ under the BS model and $L = 13$ under the VG model.

Algorithm 4.3.1: Computation of $\hat{\mathbf{C}}(x^*, b, t_m)$, equation 4.50

1: Compute w_k according to equation 4.49, for $(0 \leq k \leq N-1)$;
2: Compute m_k using equation 4.53, for $(0 \leq k \leq N-1)$;
3: Compute $\mathbf{m}^c$ according to equation 4.56 using the properties of m_k from equation 4.53 ;
4: Compute $\mathbf{m}^s$ according to equation 4.54 using the properties of m_k from equation 4.53 ;
5: Compute $\mathbf{w}^s$ according to equation 4.57 using the properties of w_k from equation 4.49;
6: Compute $\underline{\zeta}^s(x^*, b)\mathbf{w}$ in equation 4.58 via DFT using equation 4.61 such that $\underline{\zeta}^s(x^*, b)\mathbf{w}$ = the first N elements of

$$DFT_j^{-1}[DFT_n[\mathbf{m}^s(x^*, b)] \cdot DFT_n[\mathbf{w}^s(t_{m+1})]];$$

7: Compute $\underline{\zeta}^c(x^*, b)\mathbf{w}$ in equation 4.59 via DFT using equation 4.62 such that $\underline{\zeta}^c(x^*, b)\mathbf{w}$ = reverse the first N elements of

$$DFT_j^{-1}[DFT_n[\mathbf{m}^c(x^*, b)] \cdot \mathbf{sgn} \cdot DFT_n[\mathbf{w}^s(t_{m+1})]]$$

Note: $DFT[\mathbf{w}^c] = \mathbf{sgn} \cdot DFT[\mathbf{w}^s]$ with $\mathbf{sgn} = [1, -1, 1, -1, \cdot]^{\mathbb{T}}$] (this is based on the shifting property of DFT, see Press *et al.* (2007) for detail);
8: Then, compute $\hat{\mathbf{C}}(x^*, b, t_m)$ via FFT:

$$\hat{\mathbf{C}}(x^*, b, t_m) = \frac{e^{-r\Delta_t}}{\pi} \mathcal{I}\left([\underline{\zeta}^c(x^*, b)\mathbf{w} + \underline{\zeta}^s(x^*, b)\mathbf{w}]\right). \tag{4.63}$$

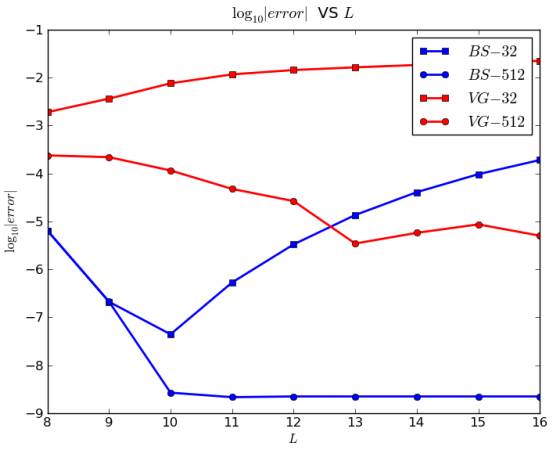

Figure 4.2: Error convergence for pricing a one-year Bermudan put under the BS model and VG model with respect to L with $M = 10$, $T = 1$, $K = 110$, $S_0 = 100$, $\sigma_{BS} = 0.2$, $\sigma_{VG} = 0.12$, $r = 0.1$, $\theta_{VG} = -0.14$, $\kappa = 0.2$, for different values of N.

4.3.4 Summary

Presented below is a pseudo-code that summarsies the implementation of the COS algorithm for pricing Bermudan option.

Algorithm 4.3.2: **Fourier-cosine series method.**

1: We begin by computing the truncation range,

$$[a,b] := [x + c_1 - L\sqrt{(c_2 + \sqrt{(c_4)})}, x + c_1 + L\sqrt{(c_2 + \sqrt{(c_4)})}],$$

where $x = \log(\frac{S_0}{K})$, as proposed by Fang and Oosterlee (2009b).

2: Then, we compute the terminal put payoff $V_n^{\text{put}}(t_M)$ using equation 4.33 where $\mathbb{X}_n(a, x_M^*)$ is given in equation 4.34, and $x_M^* = 0$, for $n = 0, 1, \ldots, N-1$.

3: Using the Newton Raphson method, we derive the early-exercise points, x_m^*, where the initial root $x_M^* = 0$, then we use backward recursion, for $m = M - 1, M-2, \ldots, 1$.

4: Then by equation 4.32, we compute

$$\mathcal{V}_n^{\text{put}}(t_m) = \mathbb{X}_n(a, x_m^*) + \mathcal{C}_n(x_m^*, b, t_m,)$$

where $\mathbb{X}_n(a, x_m^*)$ is given in equation 4.34 and $\mathcal{C}_n(x_m^*, b, t_m) = \hat{\mathbf{C}}(x_m^*, b, t_m)$ is given in equation 4.50 by

$$\hat{\mathbf{C}}(x_m^*, b, t_m) = \frac{e^{-r\Delta_t}}{\pi} \mathcal{I}\left([\underline{\zeta}^c(x_m^*, b) + \underline{\zeta}^s(x_m^*, b)]\mathbf{w}\right),$$

for $m = M-1, \ldots, 1$ and $n = 0, \ldots, N-1$. We repeat this procedure up till when $m = 1$ such that

$$\mathcal{V}_n^{\text{put}}(t_1) = \mathbb{X}_n(a, x_1^*) + \hat{\mathbf{C}}(x_1^*, b, t_1).$$

5: Lastly, the option value at time t_0 is given by equation 4.26 when $t = 0$;

$$c(x, t_0) \approx \frac{b-a}{2} e^{-r\Delta_t} {\sum_{n=0}^{N-1}}' \mathcal{R}\left(e^{-in\pi \frac{a}{b-a}} \Phi\left(\frac{n\pi}{b-a}; x\right)\right) \cdot \mathcal{V}_n^{\text{put}}(t_1),$$

where the $\mathcal{V}_n^{\text{put}}(t_1)$ coefficients would have been computed from above, and the coefficients of $\mathcal{R}(\cdot)$ are defined accordingly.

We observe the convergence of the COS method depends on the choice of L and N.

4.4 Pricing Bermudan options using FST method

In this section, we shall derive the FST formula for pricing Bermudan options from equation 3.95 by extending the FST formula for pricing European options in equation 3.101. Naturally, a time step t_{m+1} in the frequency domain requires a step backward in time t_m on the space domain. This simplifies the FST Bermudan formula. Thus, the FST formula for pricing a Bermudan put option, equation 4.2 with M-exercise dates is given as follows:

$$v_{m-1} := \max(\underbrace{\Psi(\mathbf{s})}_{\text{payoff}}, \underbrace{FFT^{-1}[FFT[v_m] \cdot e^{\varrho(\cdot)\Delta t}]}_{\text{continuation value}}), \quad \text{for } m = 2, \cdots, M-1 \tag{4.64}$$

where $\max(,)$ is taken at each point in the length of $\mathbf{s}$ (component-wise).

$$\mathbf{s} = S_0 \exp(x_n), \quad \text{for } (0 \leq n \leq N-1)$$

and x_n are points on the real space (x-grid) given in equation 3.87. At $m = M-1$,

$$v_M := e^{-r\Delta t}\Psi(\mathbf{s}) = e^{-r\Delta t}(K - S_0 \exp(x_n))^+.$$

Thus,

$$v_{M-1} := \max(\Psi(\mathbf{s}), FFT^{-1}[FFT[e^{-r\Delta t}(K - S_0 \exp(x_n))^+] \cdot e^{\varrho(\cdot)\Delta t}]).$$

To know the Bermudan put at $m = 0$, that is at time t_0, solve for $v_{m=1}$ using equation 4.64, then substitute $v_{m=1}$ into equation 3.95, that is;

$$v_0 := \mathcal{F}^{-1}[\mathcal{F}[v_1]e^{\varrho(\omega)(t_1 - t_0)}], \tag{4.65}$$

and solve accordingly.

4.4.1 Implementation details.

The selection of the grid points on the real space and the Fourier space for pricing a Bermudan option is the same as discussed in Section 3.5. The characteristic exponents $\varrho(\omega)$ are given in Table 3.5. The time step ($\Delta t = \frac{T}{M}$) is implemented on the frequency domain, the Fourier space, while the terminal condition is performed on the space domain, the real space.

Result 4.4.1 (Effect of x, the limit point on the real space on one-year Bermudan put option using the FST method under BS model)**.**

As shown in Figure 4.3, $x \in [1.5, 4.5]$ gives a more accurate result under the BS model and $x \in [0.5, 1.5]$ is preferable for pricing a Bermudan put under the VG model. Similar to the pricing of European options, the optimal value of x changes with different values of N and volatilities σ. In all numerical experiments here, we set $x = 1.5$ in the BS and VG models. That is $x_{\min} = -1.5$ and $x_{\max} = 1.5$.

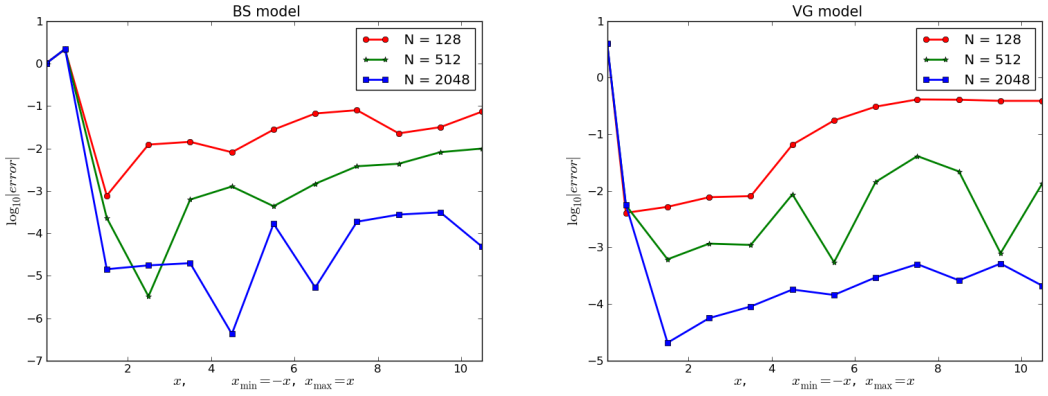

Figure 4.3: Error convergence for pricing a one-year Bermudan put using the FST method under BS and VG models, with respect to x_{grid}. Parameters used: $S_0 = 100$, $K = 110$, $r = 0.1$, $\sigma_{BS} = 0.25$, $\sigma_{VG} = 0.12$, $\theta_{VG} = -0.14$, $\kappa = 0.2$, for different values of N.

4.4.2 Summary

Presented below is a pseudo-code that summarises the implementation of the FST algorithm for pricing a Bermudan option.

Algorithm 4.4.1: **Fourier space time-stepping method.**

1: Declare the initial variables: S_0, T, x, N, M;
2: Compute the Lévy exponent of the distribution of the underlying asset, that is, $\varrho(\cdot)$;
3: Discretize the spatial domain $[0, T] \times (x_{\min}, x_{\max})$ using equation 3.87 (for $0 \leq n \leq N-1$);
4: Discretize the frequency domain $[0, T] \times (\omega_{\min}, \omega_{\max})$ according to equation 3.88 (for $0 \leq n \leq N-1$);
5: Compute V_{m-1} according to equation 4.64 via FFT (for $M-1 \leq m \leq 2$);
6: Compute V_0 via FFT using equation 4.65.

The computation requires a time-stepping procedure which is ignored in the FST formula for pricing an European option. The FST Bermudan put formula can be extended to price an American put option by increasing the exercise dates. To speed up the computation time for pricing an American put, the penalty method can be used. The numerical behaviour of approximating a Bermudan put to an American put is presented in Section 4.6.

4.5 Approximating American options by Bermudan options

An American put (call) option gives the holder of the option the opportunity to sell (buy) a financial asset for a fixed price K, at any time until the maturity date. The holder may choose whether or not to exercise the option. Obviously, only American options with finite maturity dates are of interest in practice. Again, it is never optimal to exercise an American call on a non-dividend paying asset before maturity; American calls on such are equivalent to European calls, Hull (2007), and the pricing of an American put option is not trivial. It is optimal to exercise the put if the payoff from exercising it is greater than the value of the put if it is not exercised.

To price options with early-exercise features in an exponential Lévy model with jump, the premium has an extra complex term due to the fact that the stock-price can jump from the exercise region to the continuation region without crossing the exercise boundary. The difficulty in the diffusion model comes from the non integral term. A sufficient condition which ensures that the price function of the optimal stopping problem is the unique solution of the free-boundary problem, is given in Peskir and Shiryaev (2006). In literature, different techniques have been developed to determine the early-exercise boundary for American put for different financial models. An explicit analysis of the problem of pricing of American option is to transform the optimal stopping problem into free boundary problem Almendral and Oosterlee (2007). Geske and Johnson (1984) established a closed-form solution for solving American puts by using a compound option-pricing approach. However, their formula cannot be solved analytically, numerical methods must be used to approximate the real price.

Numerical methods that involve the calculation of a series of Bermudan put options can be used to price American put options by increasing the number of exercise dates and *direct approximation*. The number of Bermudan puts required to determine an approximation for the American put option, with a desired level of accuracy, can be determined by what is known as the Repeated-Richardson Extrapolation Technique. Fang and Oosterlee (2009b) and Lord *et al.* (2008), validate these two approaches of pricing American puts. Jackson. *et al.* (2008) and Surkov (2009), employed the direct approximation approach to pricing American puts and also applied the penalty method on the FST algorithm for Bermudan puts in order to increase the efficiency of the method.

In this dissertation, we presents the numerical behaviour of pricing a one-year American put under the VG model by the direct approximation method.

4.5.1 Direct approximation.

The direct approximation of Bermudan puts to American puts describes the behaviour of Bermudan puts prices if M, the number of early-exercise dates, goes to

infinity. The only difference is the increase in the value of M, the exercise dates, in the implementation.

4.6 Numerical results

This section summarises the numerical behaviour of Fourier methods for pricing Bermudan puts under the BS and VG models, and for pricing American puts under the VG model. Reference prices are taken from Lord *et al.* (2008). The CF, characteristic exponent, and cumulants are given in Tables 2.1 and 2.2, respectively. The error convergence is the same as discussed in Section 3.6. The parameters used for implementation are stated in Table 4.1. The number of exercise dates for the Bermudan puts in all computations is 10, that is, $M = 10$. And the number of exercise dates for American puts is 100.

BS	$\sigma_{BS} = 0.25$	$r = 0.1$	$S_0 = 100$	$q = 0$	$K = 110$		
VG	$\sigma_{VG} = 0.12$	$r = 0.1$	$S_0 = 100$	$q = 0$	$\theta_{VG} = -0.14$	$\kappa = 0.2$	$K = 110$

Table 4.1: Parameters used for the implementation. Otherwise, stated.

4.6.1 Black-Scholes model

The convergence result of pricing a one-year Bermudan put under the BS model is discussed. The reference price is 11.98745352 when $K = 110$, Lord *et al.* (2008).

Result 4.6.1 (Error convergence and CPU-time for pricing a one-year Bermudan put under the BS model using the CONV, COS and FST methods)**.** We discover the convergence exhibited here is similar to that discussed in Result 3.6.1. The convergence of the CONV and FST methods is algebraic while the convergence of the COS method is exponential. This is as a result of the smooth behaviour of the transition density of the BS model. The CONV and FST methods needs $N > 120$ points to converge to an error of order $\mathcal{O}(10^{-3})$ in 100 milliseconds, while the COS method needs $N < 64$ to converge to an error of order $\mathcal{O}(10^{-8})$ in more than 100 milliseconds.

4.6.2 Variance Gamma model

Here we present the error convergence and the CPU-time for a one-year Bermudan put under the VG model. The reference price is 9.040646119 when $K = 110$, Lord *et al.* (2008).

Result 4.6.2 (Error convergence and CPU-time for pricing a one-year Bermudan put under the VG model using the CONV, COS and the FST methods)**.** Figure 4.5 shows the error convergence of the CONV, COS and FST methods to be algebraic (second-order). The convergence of the COS method is similar to Result 3.6.4, (pricing European calls under VG model when $T = 0.1$), because $(\Delta t(T/M = 0.1)) < \kappa(0.2)$. The convergence of the CONV and FST methods remains algebraic. With $N = 500$,

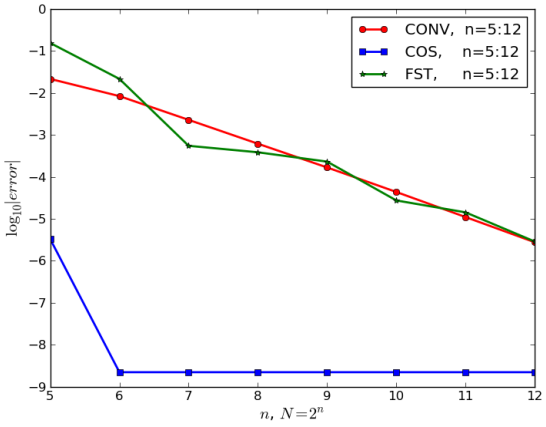

(a) Error convergence for pricing a one-year Bermudan put under the BS model.

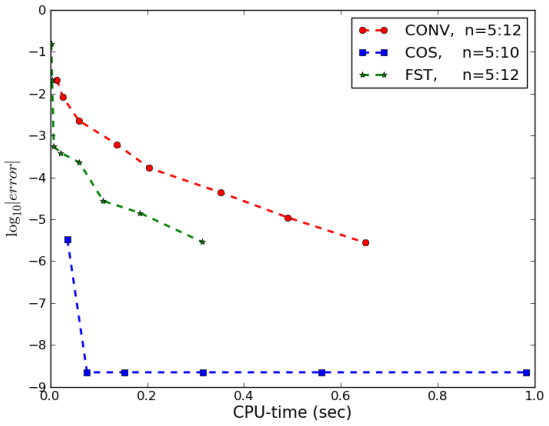

(b) CPU-time for pricing a one-year Bermudan put under the BS model.

Figure 4.4: One-year Bermudan put under the BS model. Parameters used: $T = 1$, $\alpha = 0$, $L = 10$ and $x = 1.5$

	CONV		COS		FST	
n	**|error|**	**time**	**|error|**	**time**	**|error|**	**time**
5	$4.22e^{-01}$	0.01	$3.30e^{-06}$	0.03	$1.50e^{-01}$	0.002
6	$9.35e^{-02}$	0.02	$2.22e^{-09}$	0.07	$2.14e^{-02}$	0.003
7	$3.27e^{-02}$	0.05	$2.22e^{-09}$	0.15	$5.40e^{-04}$	0.007
8	$7.14e^{-03}$	0.13	$2.22e^{-09}$	0.31	$3.84e^{-04}$	0.027
9	$1.68e^{-03}$	0.20	$2.22e^{-09}$	0.55	$2.30e^{-04}$	0.059
10	$5.35e^{-04}$	0.35	$2.22e^{-09}$	0.98	$2.73e^{-05}$	0.109
11	$2.20e^{-04}$	0.49	$2.22e^{-09}$	1.08	$1.42e^{-05}$	0.184
12	$3.66e^{-05}$	0.65	$2.22e^{-09}$	1.51	$2.86e^{-06}$	0.313

Table 4.2: Error and CPU (time-seconds) for pricing a one-year Bermudian put under the BS model, K=110.

the COS method achieves an error of order $\mathcal{O}(10^{-5})$ in less than 500 milliseconds of CPU-time, while an error of order $\mathcal{O}(10^{-3})$ is achieved in the CONV and FST methods in less CPU-time.

	CONV		COS		FST	
n	**|error|**	**time**	**|error|**	**time**	**|error|**	**time**
5	$2.6e^{-01}$	0.04	$1.62e^{-02}$	0.03	$2.61e^{-01}$	0.006
6	$4.00e^{-02}$	0.06	$1.70e^{-04}$	0.08	$2.00e^{-02}$	0.008
7	$8.26e^{-03}$	0.09	$3.00e^{-04}$	0.14	$5.21e^{-03}$	0.062
8	$1.19e^{-03}$	0.13	$3.62e^{-05}$	0.38	$6.98e^{-04}$	0.067
9	$2.51e^{-04}$	0.32	$3.43e^{-06}$	0.73	$6.16e^{-04}$	0.110
10	$6.71e^{-05}$	0.59	$1.971e^{-06}$	1.46	$7.10e^{-05}$	0.159
11	$1.76e^{-05}$	1.37	$2.93e^{-07}$	2.48	$2.06e^{-05}$	0.260
12	$4.56e^{-06}$	2.63	$1.22e^{-07}$	3.53	$3.89e^{-06}$	0.394

Table 4.3: Error and CPU (time-seconds) for pricing a one-year Bermudian put under BS model, K=110.

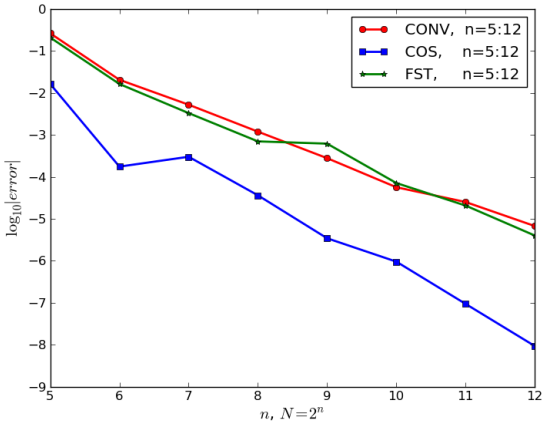

(a) Error convergence for pricing a one-year Bermudan put under the VG model.

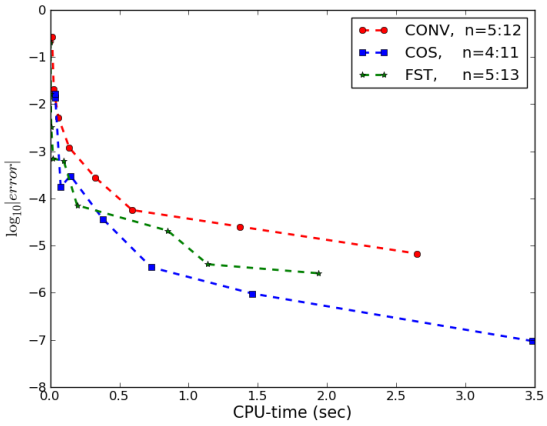

(b) CPU-time for pricing a one-year Bermudan put under the VG model.

Figure 4.5: One-year Bermudan put under the VG model. Parameters used: $T = 1$, $\alpha = 0$, $L = 13$ and $x = 1.5$

In the BS and the VG models, the FST method achieves it convergence in less computational time because it does not require any time-stepping procedure between successive dates. The error convergence of the COS method is still faster than the CONV and FST methods.

4.6.3 Speed

In cases considered here, the parameters used for implementation are the same as in Table 4.1, unless otherwise stated. $K = 110$ under the BS model and the VG model.

Result 4.6.3 (CPU-time taken to achieve a $\mathcal{O}(10^{-6})$ accuracy across the BS model and the VG model using the CONV, COS and FST methods)**.** Comparing the speed to accuracy across different models, the COS method is good for pricing a Bermudian put under the BS model because, there is no discontinuity in the computation of the CF of the model, unlike the VG model, where $\Delta t(0.1) < \kappa(0.2)$, and this introduces discontinuity in the computation of the CF of the model. The FST method is preferable for pricing a Bermudian put under the VG model because, the method does not require any time-stepping procedure between successive dates, thus, it can successfully deal with discontinuity in its algorithm.

Method	BS model	VG model
CONV	0.72	2.63
COS	0.03	1.09
FST	0.313	0.39

Table 4.4: CPU-time (milliseconds) for pricing a one-year Bermudian put that converges to an error of order $\mathcal{O}(10^{-6})$ under the BS model and VG model using the CONV, COS and FST methods.

4.6.4 Direct Approximation of Bermudan put to American put

The reference price for pricing an American put under the VG model is 10.0000, Lord *et al.* (2008). In Result 4.6.4, we set $M = 100$.

Result 4.6.4 (Error convergence for pricing a one-year American put under the VG model using the CONV, COS and the FST methods)**.**

Obviously, the convergence of the FST method is significant. With $N = 1000$, an error of order $\mathcal{O}(10^{-8})$ is achieved with the FST method in 1 second of CPU-time, while an error of order $\mathcal{O}(10^{-3})$ is achieved with the CONV and the COS method in more than 2 seconds of CPU-time. As M increases in the COS method, the convergence becomes slower compared to previous results achieved because an increase in M leads to a decrease in Δt. Thus, Δt becomes very small. Similar to the COS method, when Δt is very small, the convergence of the CONV method becomes very slow. In the case of the FST method, only a single-time step of the algorithm is required between exercise dates, which would require several steps in the CONV and COS methods. An increase in M makes the FST method more accurate.

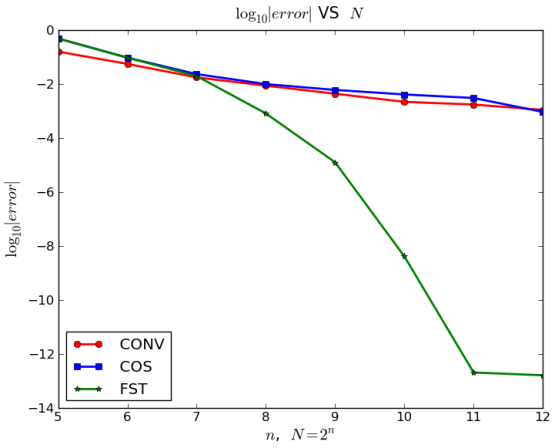

Figure 4.6: One-year American put under the VG model. Parameters used: $T = 1$, $\alpha = 0$, $L = 13$ and $x = 1.5$

4.7 Conclusion

In this chapter, we show by means of some numerical results, the pricing of a Bermudan put with 10 exercise dates under the BS and VG models, and the direct approximation of a Bermudan put to an American put using the CONV, COS and FST methods under the VG model.

Based on Figure 4.4, we conclude that the error convergence for pricing the Bermudan put under the BS model using the COS method is excellent, for the convergence is exponential. The convergence of the CONV and FST methods is algebraic. The FST method achieved its convergence with less computational effort.

The error convergence of the Fourier methods for pricing a Bermudan put under the VG model is algebraic, although the error convergence of the COS method proved outstanding. For pricing an American put, Result 4.6.4 shows that the convergence of the FST method is remarkable. The FST method is accurate up to an error of order $\mathcal{O}(10^{-8})$ with $N < 1000$ points. The FST converges in 1 second of CPU-time. Though the convergence of the CONV and COS methods for pricing American puts is similar, the CONV method demands lesser computational effort compared to that of the COS method.

Thus, the COS method is superior for pricing Bermudan puts under the BS and VG models and the FST method is outstanding in pricing American puts under the VG model. In term of CPU-time, the FST algorithm requires less computational effort to converge compared to other Fourier methods. Thus, the COS method gives more accurate results for small values of M, but the FST method works better for large values of M.

Chapter 5

Concluding remarks

In this dissertation, we have discussed and implemented four (4) Fourier methods, the Carr-Madan method, Carr and Madan (1999), the Convolution method, Lord *et al.* (2008), the COS method, Fang and Oosterlee (2008), Fang and Oosterlee (2009b) and the Fourier space time-stepping method, Jackson *et al.* (2007), Jaimungal and Surkov (2009), Surkov (2009) in pricing some options under the Black-Scholes model, the Normal Inverse Gaussian model and the Variance Gamma model. These methods can be used whenever the CF of the process of the underlying asset is known. In most of the Fourier methods, we implement the FFT algorithm. The FFT initiates the impressive improvement in the computational speed achieved by these methods without any connection to the process of the underlying asset. Thus, the involvement of the FFT in these methods is flexible and generic, given that the CF is known.

The Carr-Madan method provides platform for the development of other Fourier methods. But, this method cannot be used to price early-exercise options, neither can it price path-dependent exotic options. The satisfactory convergence of this method requires a large number of points, N, which is not desirable from a computational point of view.

The convolution method is a great improvement over the Carr-Madan method. To price a Bermudan option, we achieved a computational complexity of $\mathcal{O}(MN \log N)$. The error convergence of the CONV method is algebraic. For pricing an American put by direct approximation of Bermudan put to the American put, the error convergence exhibited by the CONV method is not as fast as those experienced in pricing European and Bermudan options.

The recovery of the density function, the exponential convergence in N for financial models with continuous density function, and the remarkable computational speed of the Fourier-cosine series expansion method makes the method outstanding for pricing plain-vanilla European and Bermudan options. The COS method gives a highly accurate results within a small number of points. In our numerical results, the convergence of the COS method is exponential in pricing European and Bermudan options except in the VG model where $\Delta t < \nu$, the convergence, is algebraic. The computational complexity for pricing a Bermudan put is $\mathcal{O}((M-1)N \log N)$.

The convergence of a Bermudan put to an American put by direct approximation (increasing M) using the COS method, is extremely slow compared to other options. This is as a result of the small interval between two successive dates. The smaller the time interval between two successive dates, the more the peakedness of the density function of the process of the underlying asset. Thus, a larger value of N is required to achieve satisfactory accuracy.

The Fourier space time-stepping method solves the pricing PIDE efficiently. The convergence of the FST method in all numerical results presented in this dissertation is algebraic. The computational complexity for pricing Bermudan put is $\mathcal{O}(MN \log N)$. This method requires less computational effort in pricing early exercise options, for it does not require any time-stepping procedure between two successive dates. For pricing American put by direct approximation of Bermudan put to American put, the result obtained is remarkable compared to the CONV and the COS methods. The FST method converges significantly faster.

These methods can be used to price options with a series of strikes at a single computation, to price options with multi-dimensional assets and to determine the hedge parameters with less modification to the original algorithm of the option of their counterparts.

The efficiency of these methods may make it possible to calibrate models to the prices of American options which are popularly traded in the financial market.

Appendices

Appendix A

Dynamics of asset price

A.1 Examples of Lévy processes

The Poisson processes and the Wiener processes are the fundamental examples of Lévy processes. They can be thought of as the building blocks of Lévy process because each every Lévy processes is a composed of a Wiener process and a possibly infinite number of independent Poisson processes, Cont and Tankov (2004).

Poisson Processes: Finite activity Lévy processes

A Poisson process N_t is defined as the counting process with independent and stationary increments. It counts the number of random times (T_n) which occur between 0 and t.

Definition A.1.1 (Exponential distribution)**.** *A positive random variable Y is said to follow an exponential distribution with parameter $\lambda > 0$, if it has a probability density function of the form,*

$$f_Y = \lambda e^{-\lambda y} \mathbb{I}_{y \geq 0}.$$

The distribution function of Y, $\forall y \in [0, \infty)$ is given by

$$F_Y(y) = \mathbb{P}(Y \leq y) = 1 - e^{-\lambda y}.$$

The mean,

$$\mathbb{E}[Y] = \frac{1}{\lambda} \text{ and the variance, } Var[Y] = \frac{1}{\lambda^2}.$$

Proposition A.1.2. *Let T be an exponential random variable $\forall t, s > 0$,*

$$\mathbb{P}(T > t + s | T > t) = \frac{\int_{t+s}^{\infty} \lambda e^{-\lambda y} dy}{\int_{t}^{\infty} \lambda e^{-\lambda y} dy} = \mathbb{P}(T > s).$$

If T is a random time, the distribution $T - t$, knowing $T > t$, is the same as the distribution of T itself. This is called an absence of memory (i.e. it does not keep records of the past) and the exponential distribution is the only distribution with this property, Schoutens (2003). This property plays an important role in defining Markov processes with jumps.

Definition A.1.3. *Let N_t be a Poisson process with intensity $\lambda > 0$[1]. The probability distribution is given by*

$$\mathbb{P}(N_t = k) = \frac{e^{-\lambda t}(\lambda t)^k}{k!} \tag{A.1}$$

Proposition A.1.4. *Let $(\tau_i)_{i\geq 1}$ be a sequence of the independent exponential random variables with parameter λ and $T_k = \sum_{i=1}^{k} \tau_i$. The process $(N_t)_{t\geq 0}$ is defined by*

$$N_t = \sum_{k\geq 1} \mathbb{I}_{t\geq T_k} \tag{A.2}$$

is called a Poission process with intensity λ, Cont and Tankov (2004).

Proposition A.1.5. *(Properties of a Poisson process). Let $(N_t)_{t\geq 0}$ be a Poisson process with intensity λ, then,* Sato (1999)*:*

- *N_t is almost surely finite.*
- *$N_{t-} = N_t$ with probability 1.*
- *N_t follows the Poisson distribution with parameter λ_t such that $\forall n \in N$;*

$$\mathbb{P}(N_t = k) = e^{-\lambda t}\frac{(\lambda t)^k}{k!}.$$

- *For any ω, the sample path $t \to N_t(\omega)$ is piecewise constant and increases by jumps of size 1.*
- *The sample paths $t \to N_t$ are right continuous with left limit.*
- *The probability of (N_t) is continuous i.e. $\forall t > 0$, $\mathbb{P}(N_t) \to \mathbb{P}(N_s)$ as $t \to s$.*
- *The CF of N_t is given by*

$$\mathbb{E}[e^{i\omega N_t}] = e^{\{\lambda t(e^{i\omega}-1)\}} \quad \forall \quad \omega \in \mathbb{R}.$$

- *The increments of N_t are independent of the past.*
- *N_t has the Markov property $\forall t \geq s$, $\mathbb{E}[f(N_t)|N_s]$.*
- *N_t increments are stationary: $N_t + N_h$ has the same distribution as N_h.*

Since pure jumps move in one dimension in a Poisson process which makes the process insignificant in financial modelling, we incorporate the compensated Poisson process.

Definition A.1.6 (Compensated Poisson process)**.** *Let $(X_t)_{t\geq 0}$ be a Poisson process such that $\mathbb{E}[|X_t|] < \infty$. A compensated Poisson process $\bar{N}$ is given by*

$$\bar{N}_t = N_t - \lambda_t$$

[1] is the average number of jumps or arrivals per unit time

$\bar{N}_t$ has independent increments. The parameter λt is deterministic and it's known as the compensator. The compensated Poisson process can be noted as the difference between the counting process and the expectation of the counting process which is the same thing. Thus, the process is no longer integer valued and therefore not a counting process. Then, we proceed in studying the compound Poisson process. The compound Poisson processes generalise this concept by sampling jumps from more general statistical distributions and this makes it significant in Financial modelling, Cont and Tankov (2004).

Definition A.1.7 (Compound Poisson Process)**.** *Let Y_i be an i.i.d. sequence of random variables with CF ϕ and distribution $\mathbb{P}$. A compound Poisson process, X_t, is defined by*

$$X_t = \sum_{i=1}^{N_t} Y_i \tag{A.3}$$

(see Cont and Tankov (2004)) for the proof.

Proposition A.1.8. *$(X_t)_{t\geq 0}$ is a compound Poisson process if, and only if, it is a Lévy process and its sample paths are piece-wise function constant. The jump sizes $[Y_i]_{i\geq 1}$ are independent and identically distributed.*

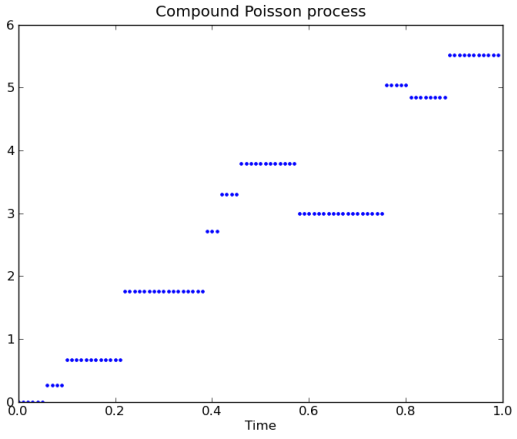

Figure A.1: Sample path of a compound Poisson process with 10 jumps. Parameters used: $T = 1$, $\lambda = 10$. Jump sizes are drawn from standard normal distribution.

Proposition A.1.9 (Characteristic function of Poisson and compound Poisson)**.** *Let $(X_t)_{t\geq 0}$ be a compound Poisson process on $\mathbb{R}$ with intensity λ, jump size of h and CF $\Phi_h(\cdot)$. The CF of a Poisson process can be derived by summing up sequence*

of an increasing function of the Poisson process:

$$\begin{aligned}\Phi(\omega) &= \sum_{k=0}^{\infty}\left[\frac{e^{\lambda t}(\lambda t)^k}{k!}\right]e^{i\omega k}\\ &= e^{\lambda t(e^{i\omega}-1)}.\end{aligned} \tag{A.4}$$

The CF of a compound Poisson process can be derived by conditioning the expectation on a Poisson process that is;

$$\begin{aligned}\mathbb{E}[e^{i\omega X_t}] &= \mathbb{E}[\mathbb{E}[e^{i\omega X_t}]|N_t] = \mathbb{E}[\Phi_h(\omega)^{N_t}]\\ &= \sum_{j=0}^{\infty}\frac{e^{\lambda t}(\lambda t)\Phi_h(\omega)^j}{j} = e^{[(\lambda t)(\Phi_h(\omega)-1)]}\\ &= e^{[t\lambda\int_{\mathbb{R}}(e^{i\omega x}-1)h(dx)]}, \qquad \omega\in\mathbb{R}.\end{aligned} \tag{A.5}$$

Comparing the CF of a Poisson with a compound Poisson, we notice that a compound Poisson random variable can be represented as a superposition of an independent Poisson process with different jumps sizes. The total density of a Poisson process with jump sizes in the interval $[y, y+dy]$ is determined by density $\lambda h(dy)$. Let $\nu(dx) = \lambda h(dx)$. Thus, equation (A.5) can be written as:

$$\mathbb{E}(e^{i\omega.X_t}) = e^{[t\lambda\int_{\mathbb{R}}(e^{i\omega x}-1)\nu(dx)]}, \qquad \omega\in\mathbb{R}. \tag{A.6}$$

ν is called the Lévy measure of a process $(X_t)_{t\geq 0}$. The Lévy measure $\nu(dx)$ of a compound Poisson process is the average number of jumps per unit time. Always note that $\nu(dx)$ is a positive measure on $\mathbb{R}$ but not a probability measure since

$$\int \nu(dx) = \lambda \neq 1.$$

The Lévy density $\nu(dx)$ of a Lévy process, $(X_t)_{t\geq 0}$, is not the same as the probability density of a Lévy process, $(X_t)_{t\geq 0}$. Hence, a Poisson process and a compound Poisson process are said to be finite-activity Lévy processes since the average number of jumps per unit time is finite, Cont and Tankov (2004):

$$\int_{\mathbb{R}} \nu(dx) < \infty.$$

Arithmetic Brownian Motion Process: The Only Continuous Lévy Process

Studying Definition 2.2.2, with great insight, we can actually deduce that most Lévy processes have jumps, but not all. A Lévy process can have a continuous sample path, (no jumps). The only example of a continuous Lévy process is a standard Brownian motion process, Schoutens (2003).

Definition A.1.10. *A real-valued standard Brownian motion $X = (B_t)_{t\geq 0}$ is a Lévy process starting from 0 on a probability space $(\Omega, \mathcal{F}, \mathbb{P})$ if,*

- $\mathbb{P}(B_0 = 0) = 1$,

- *For all* $0 \leq s \leq t$ *, the real-valued random variable* $B_t - B_s$ *is normally-distributed with mean* 0 *and variance* $t - s$*.*
- *For all* $0 = t_0 < t_1 < \cdots < t_p$*, the variables* $[B_{t_k} - B_{t_{k-1}}, 1 \leq k \leq p]$ *are independent.*

The stationary independent condition means that the distribution of increments $B_{tk} - B_{tk-1}$ do not depend on the time $tk - 1$, but they depend on the interval of time.

A.1.1 Subordination

Definition A.1.11 (Properties of Subordinator)**.** *A Lévy process* $(S_t)_{t\geq 0}$ *on* $\mathbb{R}$ *is said to be a subordinator if, and only if, it satisfies one of the following equivalent properties:*

- $S_0 = 0$ *and for every* $t \geq a$*,* $S_t \geq S_a$*.* S_t *is almost surely non-decreasing.*
- *For any* $x; (-\infty < x \leq 0]$*,* $\Phi(x) = 0$*. Thus, a negative jump does not exist since* S_t *is non-decreasing.*
- $(S_t)_{t\geq 0}$ *for all* $t > 0$ *almost surely.*
- *Let* $(\gamma_s, \sigma_s, \nu_s)$ *be a characteristic triplet of* $(S_t)_{t\geq 0}$ *where* $\sigma_s = 0$*, that is,* S_t *has no diffusion parameter, and has a positive drift and a positive jump of finite variation.*

Since the Lévy measure of an increasing Lévy process is mainly defined on the positive real-axis, S_t is a positive random variable. It is more convenient to work with the Laplace transform to the Fourier transform Cont and Tankov (2004).

Definition A.1.12 (Laplace transform)**.** *Let* s *be a random variable defined on a real positive line. The Laplace transform of a function* $f(s)$ *written on* $s \geq 0$ *is given by*

$$\mathcal{L}[f(s)] = \int_0^\infty e^{-\omega s} f(s) ds \tag{A.7}$$

and the CF of $f(s)$ *with its probability distribution function* $\mathbf{f}$ *is written as;*

$$\Phi_s(\omega) = \mathcal{L}[\mathbf{f}(s)](\omega) = \int_0^\infty e^{-\omega s} \mathbf{f}(s) ds. \tag{A.8}$$

The moment-generating function $\mathcal{M}_s(\omega)$ exists if for every positive k, $|\omega| < k$ such that;

$$\mathcal{M}_s(\omega) = \int_{-\infty}^\infty e^{\omega s} \mathbf{f}(s) ds = \mathbb{E}[e^{\omega s}] \qquad \text{for} \quad \omega \in \mathbb{R}.$$

Recall from Definition 2.6 that the moment-generation function $\mathcal{M}_s(\omega) = \Phi_s(-i\omega)$, then,

$$\mathcal{M}_s(\omega) = \Phi_s(-i\omega) = \int_0^\infty e^{i\omega s} \mathbf{f}(s) ds. \tag{A.9}$$

From the Lévy-Khinchine Representation, the CF $\Phi_s(\omega)$ can be written in terms of the moment-generating function $\mathcal{M}_s(\omega)$,

$$\mathcal{M}_s(\omega) = \mathbb{E}[e^{\omega s}] = e^{t\mathcal{L}_s(\omega)} \tag{A.10}$$

and

$$\mathcal{L}_s(\omega) = \gamma_s\omega + \int_0^\infty [e^{\omega x} - 1]\nu_s(dx)$$

is the Laplace exponent where ν_s is the Lévy measure on s that ensures the process is finite and $\gamma_s \geq 0$. The Laplace exponent $\mathcal{L}_s(\omega)$ satisfies the process, is an increasing Lévy process.

A.1.2 Brownian Subordination

A subordinating Brownian motion studies the integrate flow and arrival of new information into the model. This makes a model based on subordinated Brownian motion very simple, unlike a pure Levy process. The two models that are based on a Brownian subordinator are the Variance Gamma process and the Normal Inverse Gaussian process. The role of the Brownian class of subordinated processes were first considered in Finance by *Clark, 1997*, Madan and Seneta (1990).

Theorem A.1.13. *Let $(B_t)_{t\geq 0}$ be a standard Brownian process. Let $X(t;\omega) = \varnothing t + \sigma B(t;\omega)$ be a Brownian motion (a Lévy Process on $\mathbb{R}$), with a constant drift $\varnothing t$ and σ. Its characteristic triplet is $(\varpi, \varnothing, 0)$. Let $S(t;\omega)$ be a subordinator independent of $X(t;\omega)$ on $\mathbb{R}$, with a Laplace exponent $\mathcal{L}(\omega)$, and characteristic triplet $(b, 0, \varphi)$. The process $Z(t;\omega) = X(S_t(\omega);\omega) = \varnothing S_t(\omega) + \sigma B(S_t(\omega);\omega)$ is a Lévy with the characteristic triplet $(\varpi_z, \varnothing_z, \nu_z)$. The CF of Z_t is*

$$\Phi_{Z_t}(\omega) = \mathbb{E}[e^{i\omega.Z_t}] = e^{t\mathcal{L}[i\omega\varnothing - \frac{\omega^2\sigma^2}{2}]}. \tag{A.11}$$

For details and proof, see Cont and Tankov (2004).

Gamma Subordinator

The Gamma process is a special case of a Tempered α stable when the index stability is zero. The process can easily be seen to be a non-decreasing process, and satisfies the conditions for a subordinator.

Definition A.1.14 (Tempered α stable process)**.** *Let $(S_t)_{t\geq 0}$ be a tempered α stable subordinator with $(\gamma_s, \sigma_s, \nu_s)$ where γ_s=0 and $\sigma_s \in (0, 1)$. The Lévy measure is given by*

$$\nu_s(n) = \frac{ae^{-\lambda n}}{x^{\alpha+1}}\mathbb{I}_{n>0} \tag{A.12}$$

where a determines the intensity of jump sizes and λ determines the decay rate of large jumps, Cont and Tankov (2004). The constant a and λ are positive values. Using the Lévy-Khinchine Representation and equation (A.10), (the moment-generating function) is given as

$$\mathcal{M}_s(\omega) = \mathbb{E}[e^{(\omega S_t)}] = e^{t\mathcal{L}_s(\omega)}$$

where $\mathcal{L}_s$ is the Laplace exponent written as;

$$\mathcal{L}_s(\omega) = \gamma_s\omega + \int_0^\infty [e^{\omega x} - 1]\nu_s(dx) = a[(\lambda - \omega)^\alpha]\Gamma(-\alpha).$$

We can derive the mean of S_t, $\mathbb{E}[S_t]$. Thus,

$$\mathbb{E}[S_t] = a\alpha t\lambda^{\alpha-1}\Gamma(-\alpha). \tag{A.13}$$

When we set $\lambda = \frac{1-\alpha}{\kappa}$ and $a = \frac{1}{\Gamma(1-\alpha)}\frac{1-\alpha}{\kappa}^{(1-\alpha)}$ in equation (A.13), (A.13) becomes

$$\mathbb{E}[S_t] = \frac{1}{\Gamma(1-\alpha)}\frac{1-\alpha}{\kappa}^{(1-\alpha)} t\alpha\frac{1-\alpha}{\kappa}^{(1-\alpha)}\Gamma(1-\alpha) = t, \tag{A.14}$$

where

$$\frac{\Gamma(-a)}{\Gamma(1-a)} = -\frac{1}{a}.$$

The process $(S_t)_{t\geq 0}$, in Definition (A.1.14), is called a gamma subordinator, if $\alpha = 0$. Then the Lévy density in equation (A.12) becomes, according to Cont and Tankov (2004):

$$\nu_s(n) = \frac{ae^{-\lambda n}}{n}\mathbb{I}_{n>0}. \tag{A.15}$$

Recall from equation (A.10), the moment-generating function $[S_t]_{t\geq 0}$ can be written as:

$$\mathcal{M}_s(\omega) = \mathbb{E}[e^{(\omega S_t)}] = e^{t\mathcal{L}_s(\omega)}$$

where $\mathcal{L}_s$ is the Laplace exponent written as:

$$\begin{aligned}\mathcal{L}_s(\omega) &= \gamma_s\omega + \int_0^\infty [e^{\omega x} - 1]\nu_s(dx)\\ &= \int_0^\infty [e^{\omega x} - 1]\frac{ae^{-\lambda n}}{n}(dx)\\ &= a\ln\frac{\lambda}{\lambda - \omega}.\end{aligned}$$

The probability density of the gamma subordinator $[S_t]_{t\geq 0}$ follows a gamma distribution:

$$\mathcal{G}_t(x) = \frac{\lambda^{at}}{\Gamma at}x^{(at-1)}e^{-\lambda x} \qquad x > 0.$$

In a situation where the gamma subordinator has a unit mean rate ($\mathbb{E}[S_t] = t$), the Lévy density in equation (A.15) becomes

$$\nu_s(x) = \frac{1}{\kappa}\frac{e^{-x/\kappa}}{x}\mathbb{I}_{x>0}. \tag{A.16}$$

The moment-generating function of the gamma subordinator S_t with a unit mean rate, can be derived using equation (A.10) where the Laplace $\mathcal{L}_s$ is written as:

$$\begin{aligned}\mathcal{L}_s(\omega) &= \gamma_s\omega + \int_0^\infty [e^{\omega x} - 1]\nu_s(dx)\\ &= \int_0^\infty [e^{\omega x} - 1]\frac{1}{\kappa}\frac{e^{-x/\kappa}}{x}(dx)\\ &= \frac{-\log\kappa - \log(\frac{1}{\kappa} - \omega)}{\kappa}.\end{aligned}$$

$\kappa > 0$ is a variance rate which is equal to the variance of the subordinator at time 1. Then, κ determines the degree of the randomness of the subordinator. When the value of κ is zero, the process is deterministic. Thus, the probability density of a gamma subordinator S_t with unit mean rate $\mathbb{E}[S_t] = t$ (i.e $\frac{a}{\lambda} = 1$, where $a = \frac{1}{\kappa}$ and $\lambda = \frac{1}{\kappa}$) has a gamma density of the following form:

$$\mathcal{G}_t(x) = \frac{[1/\kappa]^{(1/\kappa)t}}{\Gamma at} x^{([1/\kappa]t-1)} e^{-[1/\kappa]x} \qquad x > 0.$$

For further studying, see Sato (1999), Schoutens (2003), Cont and Tankov (2004).

References

Albanese, C., Jackson, K. and Wiberg, P. (2004). A new Fourier transform algorithm for value-at-risk. *Quantitative Finance*, vol. 4, pp. 328–338.

Almendral, A. (2005). Numerical valuation of American options under the CGMY process. *In Exotic Option Pricing and Advanced Lévy models (A. E Kyprianou, W. Schoutens and P. Wilmott, eds.). Wiley, New york.*

Almendral, A. and Oosterlee, C. (2007). On American options under the Variance Gamma process. *Applied Mathematical Finance*, vol. 14, no. 2, pp. 131–152.

Andersen, L. and Andreasen, J. (2000). Jump diffusion process: volatility smile fitting and numerical methods for option pricing . *Review of Derivative Research*, vol. 4, pp. 231–265.

Andricopoulos, M., Widdicks, P. and Newton, D. (2003). Universal option valuation using quadrature. *Journal of Financial Economics*, vol. 67(3), pp. 447–471.

Applebaum, D. (2004). *LEVY PROCESS AND STOCHASTIC CALCULUS*. Cambridge Studies in Advanced Mathematics, Cambridge University Press.

Attari, M. (2003). Option pricing using Fourier transform: A numerically efficient simplification. *Charles River Associates working paper*.

Bachelier, L. (1900). Théorie de la spéculation. Tech. Rep., Paris: Gauthier-Villars. Translated in Cootner (1964).

Bailey, D.H and Swartztrauber, P. (1991). The fractional Fourier transform and applications. *SIAM review*, vol. 33, no. 3, pp. 389 – 404.

Barndorff-Nielsen, O.E. (1997). Normal inverse gaussian distributions and stochastic volatility modelling. *Scandinavian Journal of Statistics*, vol. 24, no. 1, pp. 1–13.

Bates, D. (1996). Jumps and stochastic volatility: Exchange rate processes implicit in Deutsche mark options. *Review of Financial Studies*, vol. 9, pp. 69–107.

Bellman, R. (1957). *DYNAMIC PROGRAMMING*. Princeton University Press, Princeton, New Jersey.

Benhamou, E. (2002). Fast Fourier tranform for discrete Asian options. *Journal of Computational Finance*, vol. 6, pp. 49–68.

Black, F. and Scholes, M. (1973). The pricing of options and corporate liabilities. *Journal of Political Economy*, vol. 81, no. 3, pp. 637–654.

Borovkov, K. and Novikov, A. (2002). On a new approach to calculating expectations for option pricing. *Journal Appl. Probab*, vol. 39, pp. 889 – 895.

Boyarchenko, S. and Levendorskii, S.Z. (2002). *NON GAUSSIAN MERTON BlACK-SCHOLES THEORY*. World scientific.

Boyd, J.P. (2000). *CHEBYSHEV FOURIER SPECTRAL METHODS*. Dover publications, Inc., 2nd edition,.

Boyle, P. (1977). Options: A Monte Carlo approach. *Journal of Financial Economics*, vol. 4, pp. 323 – 338.

Brigham, E. (1974). *THE FAST FOURIER TRANSFORM*. Prentice-Hall Inc, Englewood Cliffs, New JerseyThe Fast Fourier.

Carl, P., German, H., Madan, D. and M.Yor. (2003). Stochastic volatility for Lévy processes. *Journal of Math. Finance*, vol. 13, pp. 345–382.

Carr, P., German, H., Madan, D. and Yor, M. (2002). The fine structure of asset returns: An empirical investigation. *Journal of Business*, vol. 75, no. 2, pp. 305–332.

Carr, P. and Madan, D.B. (1999). Option valuation using fast Fourier transform. *Journal of Computational Finance*, vol. 2, pp. 61–73.

Carr, P.P. and Madan., D.B. (1998). The Variance gamma process and option pricing. *European Finance Review*, vol. 2, pp. 79–105.

Carverhill, A. and Clewlow, L. (1990). Flexible convolution. *Risk*, vol. 3, no. 4, pp. 25–29.

Cerny, A. (2008). Fast Fourier transform and option pricing. *Cass Business School Research*. Available at: http://ssrn.com/abstract=1098367

Cherubini, U., Lunga, G.D., Mulinacci, S. and Rossi, P. (2010). *FOURIER TRANSFORMS METHODS IN FINANCE*. John Wiley and Sons Ltd.

Chiarella, Carl, Ziogas and Andrew (2009). American call options under jump-diffusion processes - A Fourier transform approach . *Appl. Math. Finance*, vol. 16, no. 1, pp. 37–79.

Chourdakis, K. (2004). Option pricing using fractional FFT. *Journal of computational finance*, vol. 8, no. 2, pp. 1–18.

Cont, R. and Tankov, P. (2004). *FINANCIAL MODELLING WITH JUMP PROCESSES*. Chapman and Hall.

Cox, J. and Ross, S. (1976). The valuation of options for alternative stochastic processes. *Journal of Financial Economics*, vol. 3, pp. 145–156.

Davison, M. and Surkov, V. (2010). Efficient construction of robust hedging strategies under jump models. Working paper.
Available at: http://ssrn.com/abstract=1562685

Dempster, M. and Hong, S. (2000). Spread option valuation and the fast Fourier transform. *Technical report WP 26/2000*.

Deng, S. (2000). Pricing electricity derivatives under alternative stochastic spot price models. *Proceedings of the 33rd Hawaii International Conference on System Sciences*.

Derman, Emmanuel and Kani, I. (1994). Riding on smile. *RISK magazine*, pp. 32–39.

Dufrense, D., Garrido, J. and Morales, M. (2009). Fourier inversion formulas in option pricing and insurance. *Method of Comput Appl Prob*, vol. 11, pp. 359–383.

Dupire, B. (1994). Pricing with smile. *RISK magazine*, pp. 18–20.

Eberlein., E., Glau, K. and Papapantoleon, A. (2010). Analysis of Fourier transform valuation formulas and applications. *Appl. Math. Finance*, vol. 13, pp. 211– 240.

Eberlein, E. and Prause, K. (2000). The generalized hyperbolic model: Financial derivatives and risk measures. *In Mathematical Finance-Bachelier congress*, pp. 245–267.

Fang, F. (2010). *The COS METHOD: AN EFFICIENT FOURIER METHOD FOR PRICING FINANCIAL DERIVATIVES*. Ph.D. thesis, Delft University of Technology.

Fang, F. and Oosterlee, C. (2009b). Pricing early-exercise and discrete barrier options by Fourier-cosine series expansion. *Numerische mathematik*, vol. 114(1), pp. 27–62.

Fang, F. and Oosterlee, C. (2011). Fourier-based valuation method for Bermudan and barrier options under Heston's model. *SIAM Journal of Financial Math.*, vol. 2, pp. 439–463.

Fang, F. and Oosterlee, C.W. (2008). A novel pricing method for European options based on Fourier-cosine series expansions. *Siam Journal on Scientific Computing*, vol. 31, pp. 826–848.

F.Hubalek, Kallsen, J. and Krawczyk, L. (2006). Variance-optimal hedging for processes with stationary independent increments. *Ann. Appl. Probab*, vol. 16, pp. 853–885.

Föllmer, H. and Schweizer, M. (1991). Hedging of contingent claims under incomplete information. *In M.H.A. Davis and R.J. Elliot (ed.): Applied Stochastic Analysis*, pp. 389–414.

Förster, K. and Petras, K. (1991). Error estimates in Gaussian quadrature for functions of bounded variations. *SIAM Journal of Numerical Analysis*, vol. 28, no. 3, pp. 880–889.

Forsyth, P.A. and Vetzal, K.R. (2002). Quadratic convergence of penalty method for valuing American options. *SIAM Journal on Scientific Computing*, vol. 23, pp. 2096–2123.

Geman, H. (2002). Pure jum Lévy processes for asset price modelling. *Journal of Banking and Finance*.

Gerber, H. and Shiu, E. (1994). Option pricing by Esscher transforms. *Transactions of the Society of Actuaries XLVI*, pp. 99–191.

Geske, R. and Johnson, H.E. (1984). The American put option valued analytically. *Journal of Finance*, vol. 39, no. 5.

Gutierrez, O. (2007). Option valuation, time-changed processes and the fast Fouruer transform. *Quantitative Finance*, vol. 8, no. 2, pp. 103–108.

H.Albrecher and Predota, M. (2004). On Asian option pricing for NIG Lévy process. *Comput. Appl. Math. Finance*, vol. 172, no. 1, pp. 153–168.

Harrison, J. and Pliska, S. (1981). Martingales and stochastic integrals in the theory of continuous trading. *Stochastic processes and their application*, vol. 11, no. 11, pp. 215–260.

H.Bühlmann, Delbaen, F., Embrechts, P. and Shiryaev, A. (1996). No-arbitrage, change of measure and conditional Esscher transforms. *CWI Quarterly*, vol. 9, no. 4, pp. 291–317.

Heston, S. (1993). A closed form solution for options with stochastic volatility with applications to bond and currency options. *The Review of Financial Studies*, vol. 6, no. 2, pp. 327–243.

Hirsa, A. and Madan, D.B. (2004). Pricing American option under Variance Gamma. *Journal of Computational Finance*, vol. 7, pp. 63–80.

Hull, John and White, A. (1987). The pricing of options with stochastic volatilities. *Journal of Finance*, vol. 42, pp. 281 – 300.

Hull, J. (2007). *OPTION FUTURE AND OTHER DERIVATIVES*. Prentice Hall.

Hurd, T. and Zhou, Z. (2009). A Fourier transform method for spread option pricing. *arXiv q-fin. CP*.

Iseger, P. (2006). Numerical transform inversion using Gaussian quadrature probab. in the Eng. and Inform. *Sciences*, vol. 20, no. 1, pp. 1–44.

Jackson., K., Jaimungal, S. and Surkov, V. (2008). Fourier space time-stepping for option pricing with Lévy models . *Journal of Computational Finance*, vol. 12, no. 2, pp. 1–28.

Jackson, K.R., Jaimungal, S. and Surkov, V. (2007). Option pricing with regime switching Lévy processes using Fourier space time-stepping. pp. 92–97.

Jaimungal, S. and Surkov, V. (2008). A Lévy based framework for commodity derivative valuation via FFT. *SSRN elibrary. Technical report, University of Toronto.* Available at: papers.ssrn.com/sol3/papers.cfm?abstract_id=1302887

Jaimungal, S. and Surkov, V. (2009). Stepping through Fourier space. *Risk*, vol. July, pp. 82–87.

Ju, N. and Zhong, R. (2006). Fourier transformation and the pricing of average-rate derivatives. *Review of Derivative Research*, vol. 9, pp. 187–212.

Kahl, C. and Jäckel, P. (2005). Not-so-complex logarithms in Heston model. Tech. Rep., Wilmott magazine.

Kahl, C. and Lord, R. (2007). Optimal Fourier inversion in semi-analytical option pricing. *Journal of Computational Finance*, vol. 10(4), pp. 1–30.

Kéllezi, E. and Webber, N. (2004). Valuing Bermudan options when asset returns are Lévy proceses. *Quantitative Finance*, vol. 10(4), pp. 87–100.

Kou, S. (2002). A jump-difffusion model for option pricing. *Management science*, vol. 48, pp. 1086 – 1101.

Kypriano, A. (2010). *LEVY PROCESSES , ENCYCLOPEDIA OF QUANTATIVE FINANCE*. John Wiley and Sons, Ltd.

Kyriakos, C. (2005). Switching Lévy models in continuous time: finite distribution and option pricing. *University of Essex, Centre for Computational Finance and Economics and Agents (CCFEA) Working Papers.*

Lee, R.W. (2004). Option pricing by transform method: extensions, unification and error control. *Journal of Computational Finance*, vol. 7, no. 3, pp. 53–86.

Levendorskiĭ, S. (2004). Early exercise boundary and option prices in Lévy models. *Quantitative Finance*, vol. 4, no. 5, pp. 525–547.

Lewis, A.L. (2001). A simple option formula for general jump diffusion and other exponential Lévy processes. *Envision Financial Systems and OptionCity.net, Newport Beach, California, USA*.

Loan, V. (1992). Computational frameworks for the fast Fourier transform. *Frontier in Applied Mathematics SIAM*, vol. 10.

Lord, R. (2008). *EFFICIENT PRICING ALGORITHM FOR EXOTIC DERIVATIVES*. Ph.D. thesis, Erasmus Universiteit Rotterdam.

Lord, R., Fang, F., Bervoets, B. and Osterlee, C. (2008). A fast and accurate FFT-Based methof for pricing early exercise under Lévy processes. *SIAM Journal on Scientific Computing*, vol. 30(4), pp. 1678–1705.

Lord, R. and Kahl, C. (2010). Complex logarithm in Heston model. *Mathematical Finance*, vol. 20, no. 4, pp. 671–694.

Madan, D.B. and Seneta, E. (1990). The Variance Gamma model for share market return. *Journal of Business*, vol. 63(4), pp. 511–524.

Merton, R. (1973). Theory of rational option pricing. *Bell Journal of Economics and Management Science*, vol. 4, pp. 141–183.

Merton, R. (1976). Option pricing when underlying stock returns are discontinuous. *Journal of Economics*, vol. 3, pp. 125–144.

Miyahara, Y. (1999). Minimal entropy martingale measures of jump type price processes in incomplete assets markets. *Asian-Pacific Financial Markets*, vol. 6, no. 2, pp. 97–113.

Miyahara, Y. (2002). A note on Esscher transformed martingale measures for geometric Lévy processes. *Discussion papers in Economics. Nagoya city University*, , no. 379, pp. 1–14.

M.Minenna and Verzella, P. (2008). A revisited and stable Fourier transform method for affine jump-diffusion models. *Journal of Banking and Finance*, vol. 32, pp. 2064–2075.

M.Schmelzle (2010). *OPTION PRICING PRICING FORMULAE USING FOURIER TRANSFORM: THEORY AND APPLICATION*. Ph.D. thesis.
Available at: http://pfadintegral.com/docs/Schmelzle2010%20Fourier%20Pricing.pdf.38,47.

Nualart and Schoutens, W. (2001). Backwards stochastic differential equation and Feynman-Kač formula for Lévy processes with applications in finance. *Bernoulli*, vol. 7, no. 5, pp. 761–776.

Pascucci, A. (2011). *PDE AND MARTINGALE METHODS IN OPTION PRICING*. Springer.

Peskir, G. and Shiryaev, A. (2006). *OPTIMAL STOPPING AND FREE BOUNDARY PROBLEMS*. Springer.

Press, W.H., Teukolsky, S.A., Vetterling, W.T. and Flannery, B.P. (2007). *NUMERICAL RECIPES: THE ART OF SCIENTIFIC COMPUTING*. Third edition edn. Cambridge University Press.

Raible, S. (2000). *LEVY PROCESSES IN FINANCE: THEORY, NUMERICS AND EMPIRICAL FACTS*. Ph.D. thesis, Albert-Ludwigs-Unversität Freiburg, Germany.

Reiner, E. (2001). Convolution methods for Exotic options. *Technical reports, UBS Warburg, 2001*.
Available at: http://www.ipam.ucla.edu/publications/fm2001_4272.pdf.6.

Rydberg, T. (1997). The normal inverse Gaussian Lévy proceses: Simulations and approximations . *Stochastic models*, vol. 13, pp. 887–910.

Samuelson, P. (1965). A rational theory of warrant pricing . *Industrial Management Review*, vol. 6, pp. 13–31.

Sato (1999). *LEVY PROCESS AND INFINITELY DIVISIBLE DISTRIBUTION*. Cambridge Studies in Advanced Mathematics, Cambridge University Press.

Schoutens, W. (2003). *LEVY PROCESSES IN FINANCE: PRICING FINANCIAL DERIVATIVES*. Wiley.

Schoutens, W., E.Simons and Tistaert, J. (2004). Perfect calibration. Wilmott Magazine.

Schweizer, M. (1995). On the minimal martingale measure and the Föllmer Schweizer decomposition. *Stochastic Analysis and Applications*, vol. 13, no. 5, pp. 573–599.

Schweizer, M. (2002). On Bermudan options. *Advances in Finance and Stochastics. Essays in Honour of Dieter Sondermann, Springer*, pp. 257–269.

Scott, L. (1997). Pricing stock options in jump-diffusion model with stochastic volatility and interest rates: Application of Fourier transform methods. *Mathematical Finance*, vol. 7, pp. 413–426.

Sepp, A. (2003). Fourier transform for option pricing under affine jump-diffusion. *An Overview available at SSRN*, pp. 1–7.

Stein, Elias and Stein, J. (1991). Stock price distribution with stochastic volatiltiy: An analytic approach. *Review of Financial Studies*, vol. 4, no. 4, pp. 727–752.

Sullivan, O. (2005). Path dependent option pricing under Lévy processes. pp. 1–13.
Available at: http://ssrn.com/paper=673424.

Surkov, V. (2009). *OPTION PRICING USING FOURIER SPACE TIME-STEPPING FRAMEWORK*. Ph.D. thesis, University of Toronto.

Tankov, P. (2010). Pricing and hedging in exponential L évy models: Reviews of recent results. *In Paris-Princeton Lectures on Mathematical Finance 2010, volume 2003 of Lecture Notes in Math., Spring, Berlin*, pp. 319–359.

Walker, J.S. (1996). *FOURIER ANALYSIS*. Springer, CRC Press, Boca Raton, Florida.

Wang, I., Wan, J. and Forsyth, P. (2007). Robust numerical valuation of European and American options under the CGMY process . *Journal of Computational Finance*, vol. 10, no. 4, pp. 31–70.

Webber, N. and Ribeiro, C. (2003). A Monte Carlo method for the normal inverse Gaussian option valuation model using an inverse Gaussian bridge. *Computing in Economics and Finace 2003 5, Society for Comput. Economics*.

Wong, H. and Guan, P. (2011). An FFT network for Lévy option pricing. *Journal of Banking and Finance*, vol. 35, no. 4, pp. 988–999.